Analysis of semi-inclusive neutrino scattering within the relativistic distorted wave approach

Juan Manuel Franco Patiño
jfpatino@ific.uv.es

ANL, 17/09/2024

Contents

Contents

What do we need neutrino-nucleus scattering for?

AIM: Realistic description of semi-inclusive neutrino-nucleus scattering for neutrino oscillation experiments.

WHY: In neutrino oscillation experiments the information about the oscillation signal comes from the detection of final-state muons only $\rightarrow$ little dependence with the nuclear model used.

Semi-inclusive scattering is more sensitive to nuclear-medium effects

Large systematic uncertainty from modeling of neutrino interactions $\rightarrow$ room to improve oscillation measurements

Type of Uncertainty	$\nu_e/\bar{\nu}_e$ Candidate Relative Uncertainty (%)
Super-K Detector Model	1.5
Pion Final State Interaction and Rescattering Model	1.6
Neutrino Production and Interaction Model Constrained by ND280 Data	2.7
Electron Neutrino and Antineutrino Interaction Model	3.0
Nucleon Removal Energy in Interaction Model	3.7
Modeling of Neutral Current Interactions with Single γ Production	1.5
Modeling of Other Neutral Current Interactions	0.2
Total Systematic Uncertainty	6.0

HOW: Using the relativistic distorted-wave impulse approximation (RDWIA)

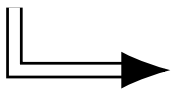

Unfactorized relativistic and fully quantum approach extensively applied in the past to inclusive and exclusive electron scattering

Contents

Inclusive vs semi-inclusive scattering

One proton knockout process in the IA

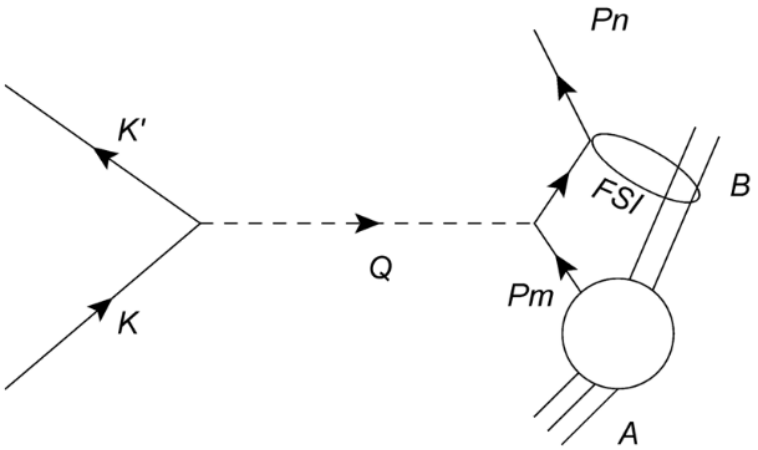

Inclusive vs semi-inclusive scattering

One proton knockout process in the IA

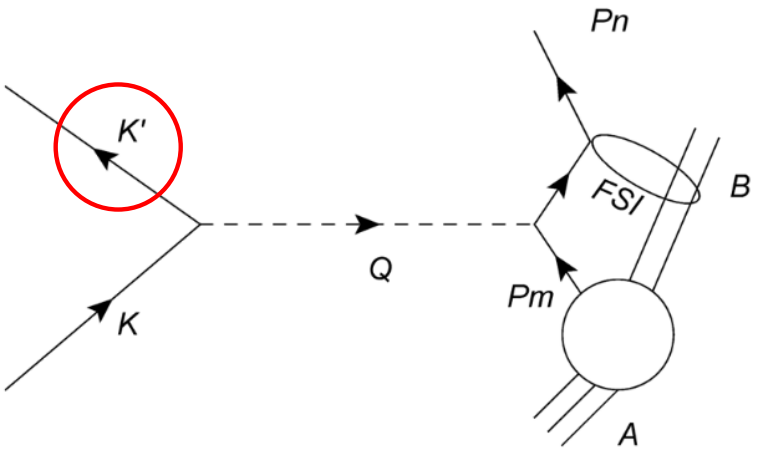

$\longrightarrow$ Inclusive process: only the final lepton k' is detected

Inclusive vs semi-inclusive scattering

One proton knockout process in the IA

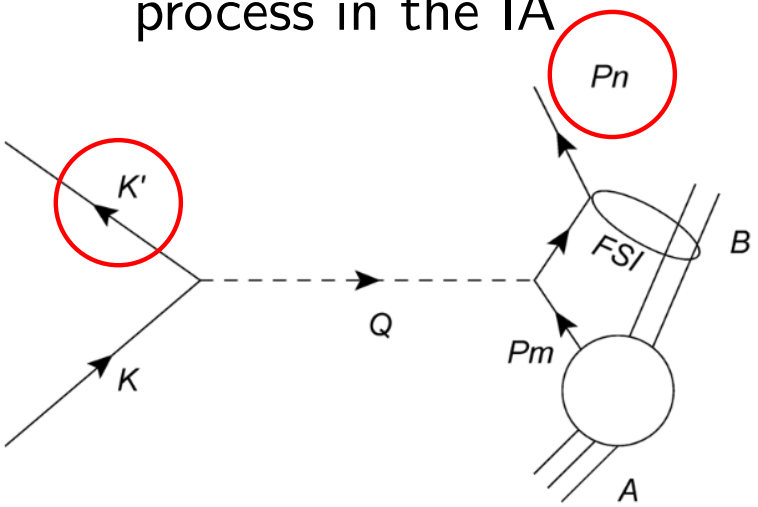

$\longrightarrow$ Semi-inclusive process: one or more particles are detected in coincidence with the final lepton (k' and p_N)

Inclusive vs semi-inclusive scattering

One proton knockout process in the IA

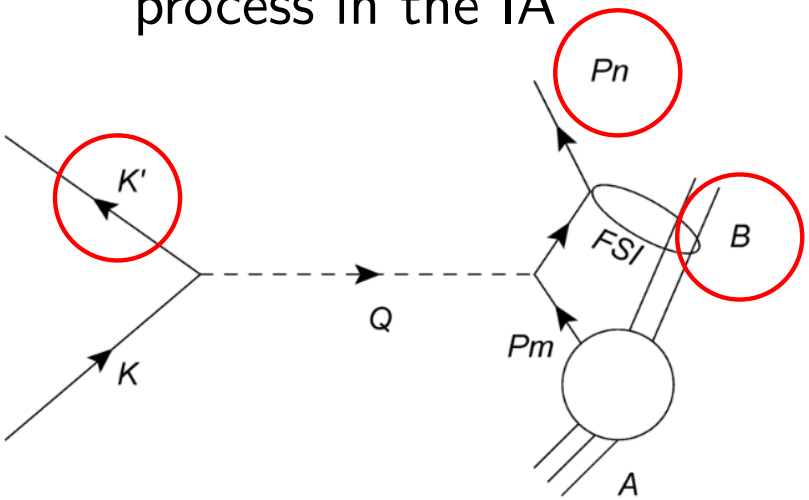

$\longrightarrow$

Exclusive process: the complete final system is known, including the residual nucleus (possible for electron but not for neutrino scattering)

Inclusive vs semi-inclusive scattering

One proton knockout process in the IA

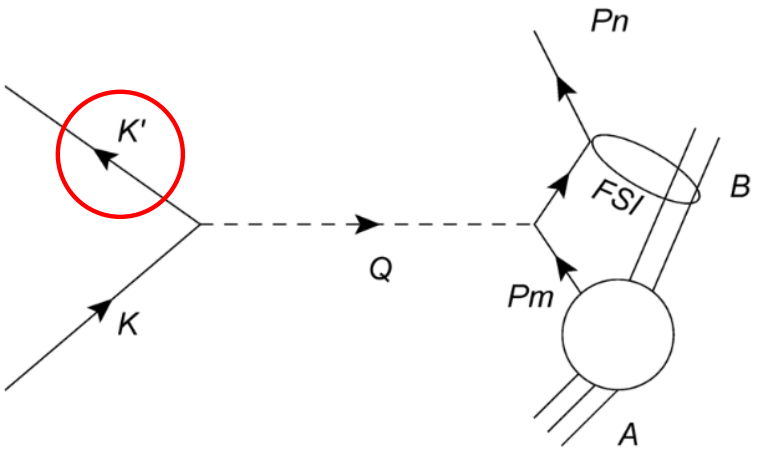

$\longrightarrow$

Until not many years ago, the majority of the experimental and theoretical work in neutrino reactions have focused on inclusive reactions.

Inclusive vs semi-inclusive scattering

One proton knockout process in the IA

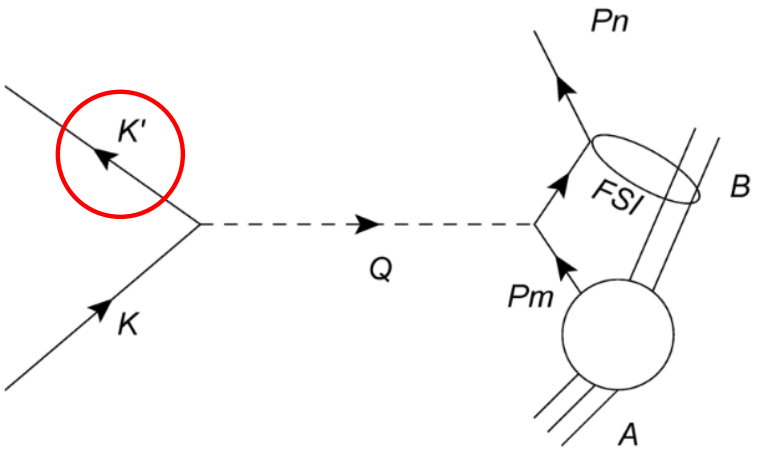

$\longrightarrow$

Until not many years ago, the majority of the experimental and theoretical work in neutrino reactions have focused on inclusive reactions.

A good agreement between theory and experiment for this kind of reactions can be achieved using very different approaches.

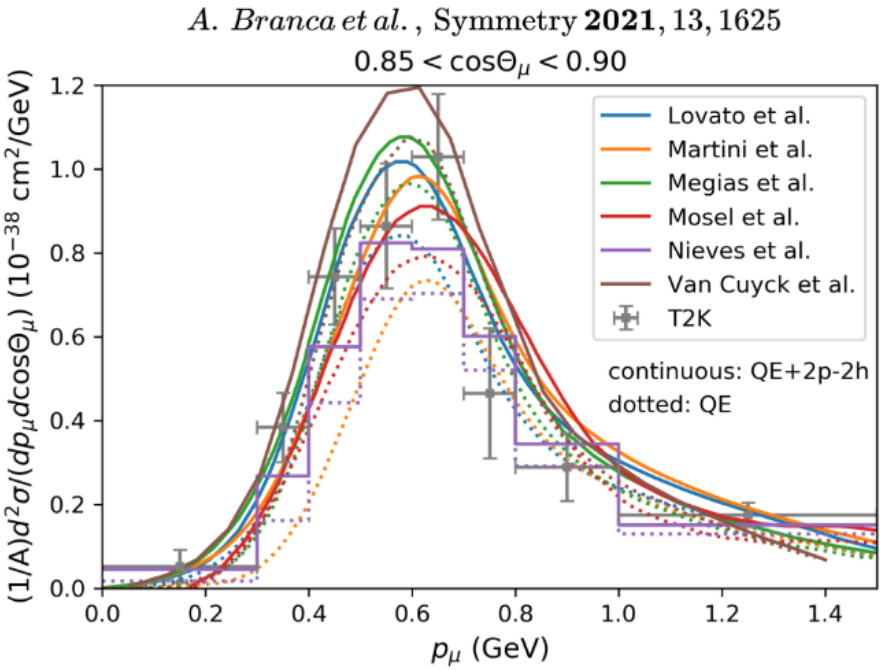

Contents

Semi-inclusive neutrino-nucleus formalism

$$\left\langle \frac{d^6\sigma}{dk' d\Omega_{k'} dp_N d\Omega_N^L} \right\rangle = \int dk\, P(k) \times K \times L_{\mu\nu} H^{\mu\nu} \longrightarrow$$

The leptonic tensor $L_{\mu\nu}$: function of initial and final leptons kinematics.

Semi-inclusive neutrino-nucleus formalism

$$\left\langle \frac{d^6\sigma}{dk' d\Omega_{k'} dp_N d\Omega_N^L} \right\rangle = \int dk\, P(k) \times K \times L_{\mu\nu} H^{\mu\nu} \longrightarrow$$

The hadronic tensor $H^{\mu\nu}$: contains the information about nuclear dynamics

$$H_\kappa^{\mu\nu} = \rho_\kappa(E_m) \times \sum_{m_j, s_N} \left[J_{\kappa, m_j, s_N}(Q, p_N) \right]^* J_{\kappa, m_j, s_N}(Q, p_N)$$

$$J^\mu_{\kappa, m_j, s_N} = \int d\mathbf{r} \overline{\Psi}_{s_N}(\mathbf{p_N}, \mathbf{r}) \left(F_1 \gamma^\mu + \frac{iF_2}{2m_N} \sigma^{\mu\nu} Q_\nu + G_A \gamma^\mu \gamma^5 + \frac{G_P}{2m_N} Q^\mu \gamma^5 \right) \Psi_\kappa^{m_j}(\mathbf{r})$$

- Scattered W.F.
- CC2 operator
- Bound W.F.

Description of the initial nuclear state:

- Pure shell model: missing energy profile is given by a Dirac delta per shell
- Realistic model, *i.e.* Benhar spectral function: short- and long-range correlations included

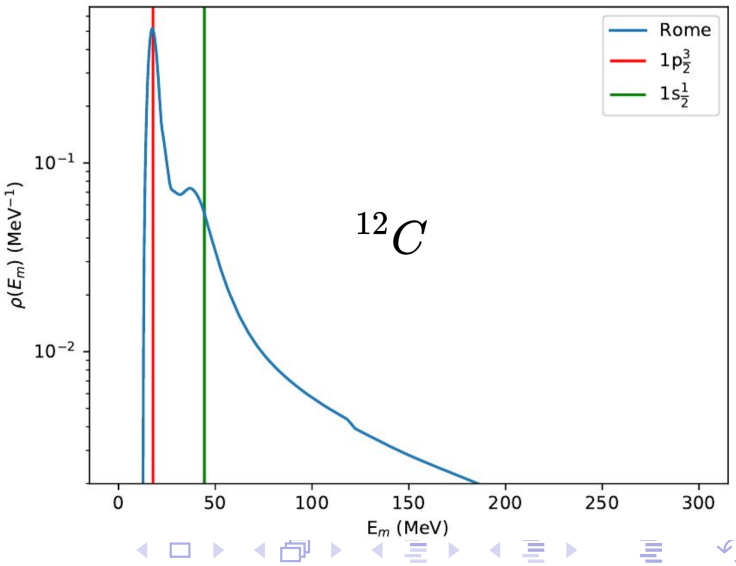

Scattered nucleon description: RPWIA and RDWIA

Regarding the scattered nucleon, we consider different models:

- Relativistic plane-wave impulse approximation (RPWIA): The ejected nucleon is considered a plane-wave (no FSI).

Scattered nucleon description: RPWIA and RDWIA

Regarding the scattered nucleon, we consider different models:

- Relativistic plane-wave impulse approximation (RPWIA): The ejected nucleon is considered a plane-wave (no FSI).
- Energy-dependent relativistic mean field (ED-RMF): W.F. solution of the Dirac Eq. in the continuum using the same RMF potential that describes the initial state times a phenomenological function that weakens the potentials at high energies.

$$f_b\left(T_N\right) = \frac{0.85}{\left(T_N/200\right)^2+3.5} + \frac{0.48}{exp((T_N-90)/23)+1} + 0.29$$

T_N = Proton kinetic energy in MeV

For small T_N the ED-RMF potential agrees with RMF. For larger values of T_N, the blending function reduces the magnitude of the strong RMF potential

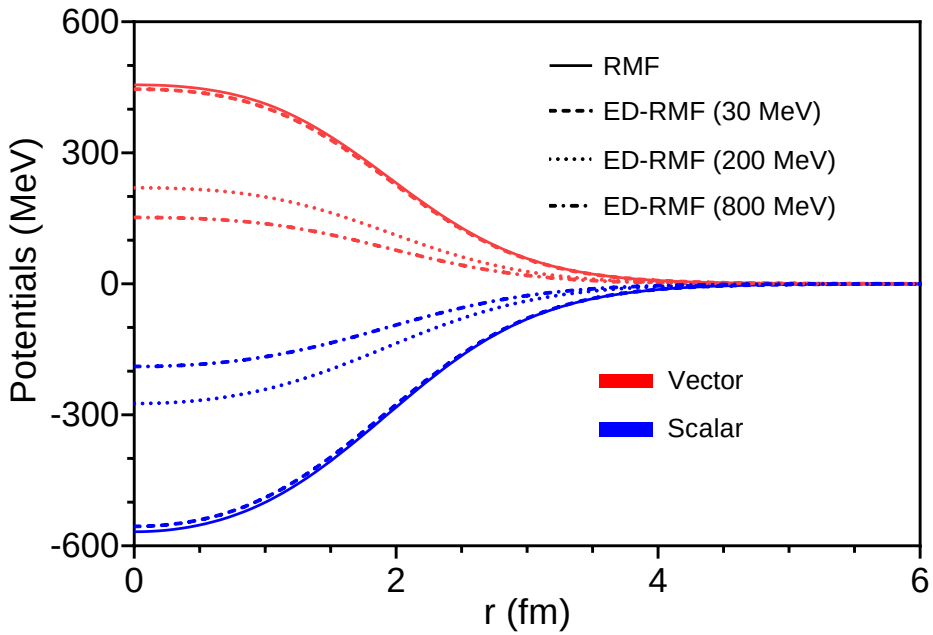

Scattered nucleon description:RPWIA and RDWIA

Regarding the scattered nucleon, we consider different models:

- Relativistic plane-wave impulse approximation (RPWIA): The ejected nucleon is considered a plane-wave (no FSI).
- Energy-dependent relativistic mean field (ED-RMF): W.F. solution of the Dirac Eq. in the continuum using the same RMF potential that describes the initial state times a phenomenological function that weakens the potentials at high energies.
- Relativistic optical potential (ROP): The scattered nucleon travels under the influence of a phenomenological relativistic optical potential fitted to elastic proton-nucleus scattering data.

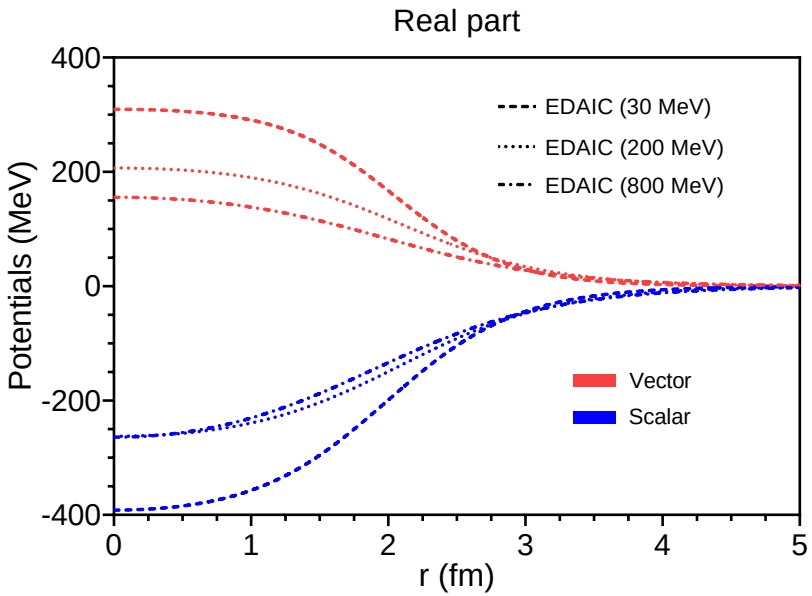

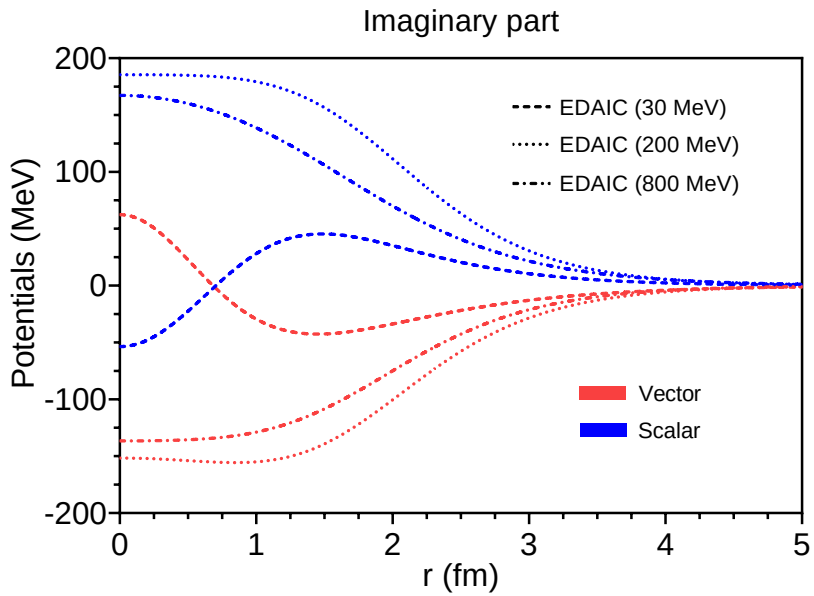

Scattered nucleon description:RPWIA and RDWIA

Regarding the scattered nucleon, we consider different models:

- Relativistic plane-wave impulse approximation (RPWIA): The ejected nucleon is considered a plane-wave (no FSI).
- Energy-dependent relativistic mean field (ED-RMF): W.F. solution of the Dirac Eq. in the continuum using the same RMF potential that describes the initial state times a phenomenological function that weakens the potentials at high energies.
- Relativistic optical potential (ROP): The scattered nucleon travels under the influence of a phenomenological relativistic optical potential fitted to elastic proton-nucleus scattering data.

$$\Psi_{s_N}(\mathbf{r},\mathbf{p_N}) = 4\pi\sqrt{\frac{E_N+m_N}{2E_N}}\sum_{\kappa,m_l,m_j} e^{-i\delta^*_\kappa} i^l \langle l\, m_l\, 1/2\, s_N | j\, m_j\rangle\, Y^*_{l\,m_l}(\Omega_N)\,\psi^{m_j}_\kappa(\mathbf{r},\mathbf{p_N})$$

$$\Psi^{m_j}_\kappa(\mathbf{r}) = \begin{pmatrix} g_\kappa(r)\Phi^{m_j}_\kappa(\hat{\mathbf{r}}) \\ i f_\kappa(r)\Phi^{m_j}_{-\kappa}(\hat{\mathbf{r}}) \end{pmatrix}$$

$$\frac{df_\kappa}{dr} = \frac{\kappa-1}{r} f_\kappa - [E_N - m_N - S(r) - V(r)]\, g_\kappa$$
$$\frac{dg_\kappa}{dr} = -\frac{\kappa+1}{r} g_\kappa + [E_N + m_N + S(r) - V(r)]\, f_\kappa.$$

RDWIA and $(e, e'p)$ data

RDWIA using the RMF model for the initial nuclear state has been compared successfully in the past with exclusive electron measurements from Saclay, NIKHEF, MAMI and JLab

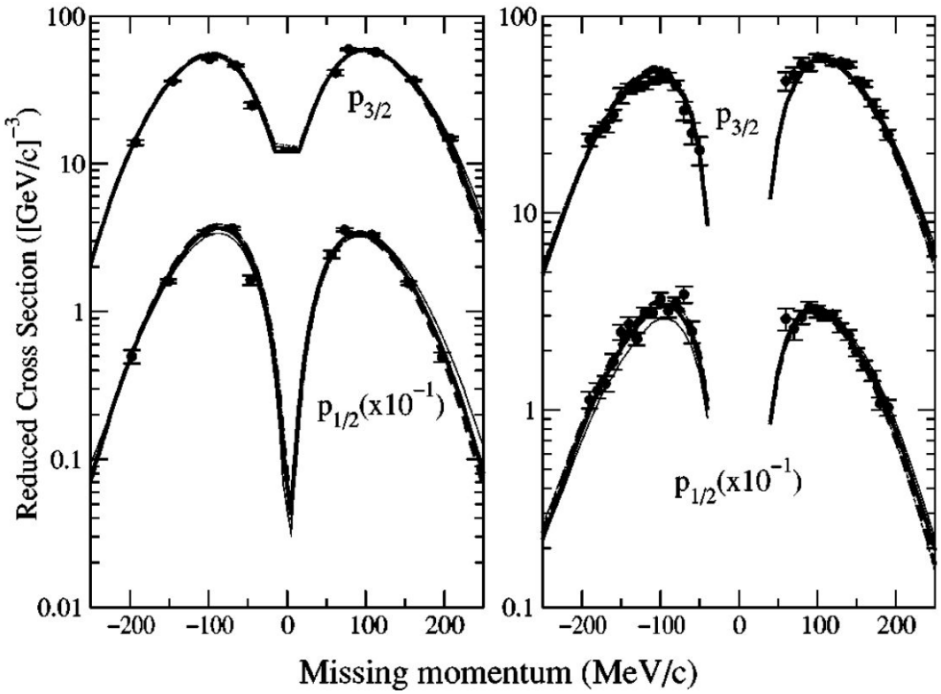

J.M. Udias *et. al.* PRC 64 024614 (2001)

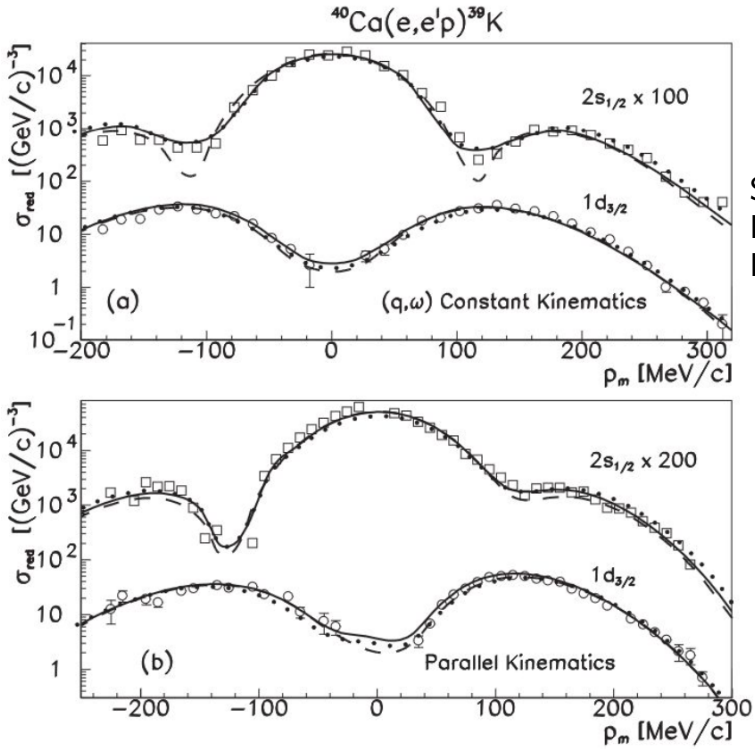

Solid: WS
Dotted: HF
Dashed: RMF

C. Giusti *et. al.* PRC 84 024615 (2011)

RDWIA: correct shape but spectroscopic factors are still needed

Contents

SuSAv2-MEC implementation in GENIE

The SuSAv2 model (PRC 90 035501 (2014) and PRD 94 013012 (2016) for details) is an inclusive model based on the SuperScaling approach and RMF results used to describe electron and neutrino inclusive data at intermediate and high momentum transfer ($q > 300$ MeV)

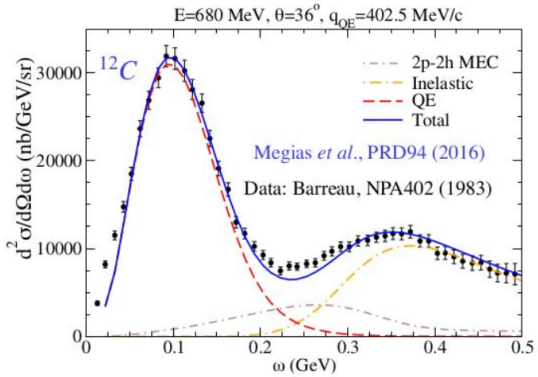

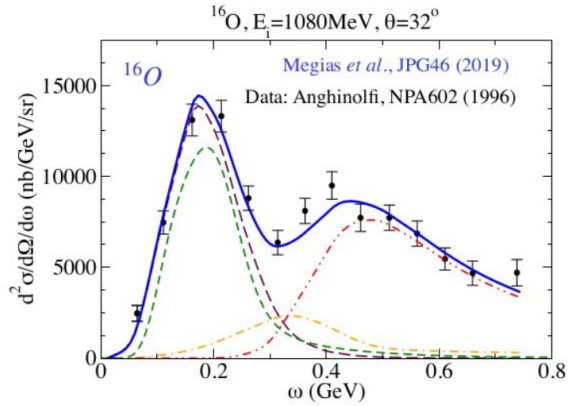

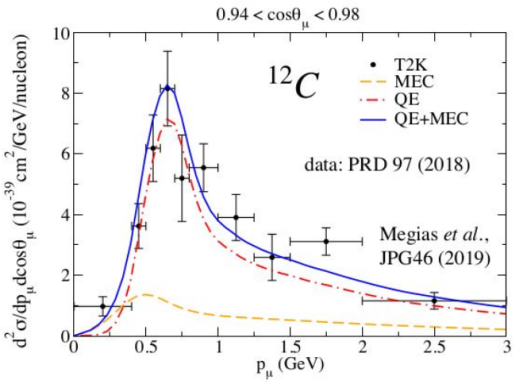

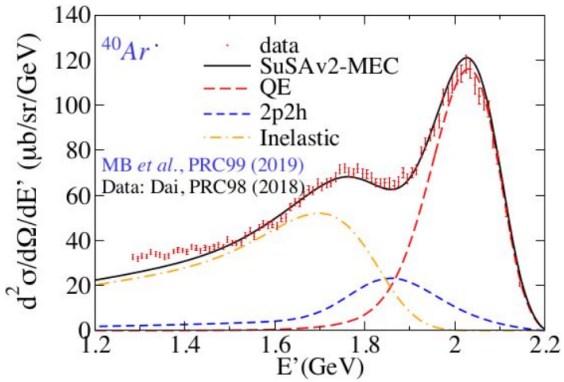

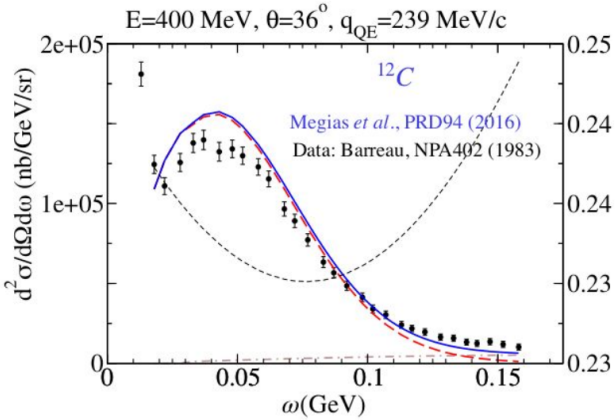

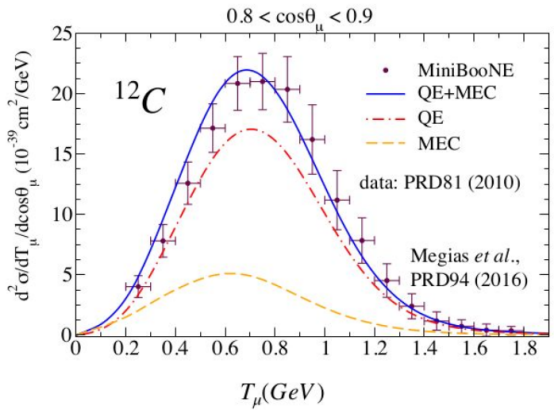

SuSAv2-MEC implementation in GENIE

SuSAv2 QE and 2p2h models were implemented in GENIE neutrino generator for (e,e') and CC ν_μ

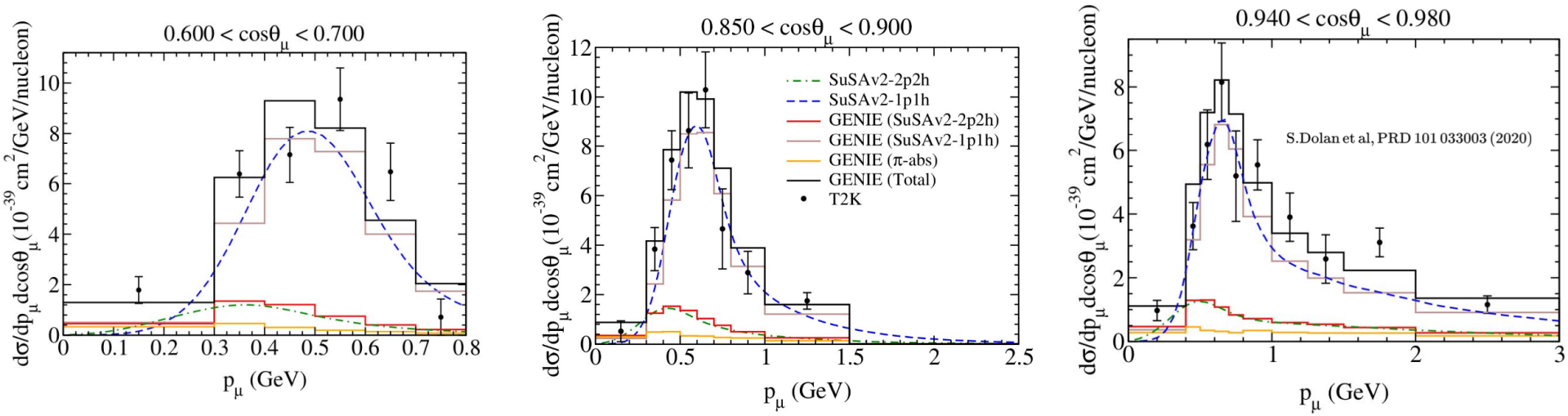

The implementation was tested against the original calculation and the agreement was found to be very good all for all the kinematics

Assuming a factorization of the leptons and hadrons kinematics, the SuSAv2-1p1h (2p2h) model implemented in GENIE can generate semi-inclusive results by independently sampling from a local (global) Fermi gas the momentum of the initial nucleon.

Contents

Cross sections vs proton kinematics:T2K and MINERνA

T2K

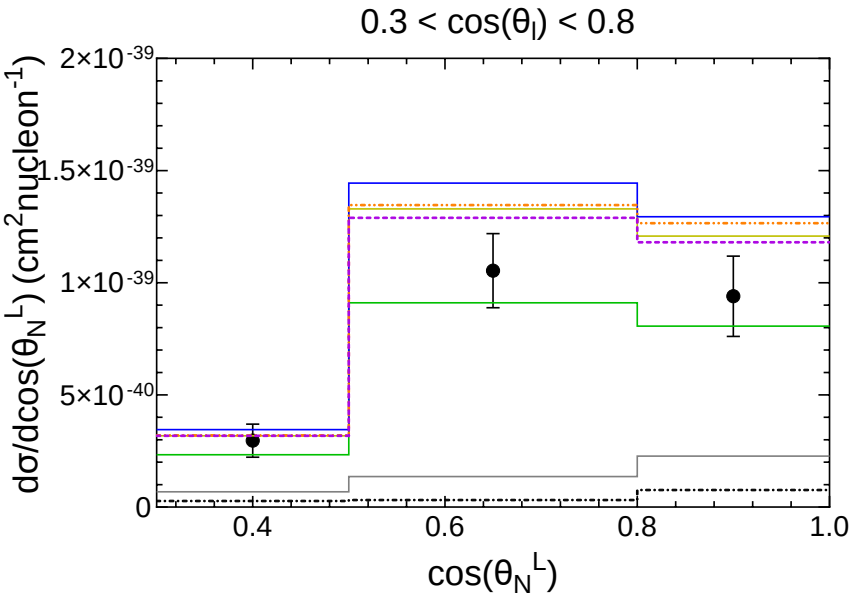

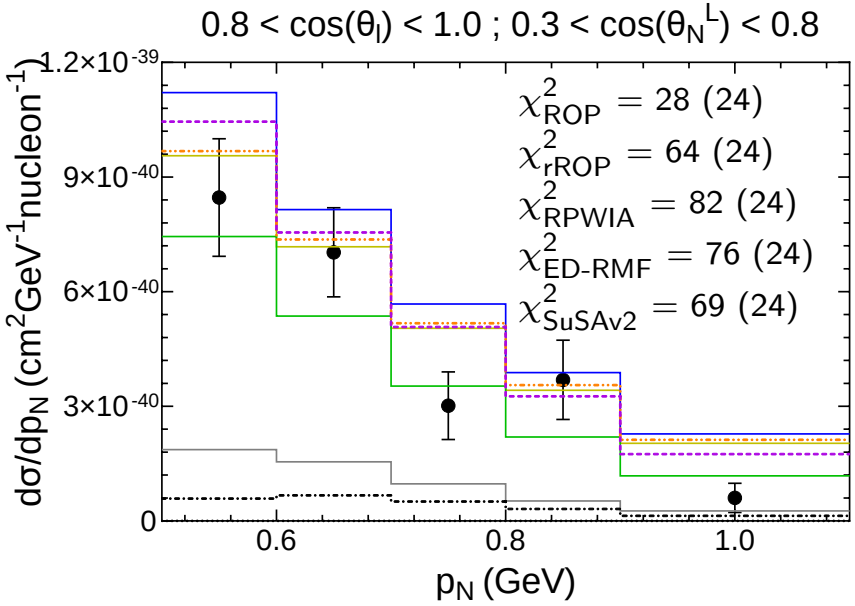

MINERνA

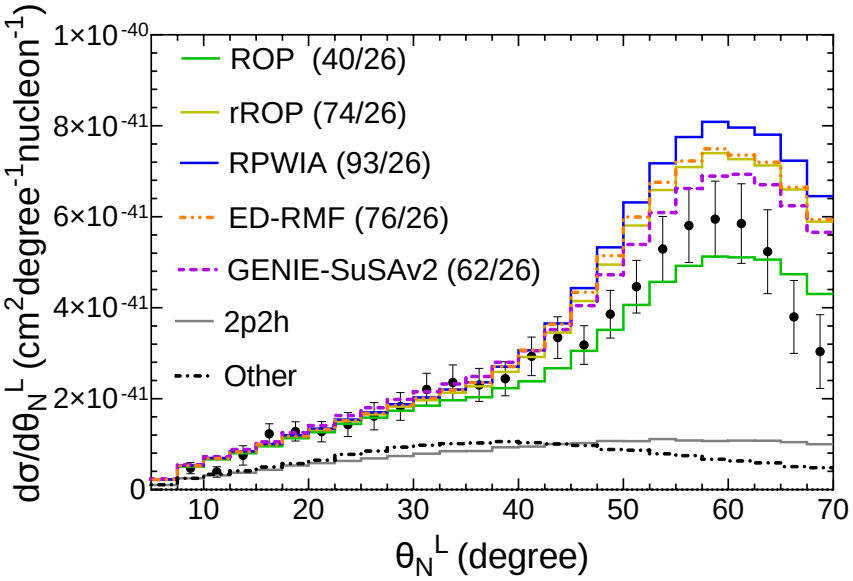

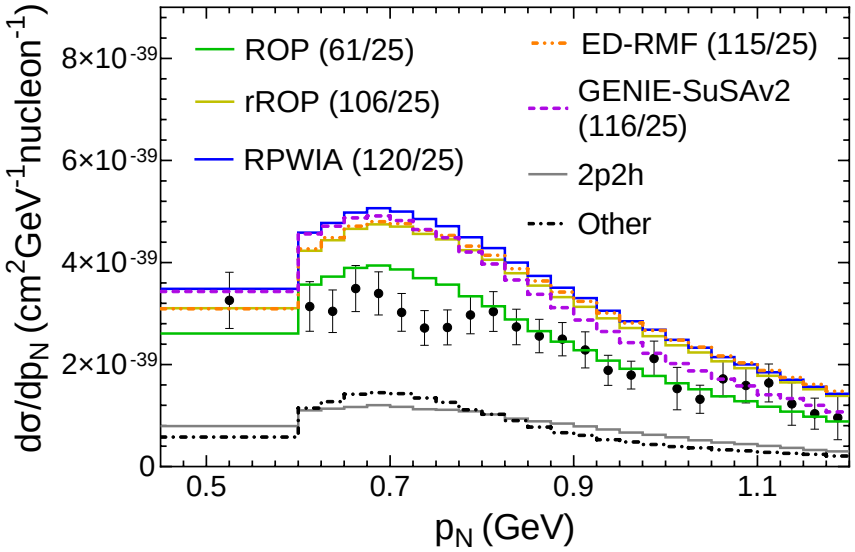

Cross sections vs transverse kinematic imbalances

$$\delta p_T = \left| \mathbf{k'_T} + \mathbf{p^N_T} \right| \longrightarrow \text{Peaked distribution at zero}$$

$$\delta\alpha_T = \arccos\left(\frac{-\mathbf{k'_T} \cdot \delta\mathbf{p_T}}{k'_T \delta p_T} \right) \longrightarrow \text{Undefined, flat distribution}$$

$$\delta\phi_T = \arccos\left(\frac{-\mathbf{k'_T} \cdot \delta\mathbf{p^N_T}}{k'_T p^N_T} \right) \longrightarrow \text{Peaked distribution at zero}$$

- T2K
- MINERνA

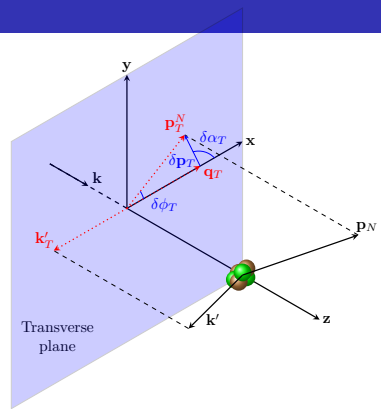

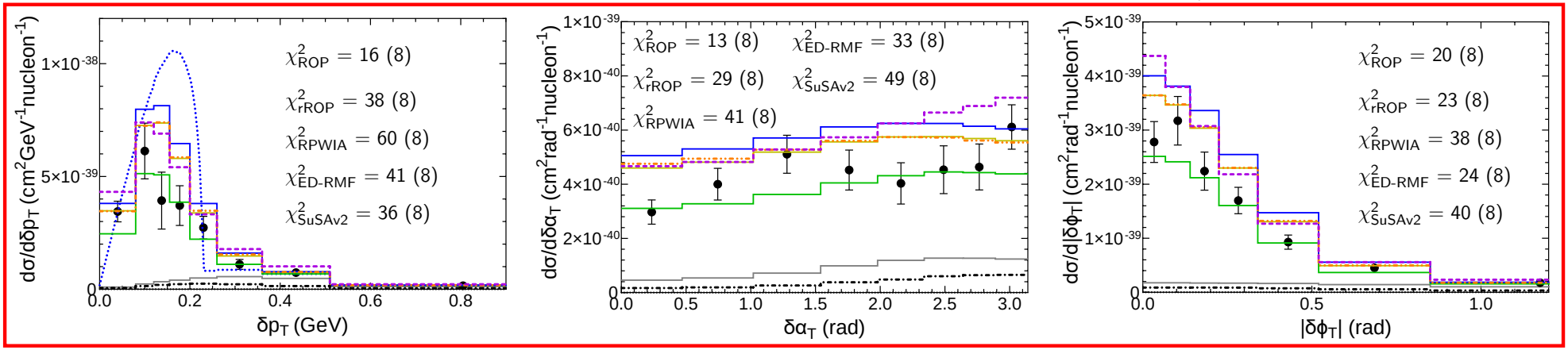

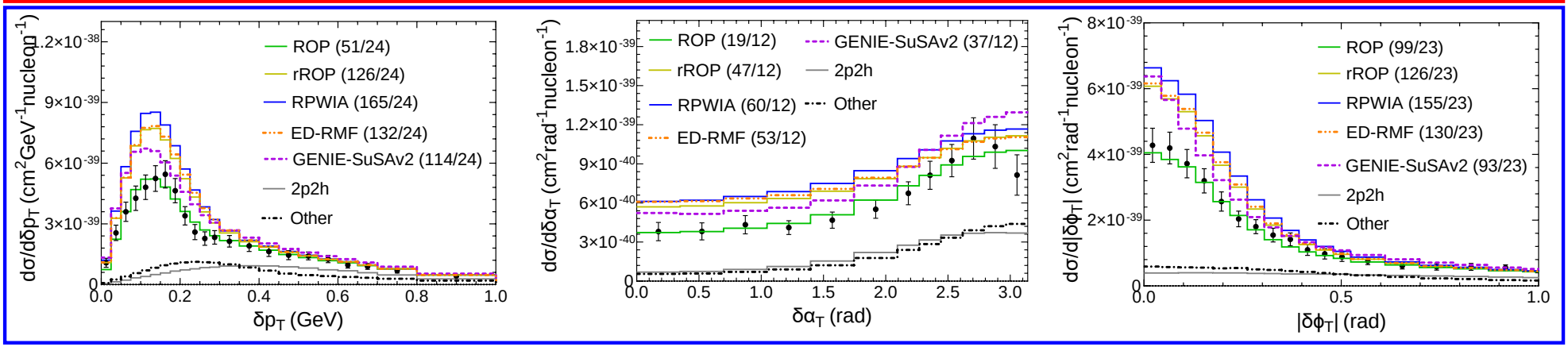

Cross sections vs TKI: MINERνA projections

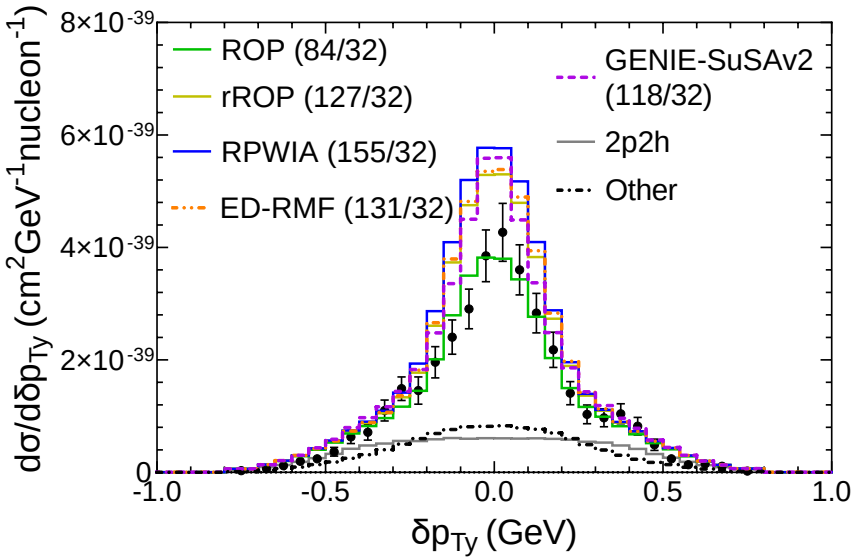

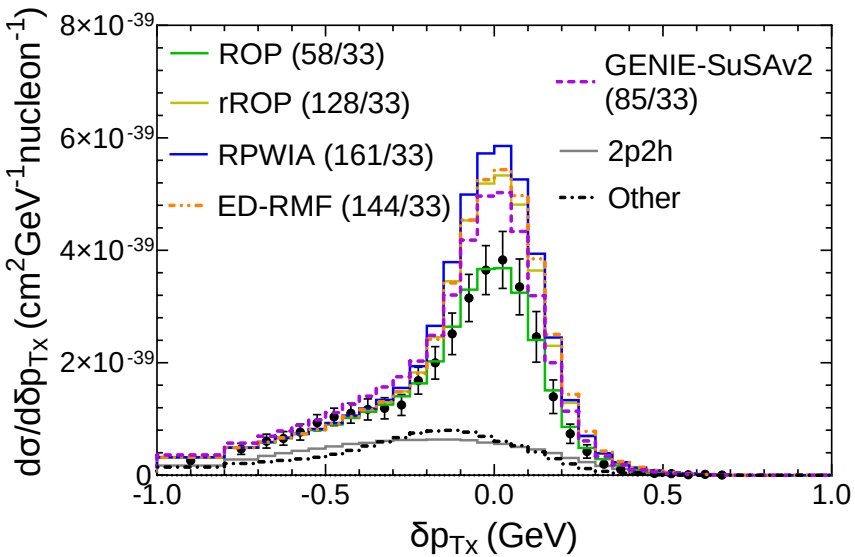

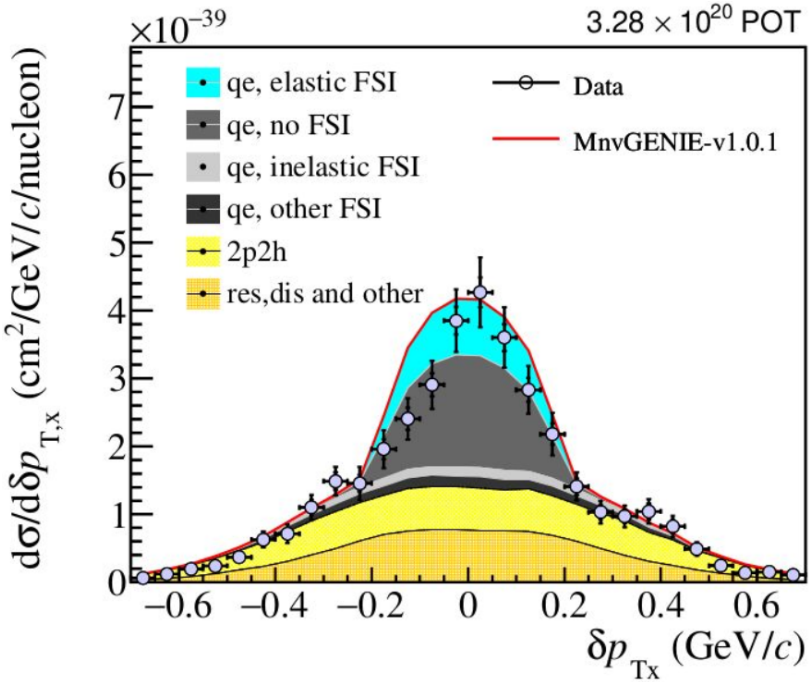

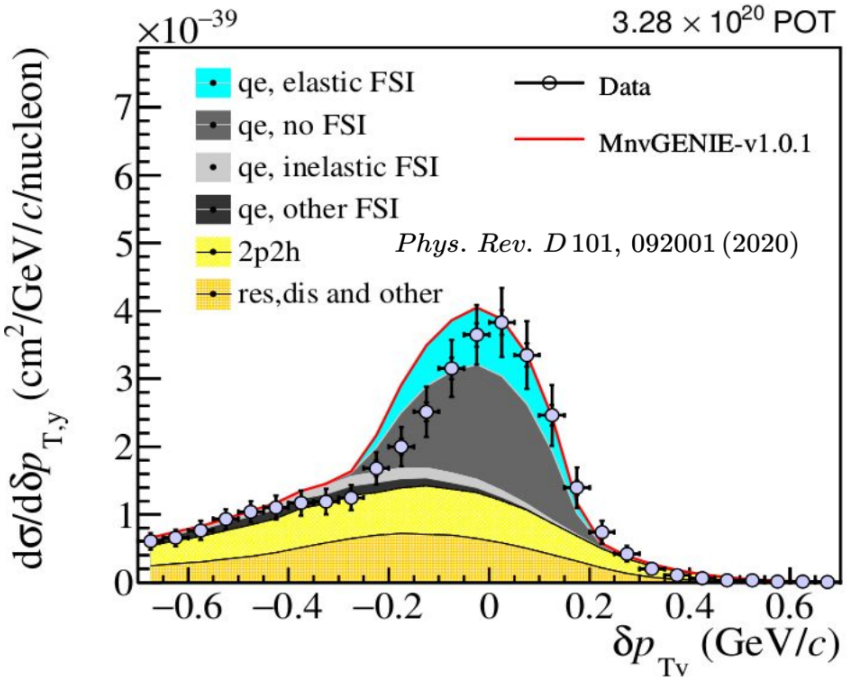

Proposal of realistic SF model for neutrons in ^{40}Ar

α	E_κ (MeV)	σ_κ (MeV)	S_κ
$1s_{1/2}$	55 ± 6	30 ± 15	0.9 ± 0.15
$1p_{3/2}$	39 ± 4	12 ± 6	0.9 ± 0.15
$1p_{1/2}$	34 ± 3	12 ± 6	0.9 ± 0.15
$1d_{5/2}$	23 ± 2	5 ± 3	0.75 ± 0.15
$2s_{1/2}$	16.1 ± 1.6	5 ± 3	0.75 ± 0.15
$1d_{3/2}$	16.0 ± 1.6	5 ± 3	0.75 ± 0.15
$1f_{7/2}$	9.869 ± 0.005	5 ± 3	0.75 ± 0.15

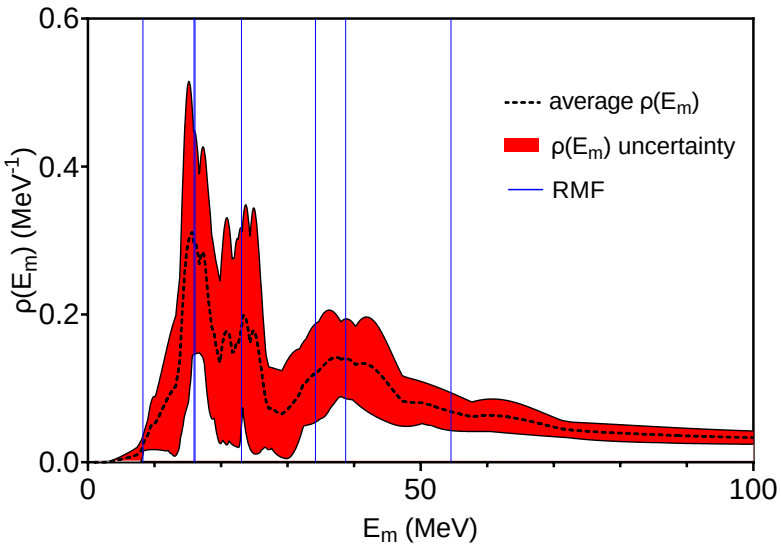

- RMF values
- Exp. neutron separation energy
- Inspired by ^{40}Ar(e,e'p)^{39}Cl measurements by JLab
- Phenomenological spec. factors
- An additional $s_{1/2}$ shell models the background (correlated part of the SF)

The RDWIA results for ^{40}Ar include a band related with the uncertainties of the parameterization of missing energy profile

J.M. Franco-Patino *et. al.*
PRD 109, 013004 (2024)

MicroBooNE $1\mu CC0\pi Np$: muon and proton kinematics

$1\mu CC0\pi Np$	k' (GeV)	$\cos\theta_l$	p_N (GeV)
	> 0.1	-	0.3-1.2

Uncert. band: 5%

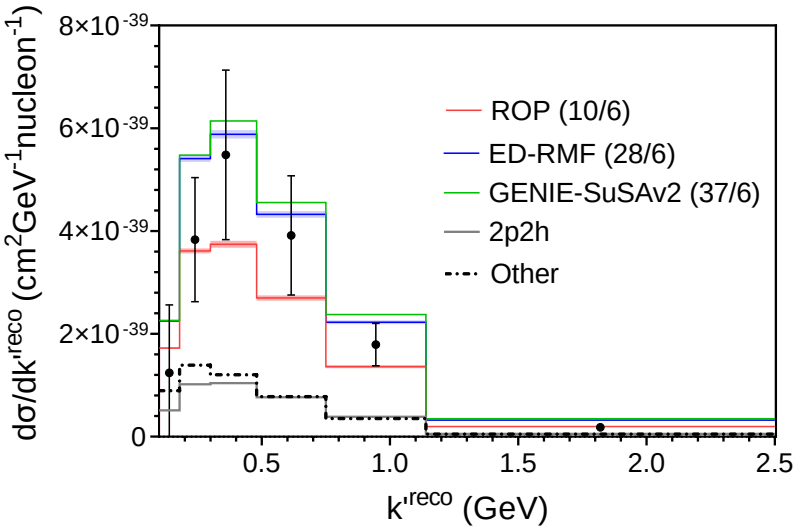

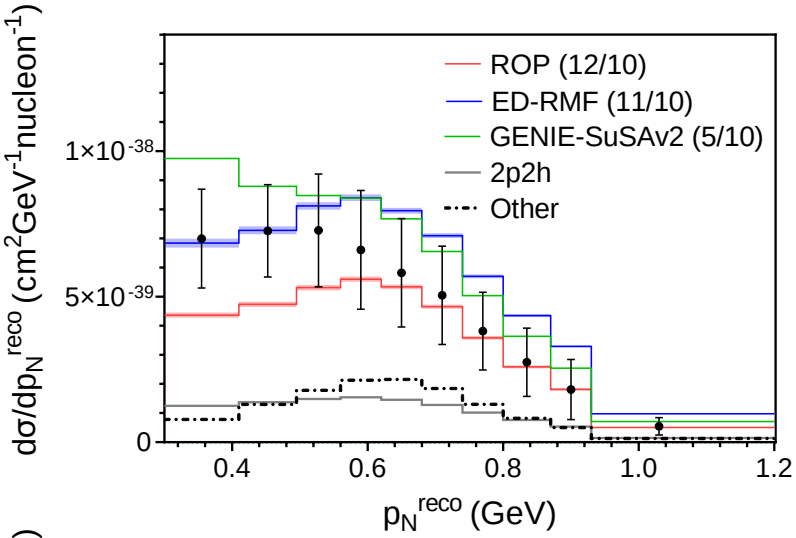

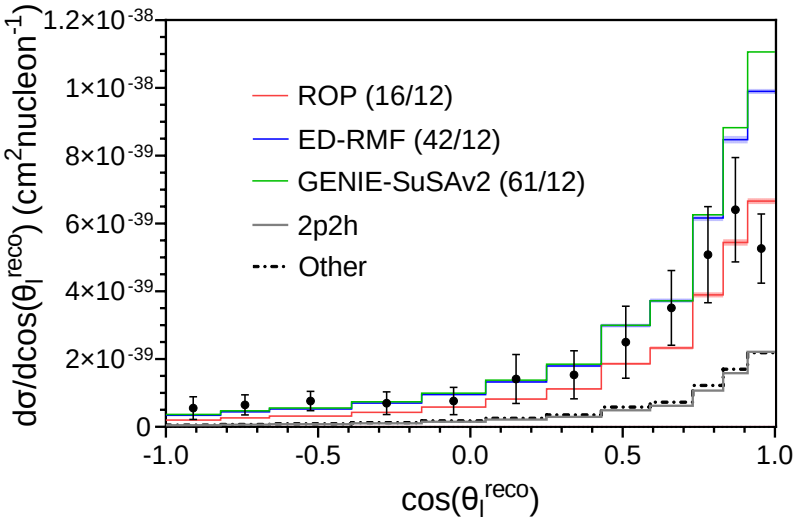

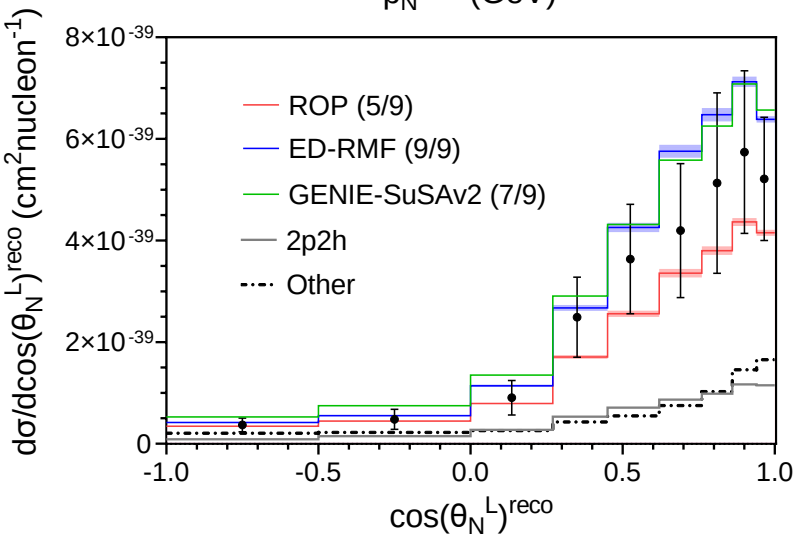

MicroBooNE $1\mu CC0\pi 1p$: proton kinematics

$1\mu CC0\pi 1p$	k' (GeV)	$\cos\theta_l$	p_N (GeV)	$\cos\theta_N^L$	ϕ_N^L (°)	$\theta_{\mu p}$ (°)	δp_T (GeV)
	0.1-1.5	-0.65-0.95	0.3-1.0	> 0.15	145-215	35-145	< 0.35

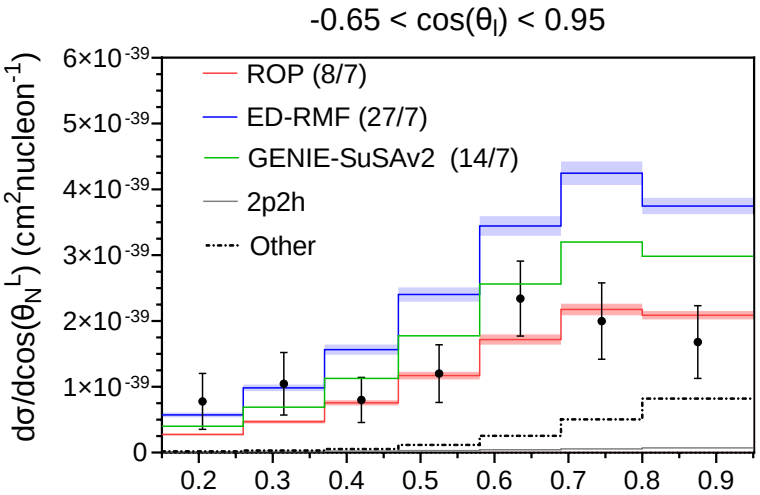

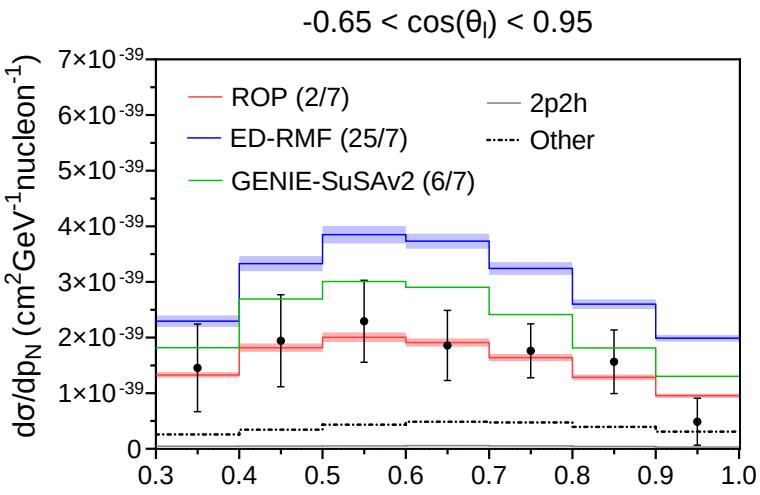

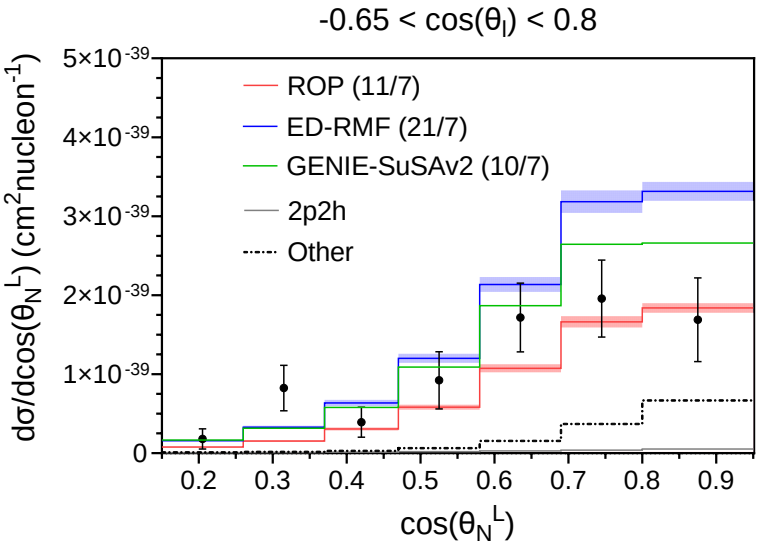

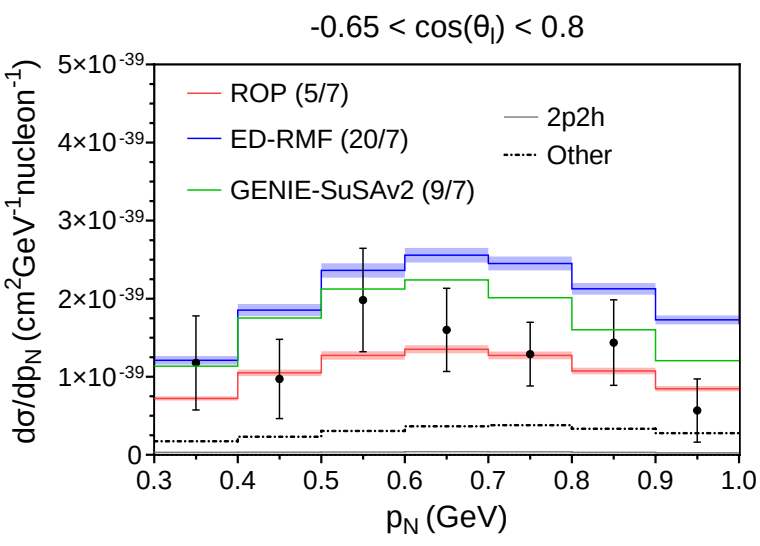

MicroBooNE 1μCC0π1p: Latest TKI measurements

RDWIA comparison with latest semi-inclusive measurements by MicroBooNE vs transverse kinematic imbalances (PRD 108, 053002 (2023))

J.M. Franco-Patino *et. al.* **In preparation**

1μCC0π1p	k' (GeV)	$\cos\theta_l$	p_N (GeV)
	0.1 – 1.2	-	0.3-1.0

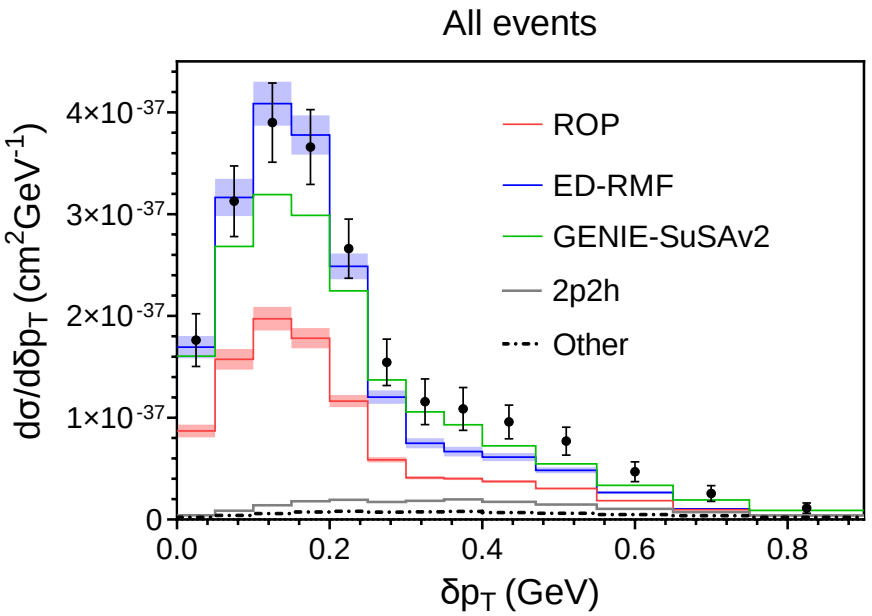

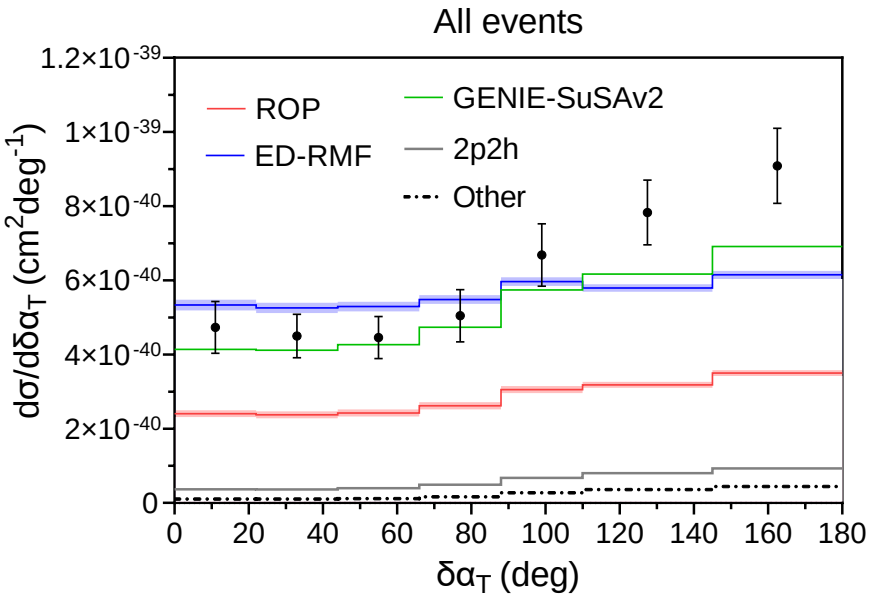

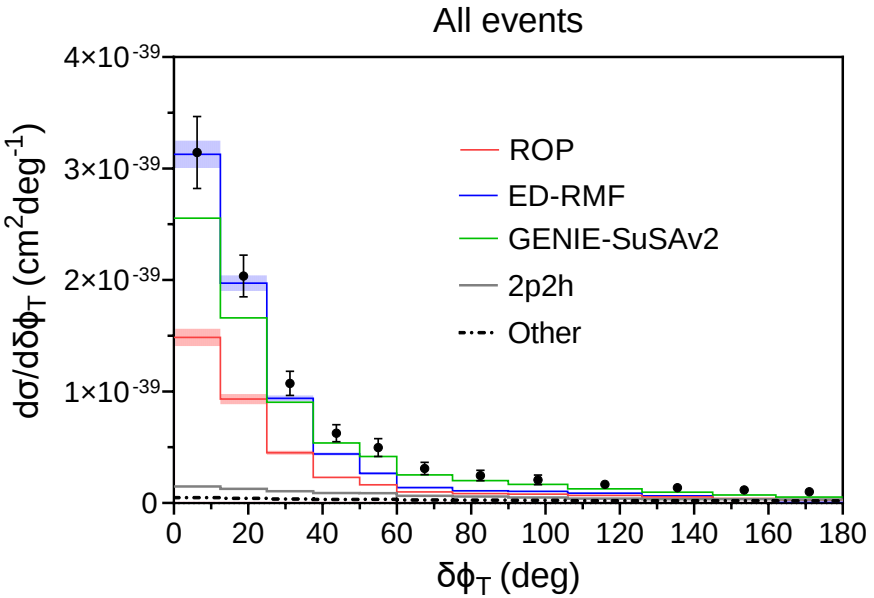

Contents

Summary

- Experimental and theoretical efforts to measure and describe semi-inclusive cross sections to help constrain nuclear models for oscillation experiments.
- The RMF and ROP models have been successfully applied in the past to the study of inclusive and exclusive electron scattering. The same analysis has now been extended to neutrino scattering.
- We have described several ways to include FSI in our theoretical model which improves in general the agreement with experimental data. Variables that measure correlations between both particles in the final state allow us to discriminate between nuclear models and separate contributions from different channels.
- The microscopic calculation based on RMF theory improves the agreement with exp. measurements at low momentum and energy transfer kinematics where factorization and SuSAv2 model fail.

Thanks for your attention!

Backup slides

JLAB ^{40}Ar(e,e') $E_i = 2.222$ GeV, $\theta_e = 15.541°$

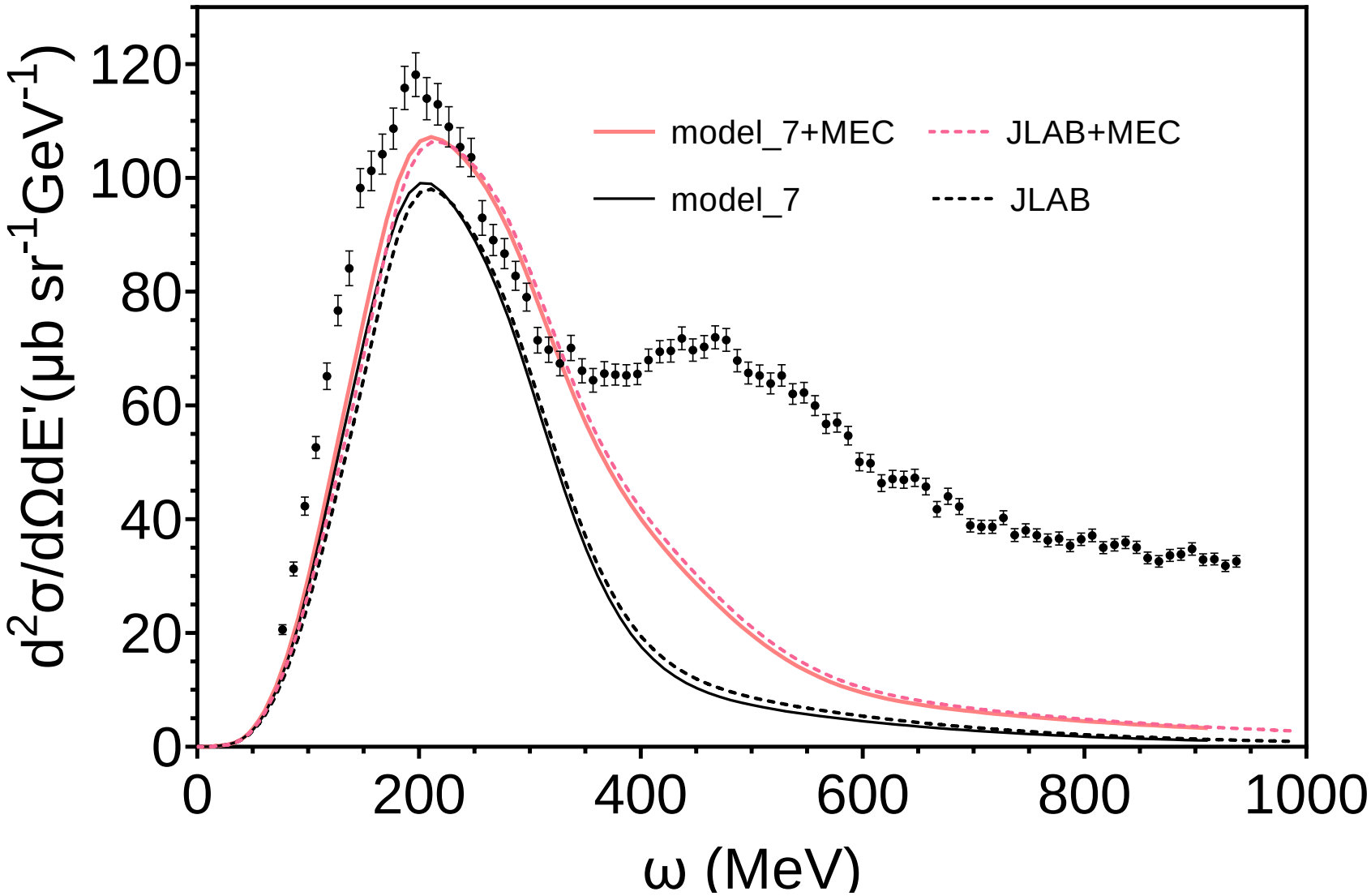

MicroBooNE 1eCC0πNp: electron and proton kinematics

1eCC0πNp	k' (GeV)	$\cos\theta_l$	p_N (GeV)
	> 0.0305	-	> 0.3105

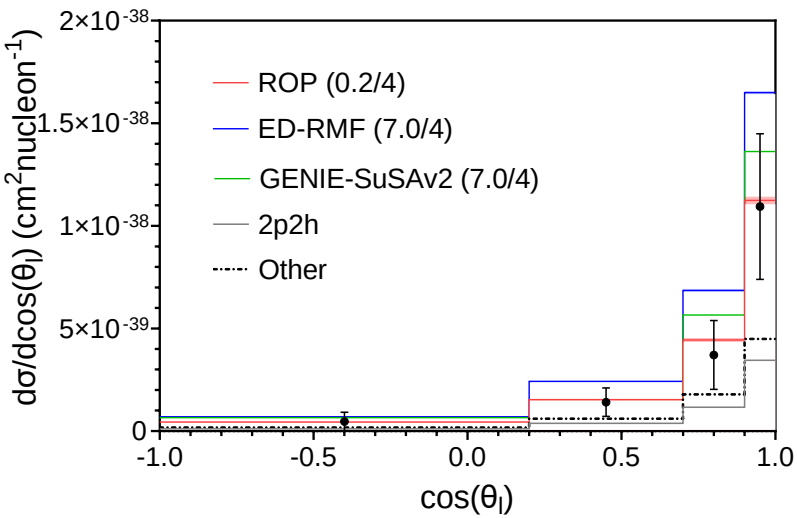

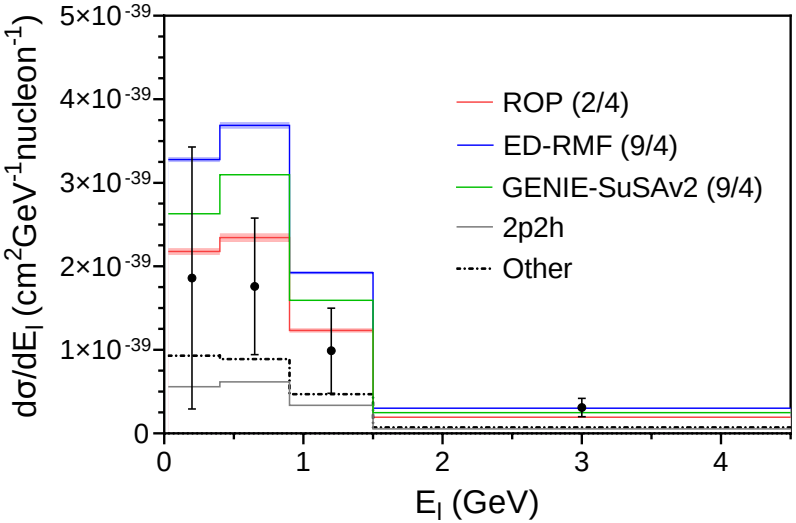

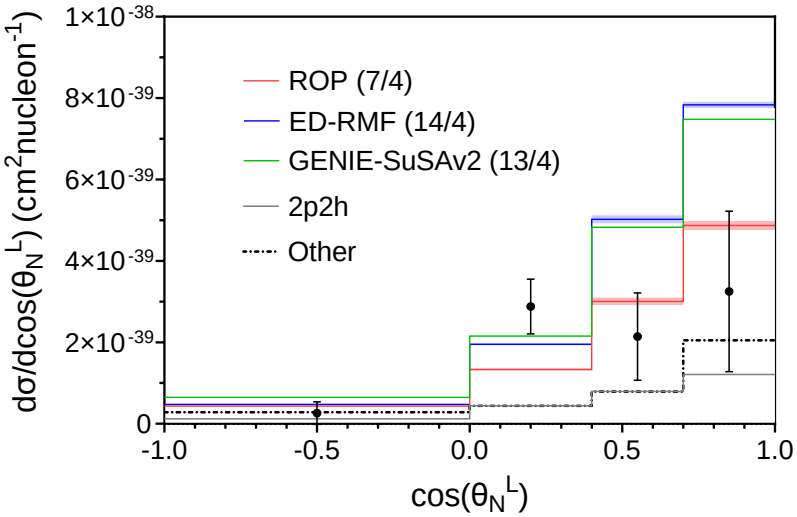

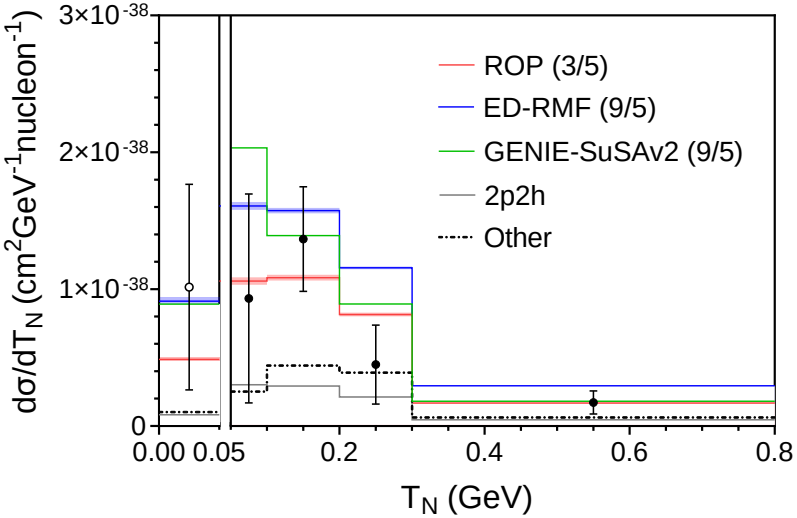

^{12}C and ^{16}O Benhar SF

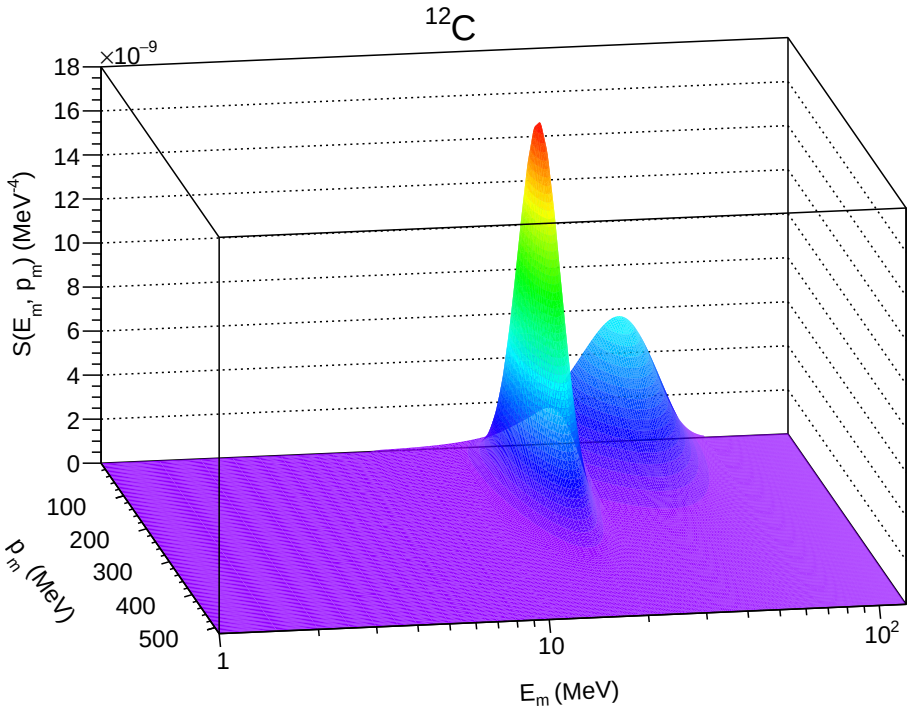

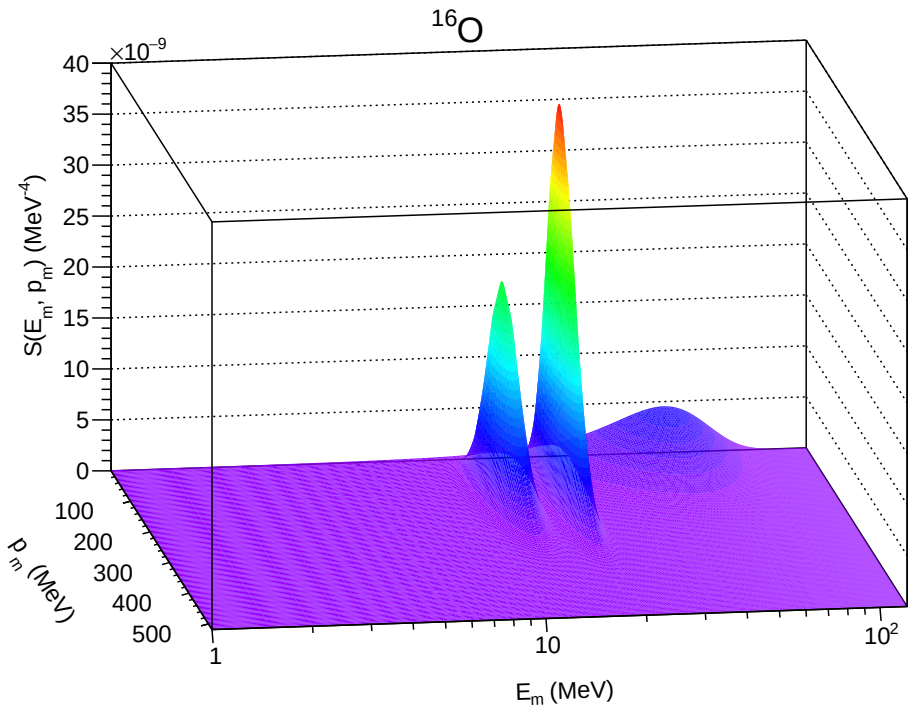

3-D plot of the carbon (left) and oxygen (right) spectral functions calculated using the Rome approach, i.e. the single-particle contribution extracted from the analysis of $(e, e'p)$ experimental data and using the LDA for the correlated part.

Momentum distributions of different ^{12}C nuclear models

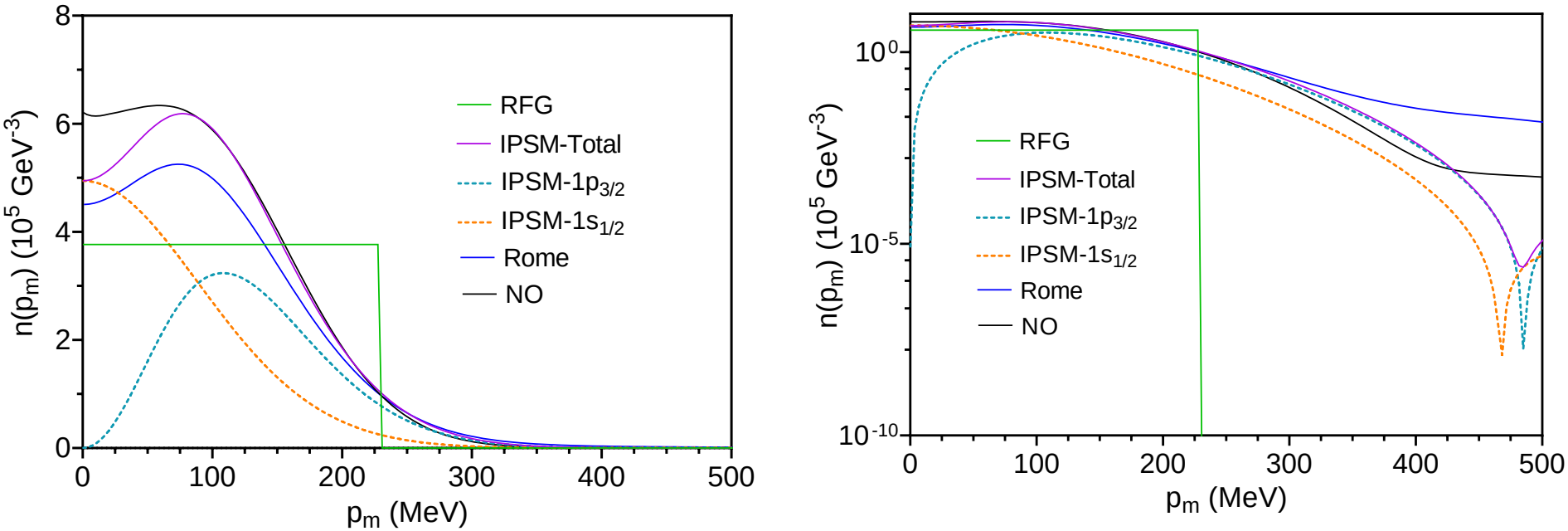

Momentum distribution $n(p_m)$ calculated by integrating the spectral function of different nuclear models of ^{12}C. The value of the Fermi momentum for ^{12}C is $k_F = 0.228$ GeV and the individual shells that are included in the IPSM are shown separately. The distributions are shown in linear (left) and semi-logarithmic (right) scales to expose the differences between the models in the low- and high-missing momentum zones.

Semi-inclusive ^{40}Ar DUNE cross sections: RFG

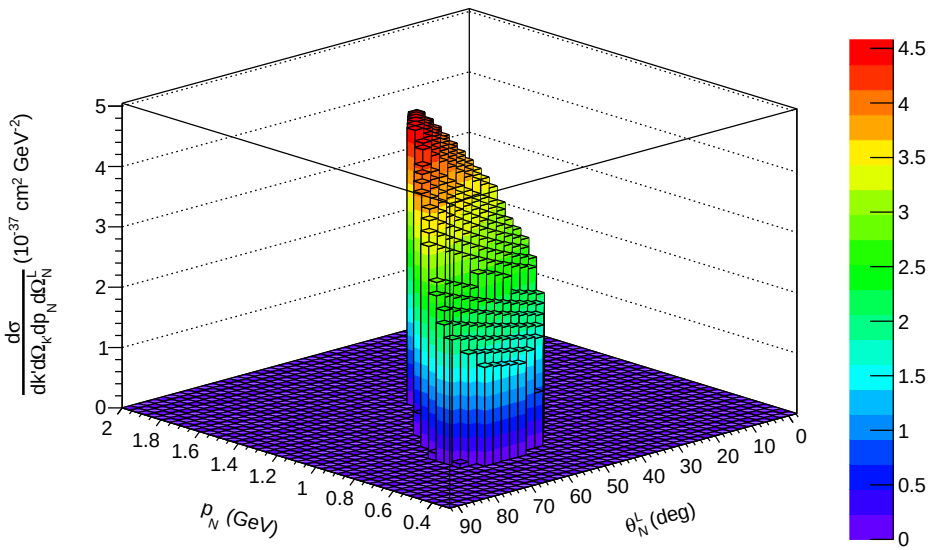

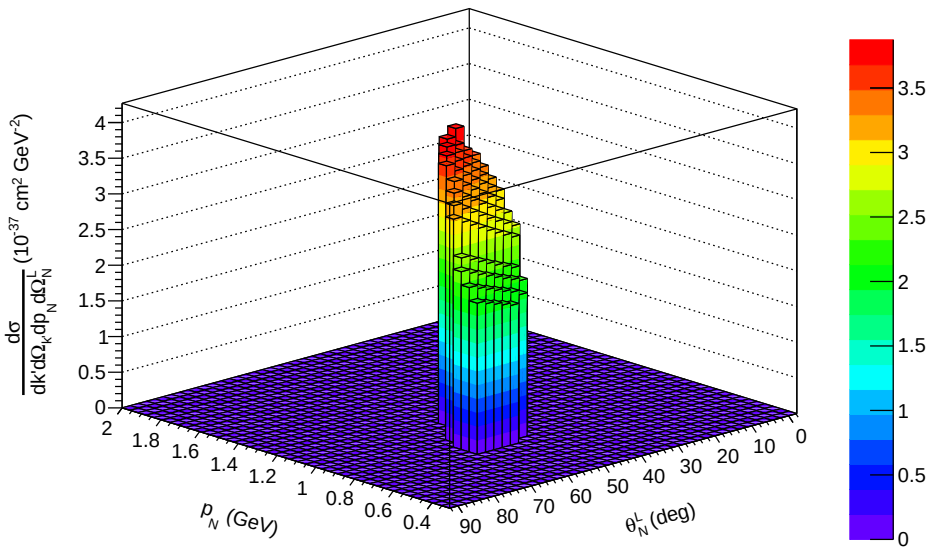

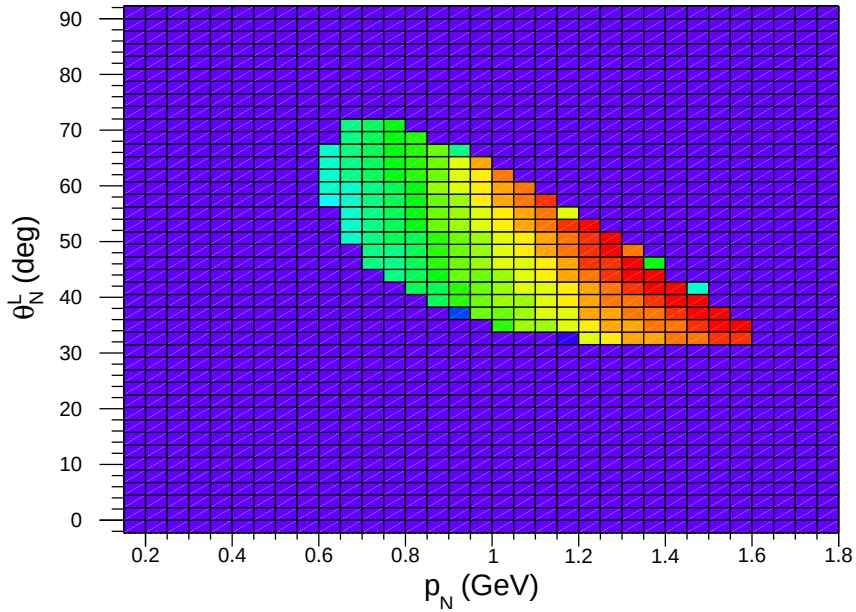

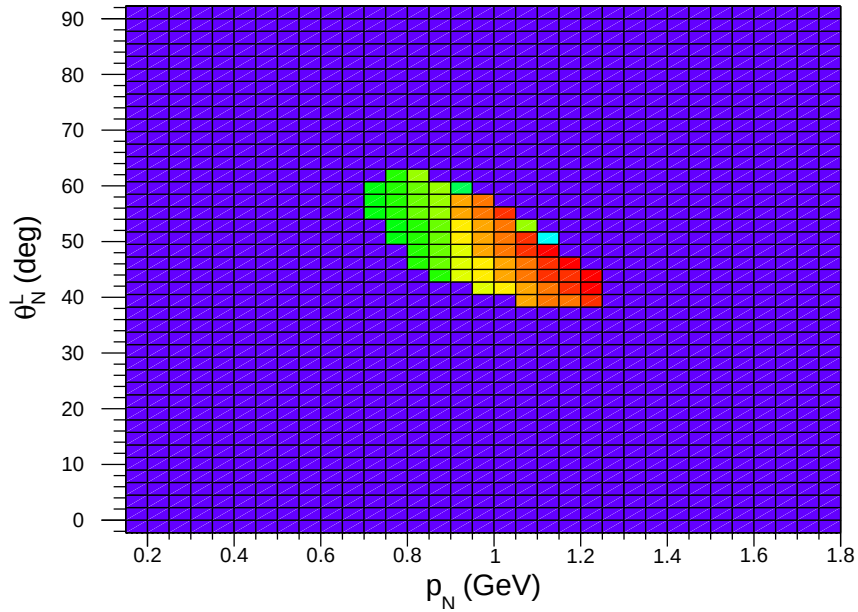

Semi-inclusive ^{40}Ar DUNE cross sections: RMF

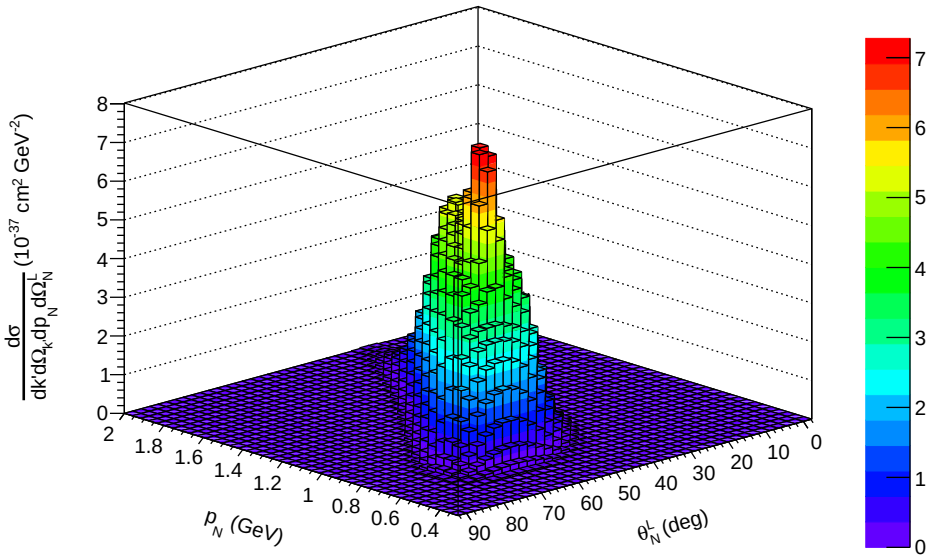

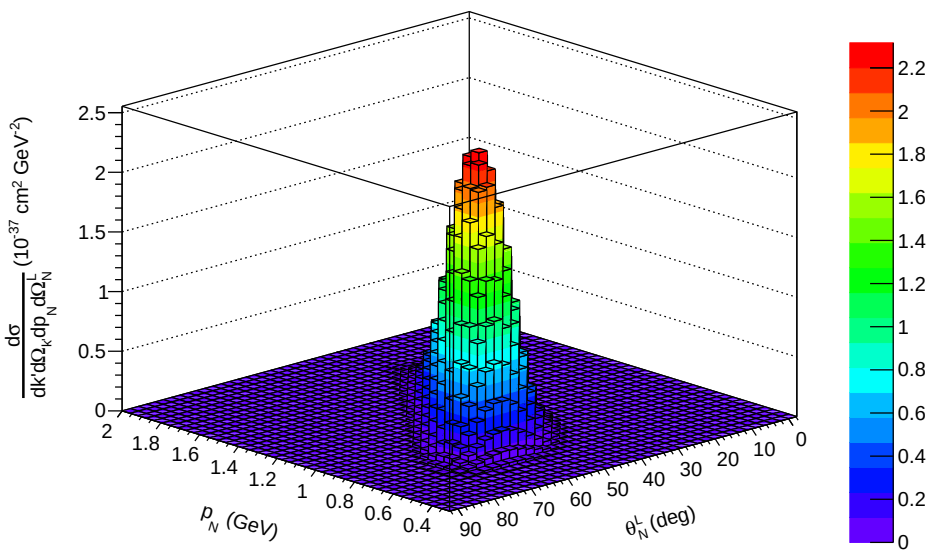

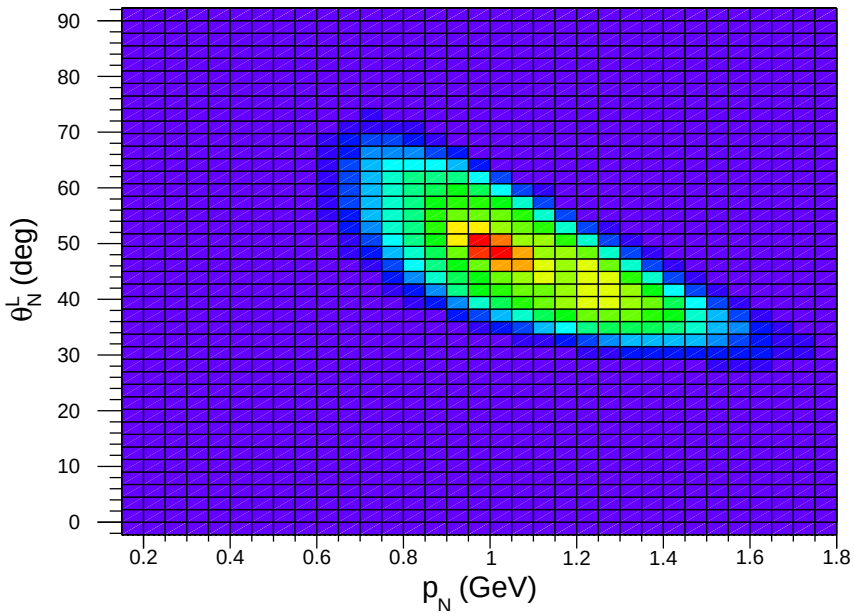

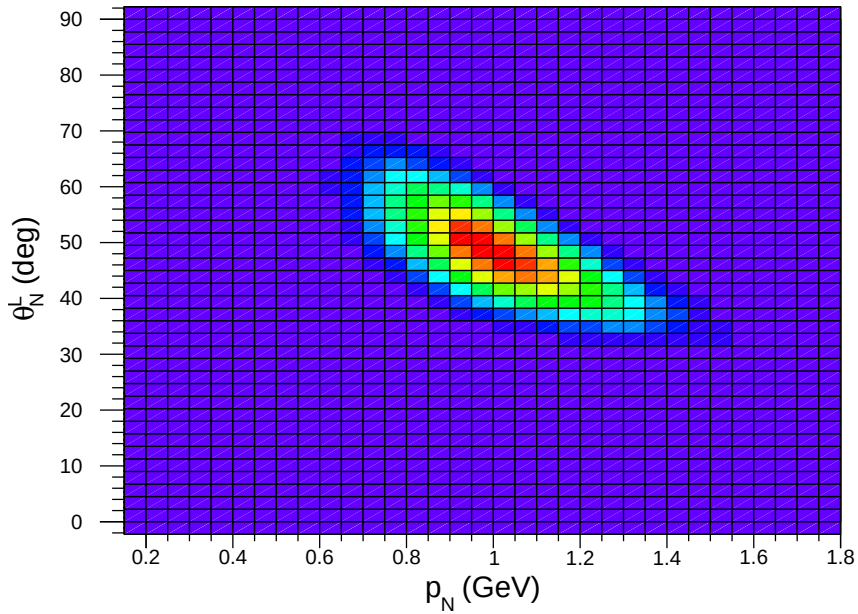

Semi-inclusive ^{12}C T2K cross sections: $\phi_N^L = 180^\circ$ RFG and RMF

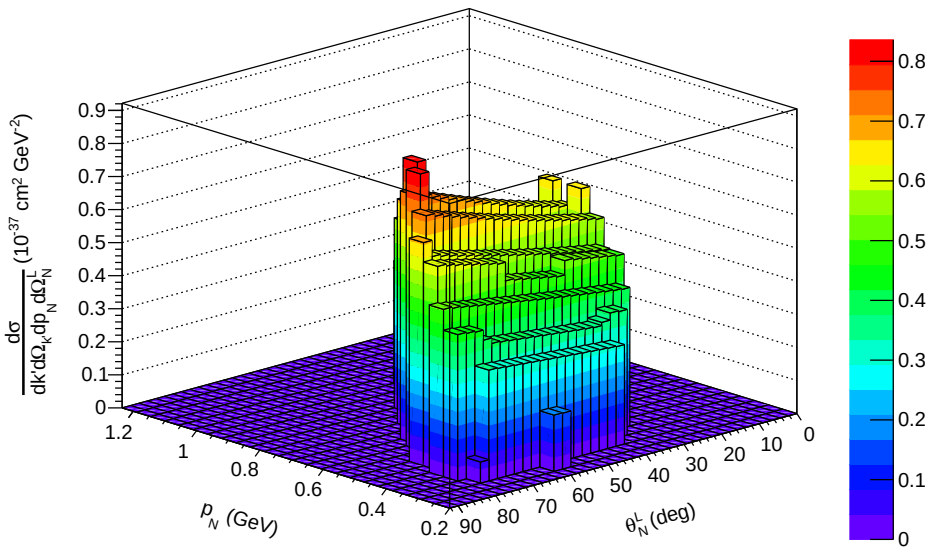

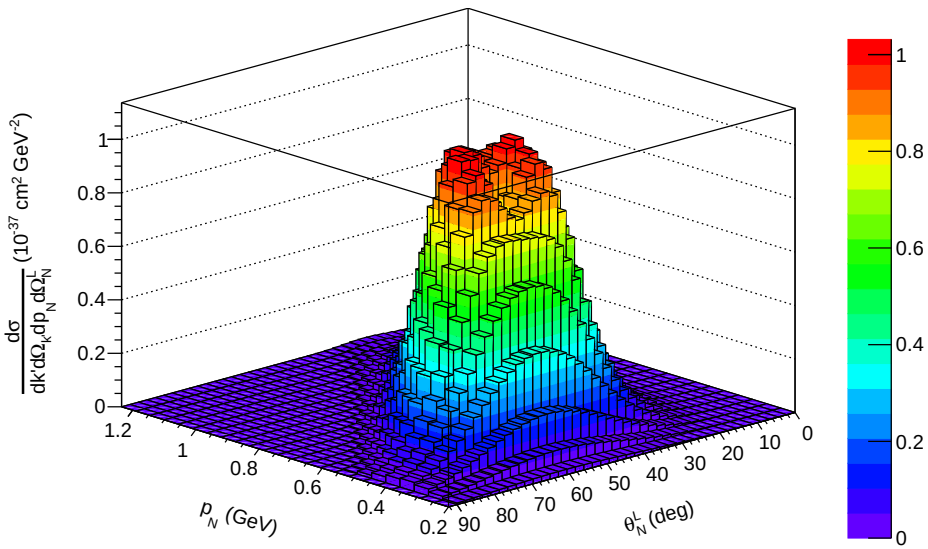

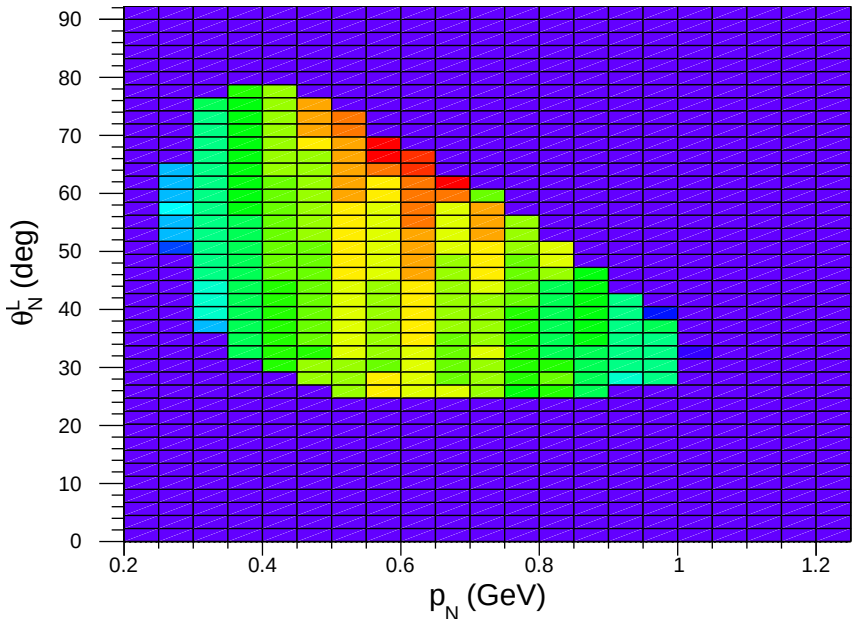

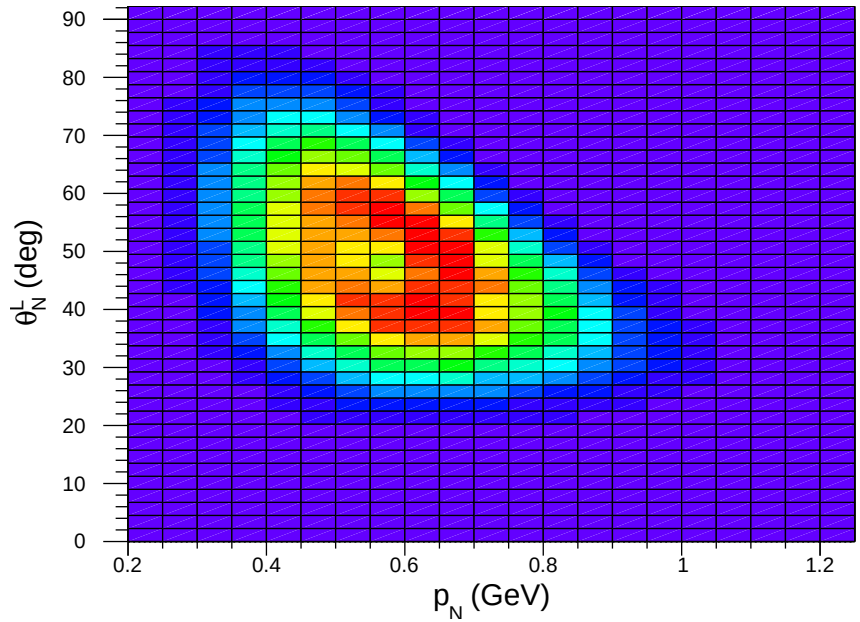

Semi-inclusive ^{12}C T2K cross sections: $\phi_N^L = 180^\circ$ NO and RMF

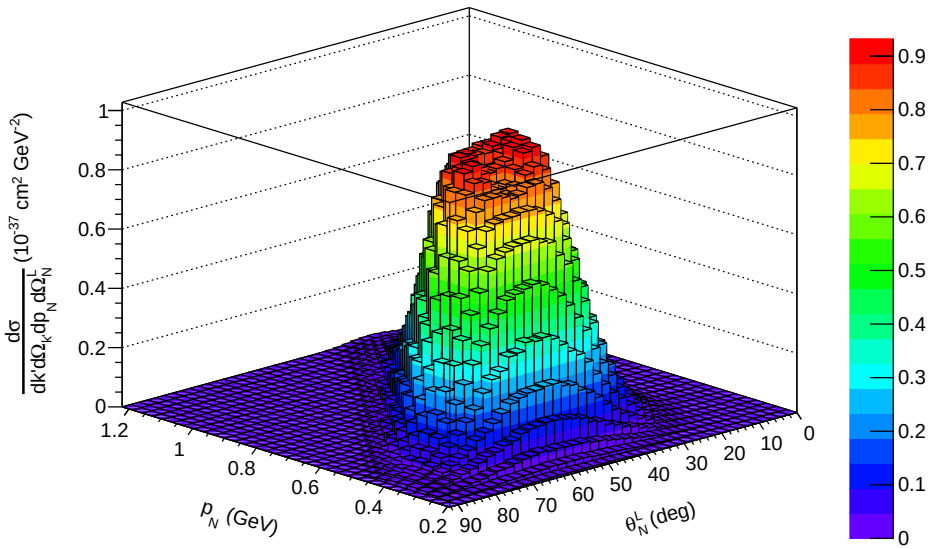

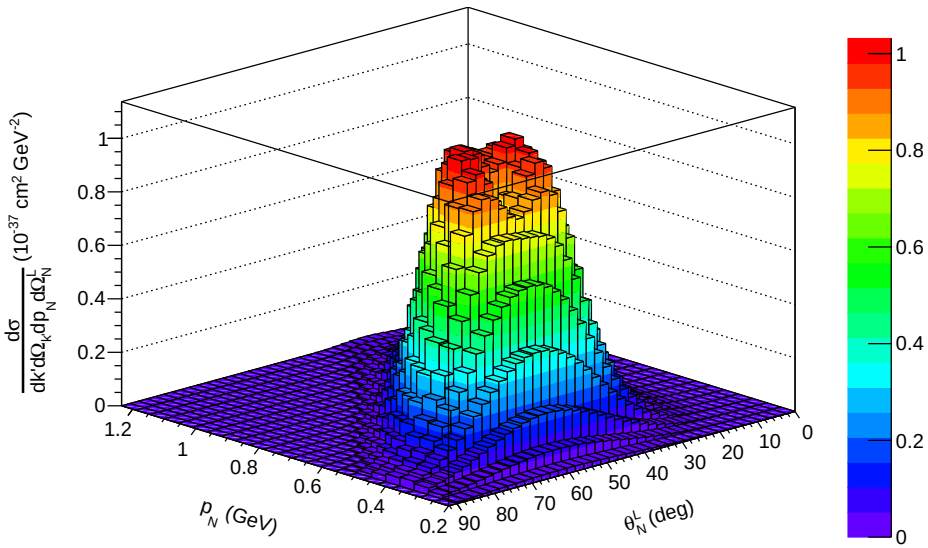

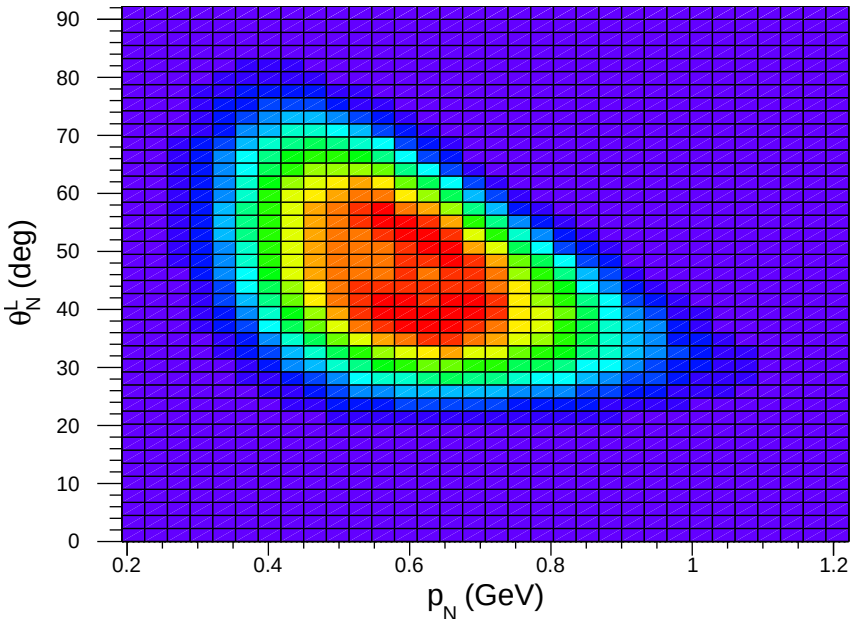

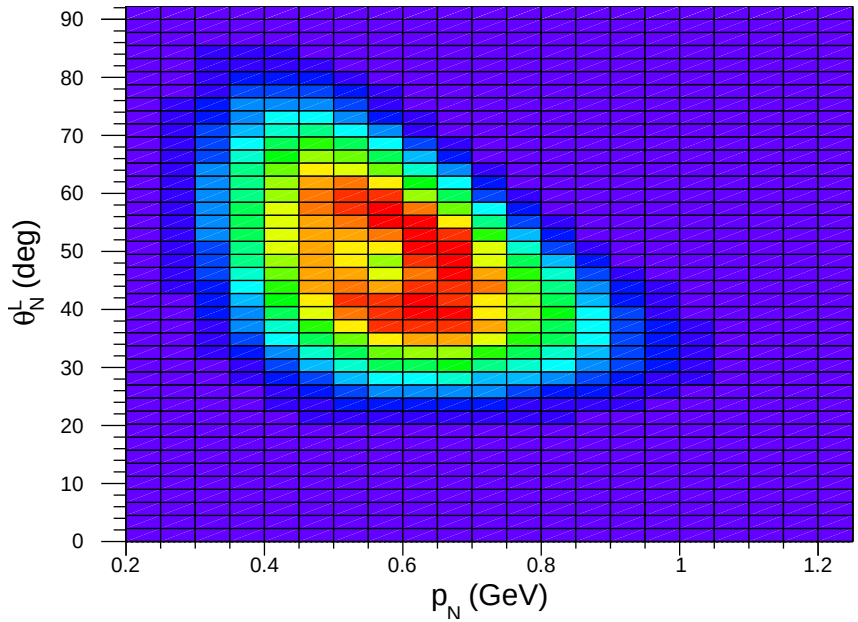

Semi-inclusive ^{40}Ar DUNE cross sections at maximum

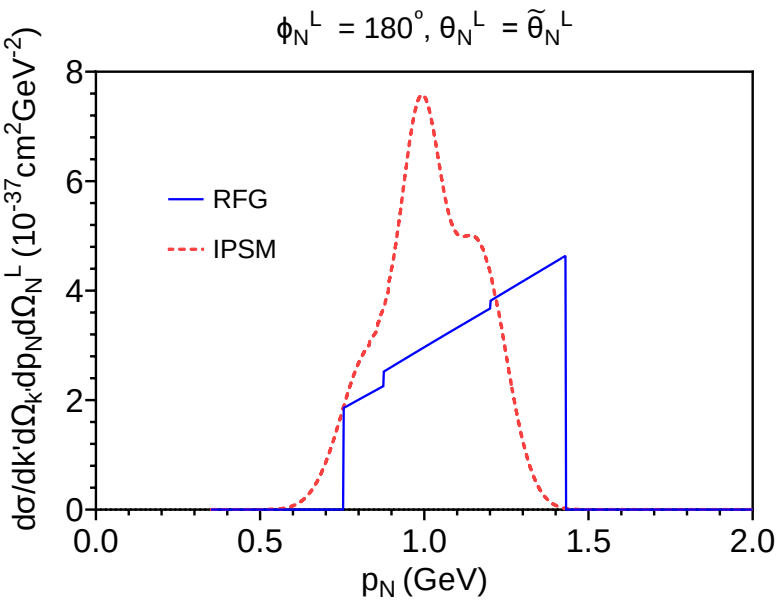

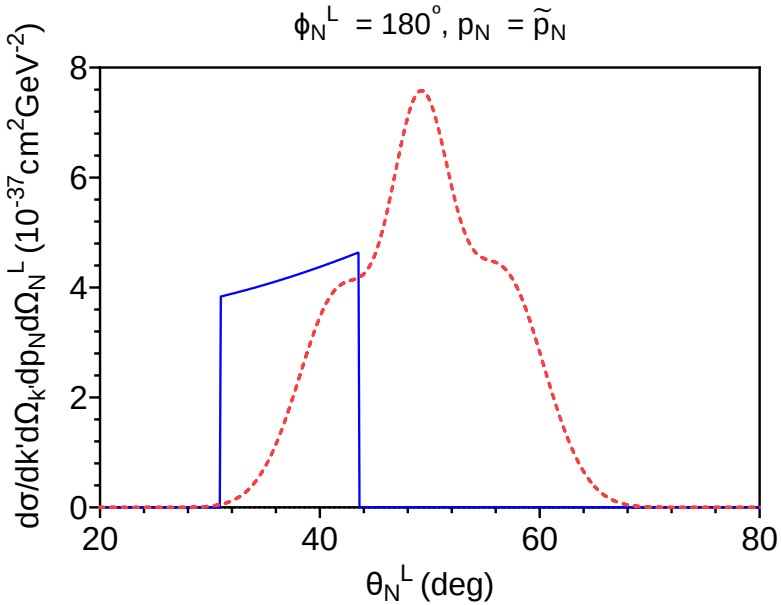

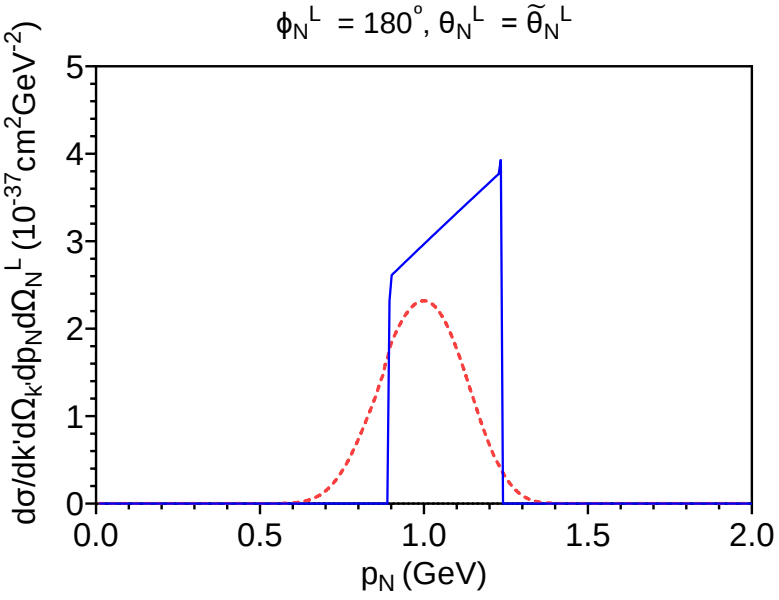

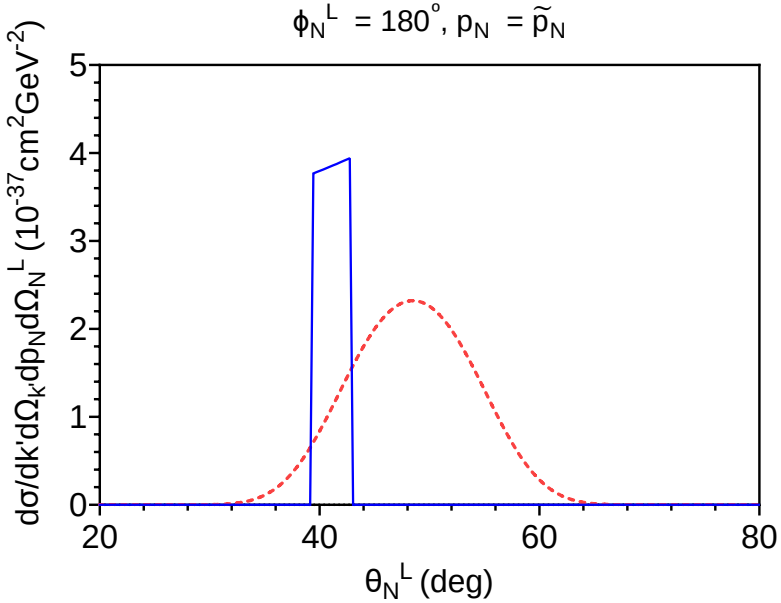

Semi-inclusive ^{40}Ar DUNE cross sections at maximum by shells

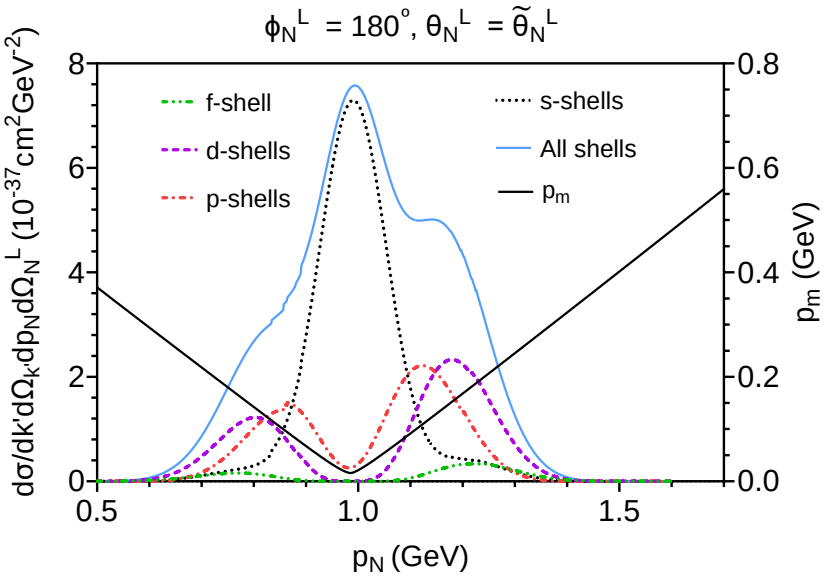

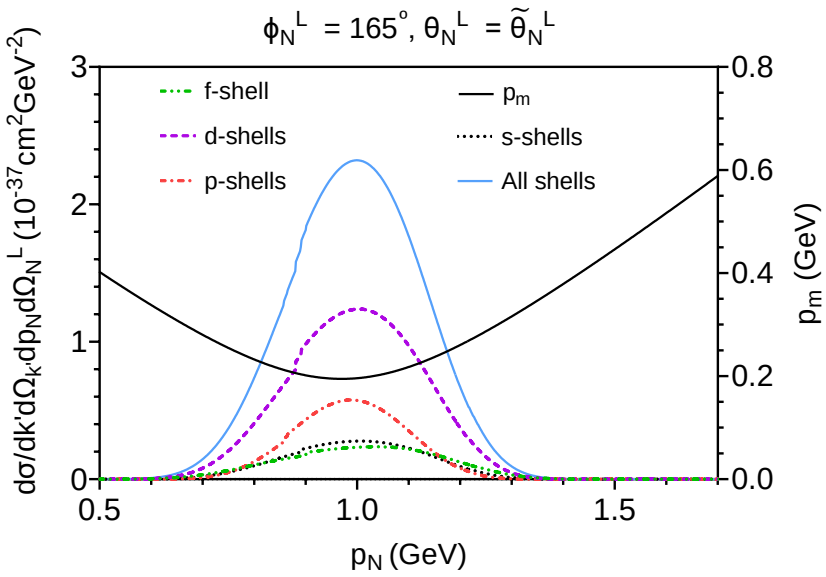

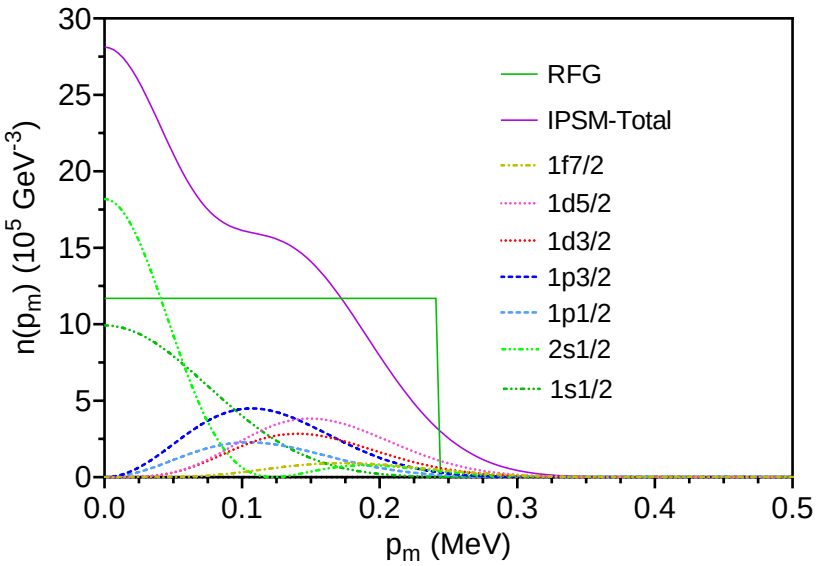

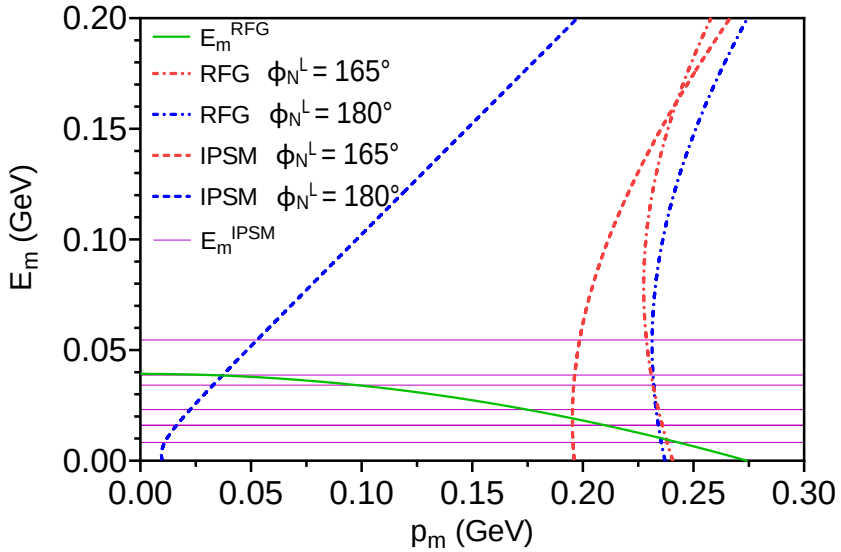

Missing energy profiles $\rho(E_m)$ for ^{12}C and ^{40}Ar

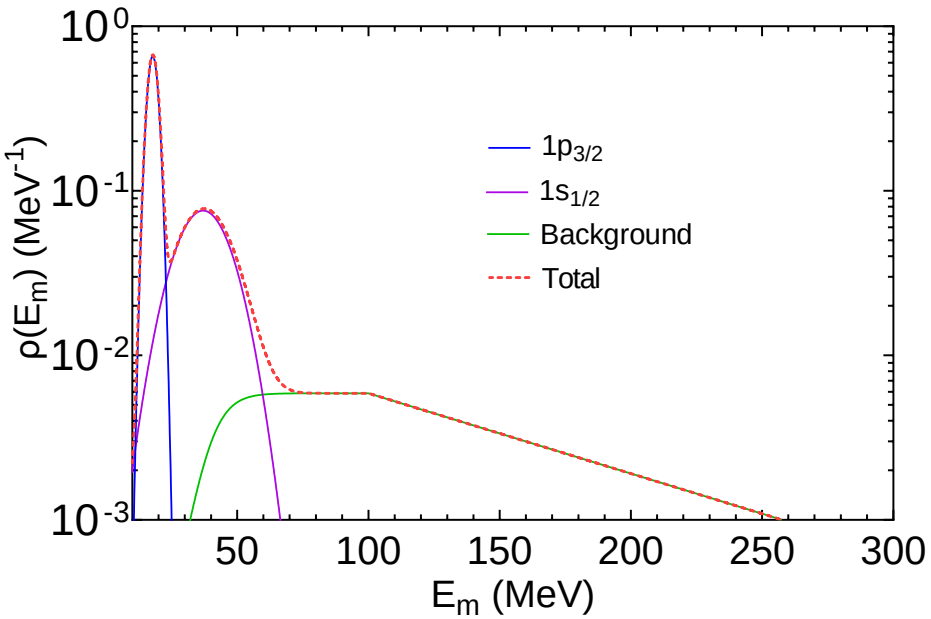

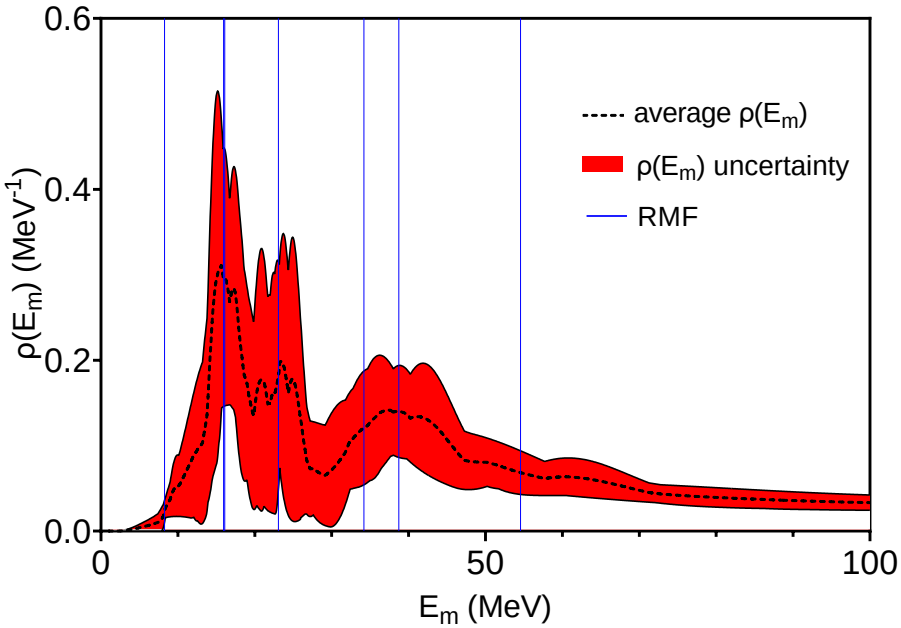

κ	E_κ (MeV)	σ_κ (MeV)	n_κ
$1s_{1/2}$	37.0	10.0	1.9
$1p_{3/2}$	17.8	2.0	3.3

α	E_κ (MeV)	σ_κ (MeV)	S_κ
$1s_{1/2}$	55 ± 6	30 ± 15	0.9 ± 0.15
$1p_{3/2}$	39 ± 4	12 ± 6	0.9 ± 0.15
$1p_{1/2}$	34 ± 3	12 ± 6	0.9 ± 0.15
$1d_{5/2}$	23 ± 2	5 ± 3	0.75 ± 0.15
$2s_{1/2}$	16.1 ± 1.6	5 ± 3	0.75 ± 0.15
$1d_{3/2}$	16.0 ± 1.6	5 ± 3	0.75 ± 0.15
$1f_{7/2}$	9.869 ± 0.005	5 ± 3	0.75 ± 0.15

Final nucleon kinematics generation in GENIE-SuSAv2 model

- Draw initial nucleon momentum $\mathbf{p_m}$ from a Fermi gas momentum distribution.
- Compute $E_m^2 = p_m^2 + m_N^2$.
- $E_N = E_m + \omega - E_b\,(q)$
- $p_N^2 = E_N^2 - m_N^2;\ |\mathbf{p_m} + \mathbf{q}| \neq p_N = \sqrt{E_N^2 - m_N^2};\ \mathbf{p_N} = \frac{p_N}{|\mathbf{p_m}+\mathbf{q}|}\,(\mathbf{p_m} + \mathbf{q})$
- Give the residual momentum to the remnant.

Final nucleon kinematics generation in GENIE-SuSAv2 model

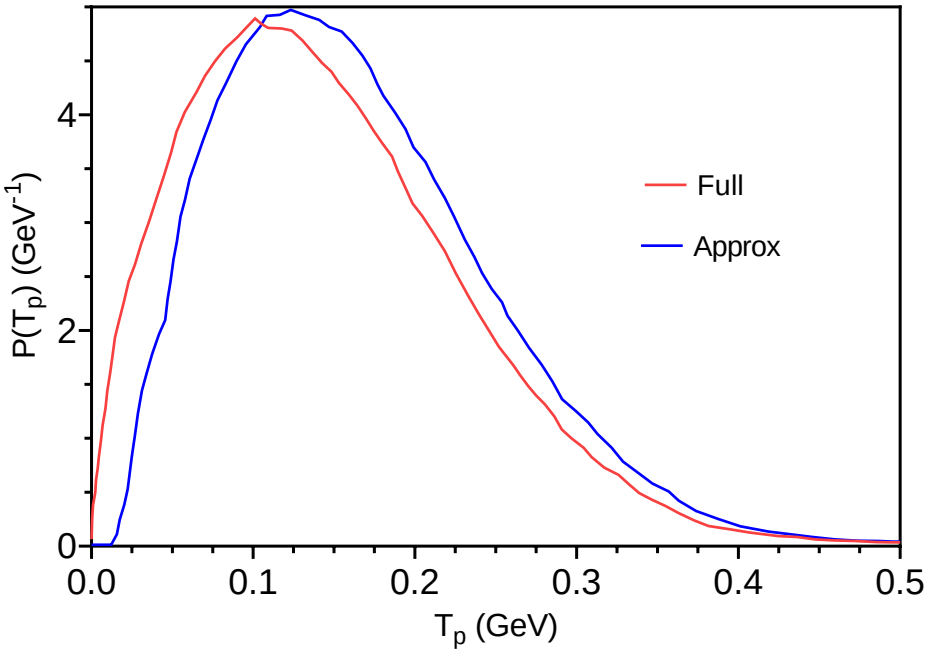

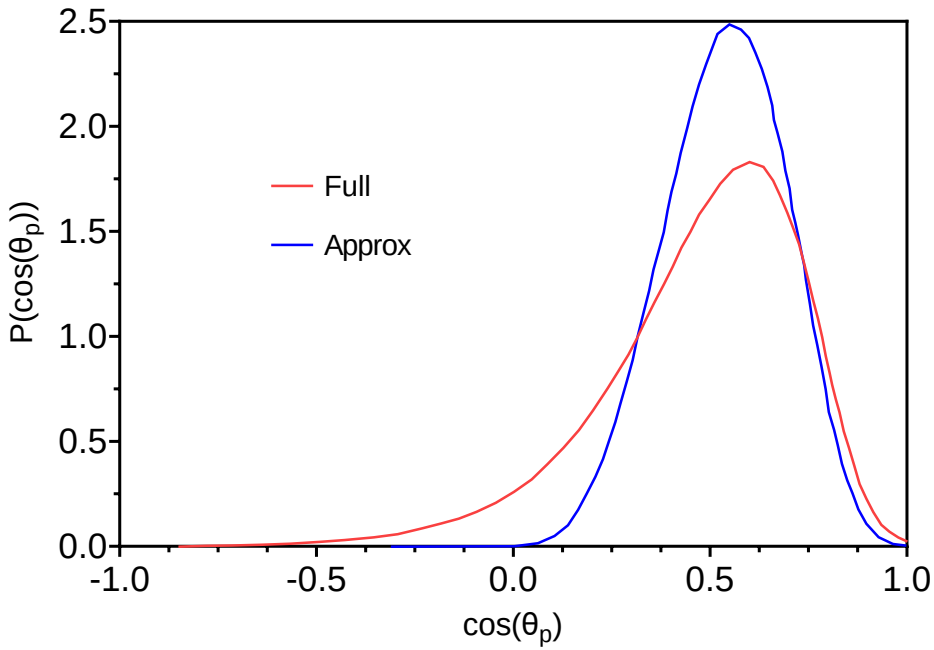

Proton kinetic energy (left) and scattering angle (right) distributions for the process $e + A \to e' + p + B$. The electron beam energy is fixed to 1.159 GeV and the outgoing electron phase-space is limited to $17^\circ < \theta_{e'} < 40^\circ$ and $E_{e'} > 0.4$ GeV. The red lines show the unfactorized RDWIA predictions obtained with ED-RMF potential for carbon (named "Full") while the blue lines show the equivalent distributions obtained after applying the GENIE algorithm and before adding GENIE cascade FSI (named "Approx"). Figure from **A. Nikolakopoulos *et. al.* 2302.12182**

T2K Semi-inclusive cross sections: $p_N < 0.5$ GeV

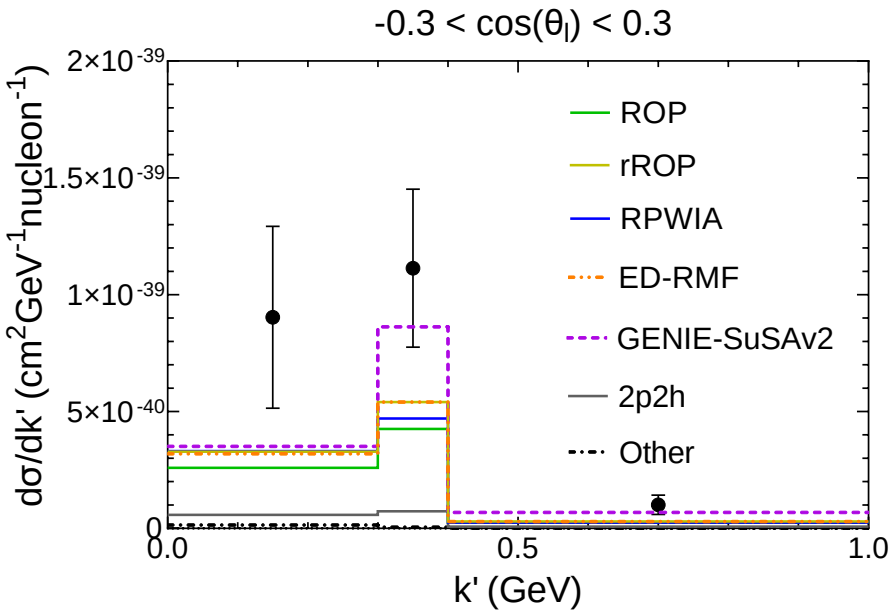

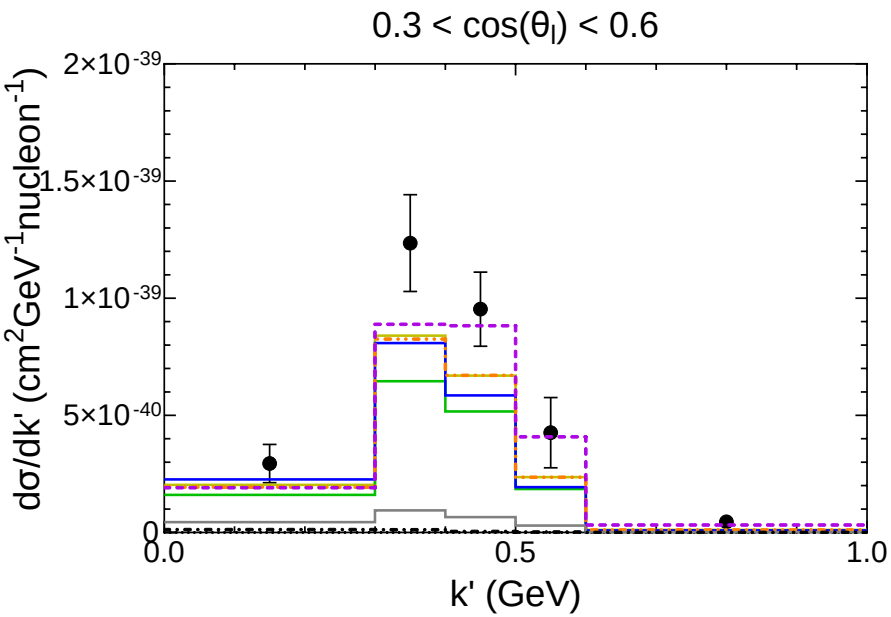

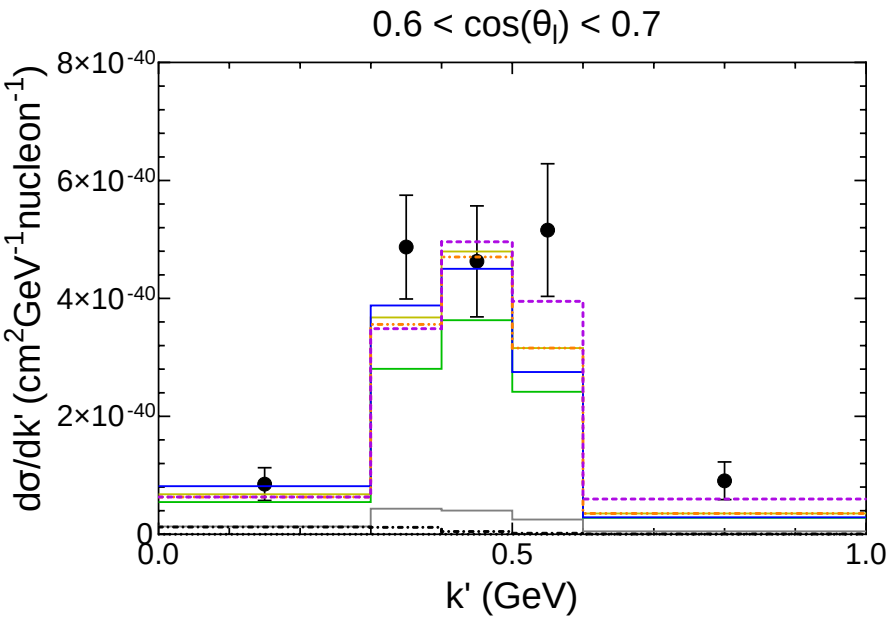

T2K Semi-inclusive cross sections: $p_N < 0.5$ GeV

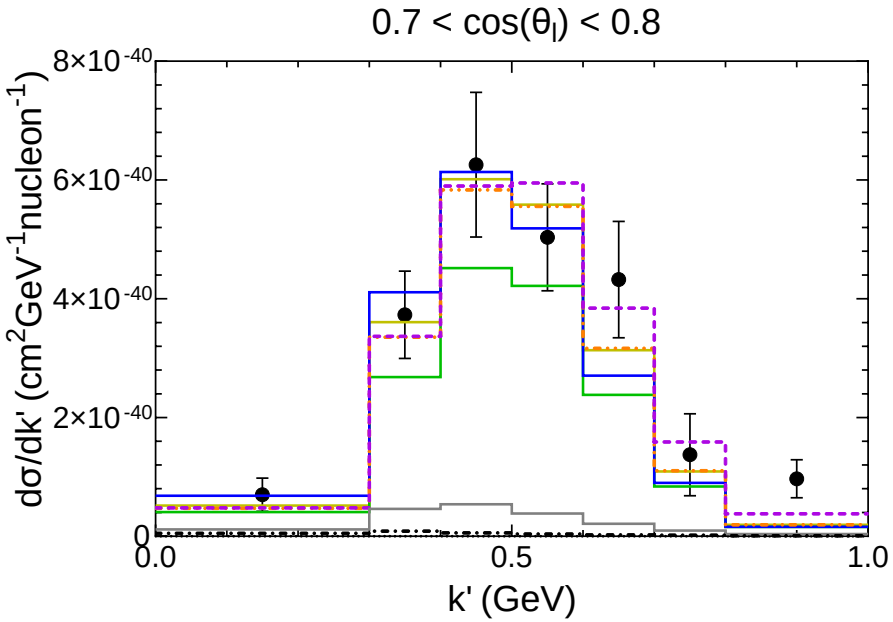

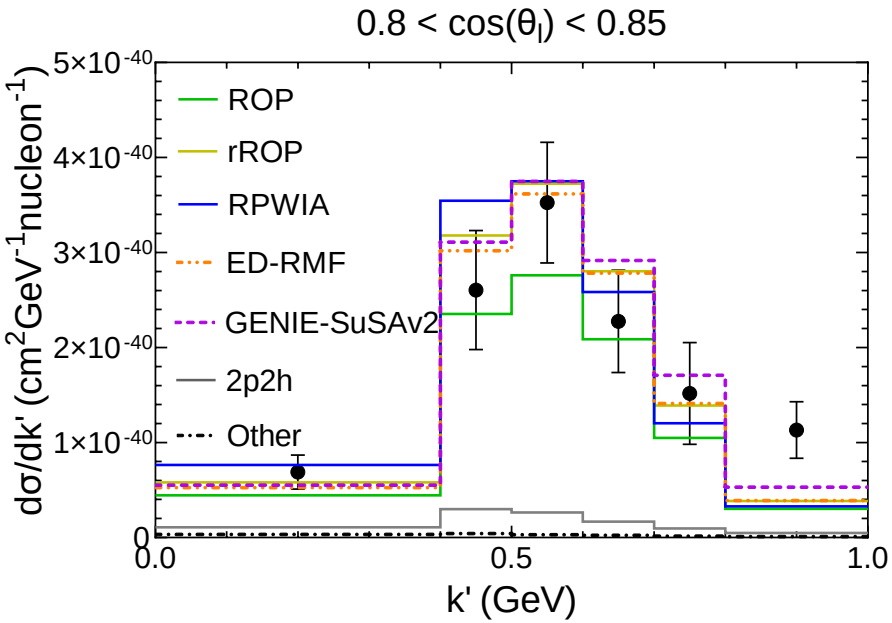

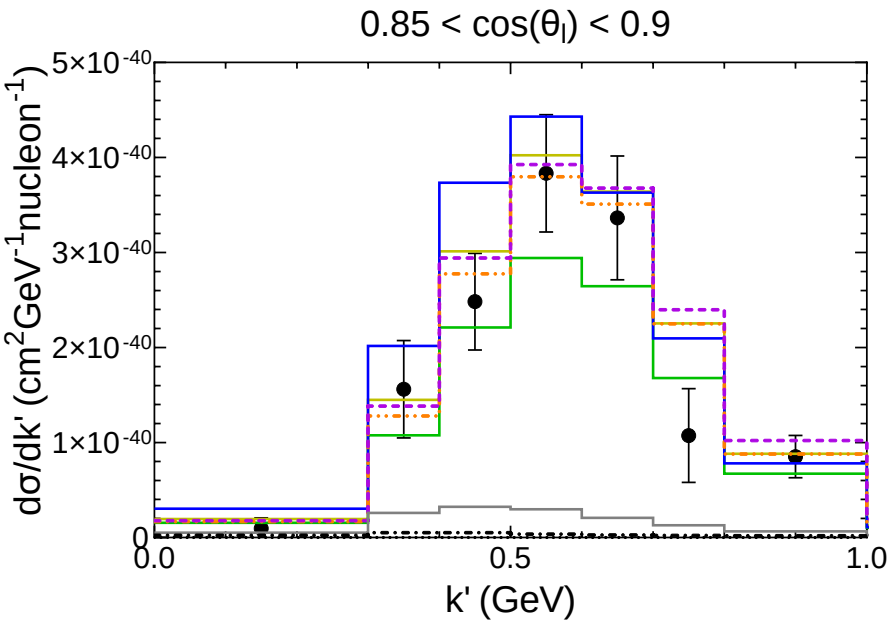

T2K semi-inclusive cross sections: $p_N < 0.5$ GeV

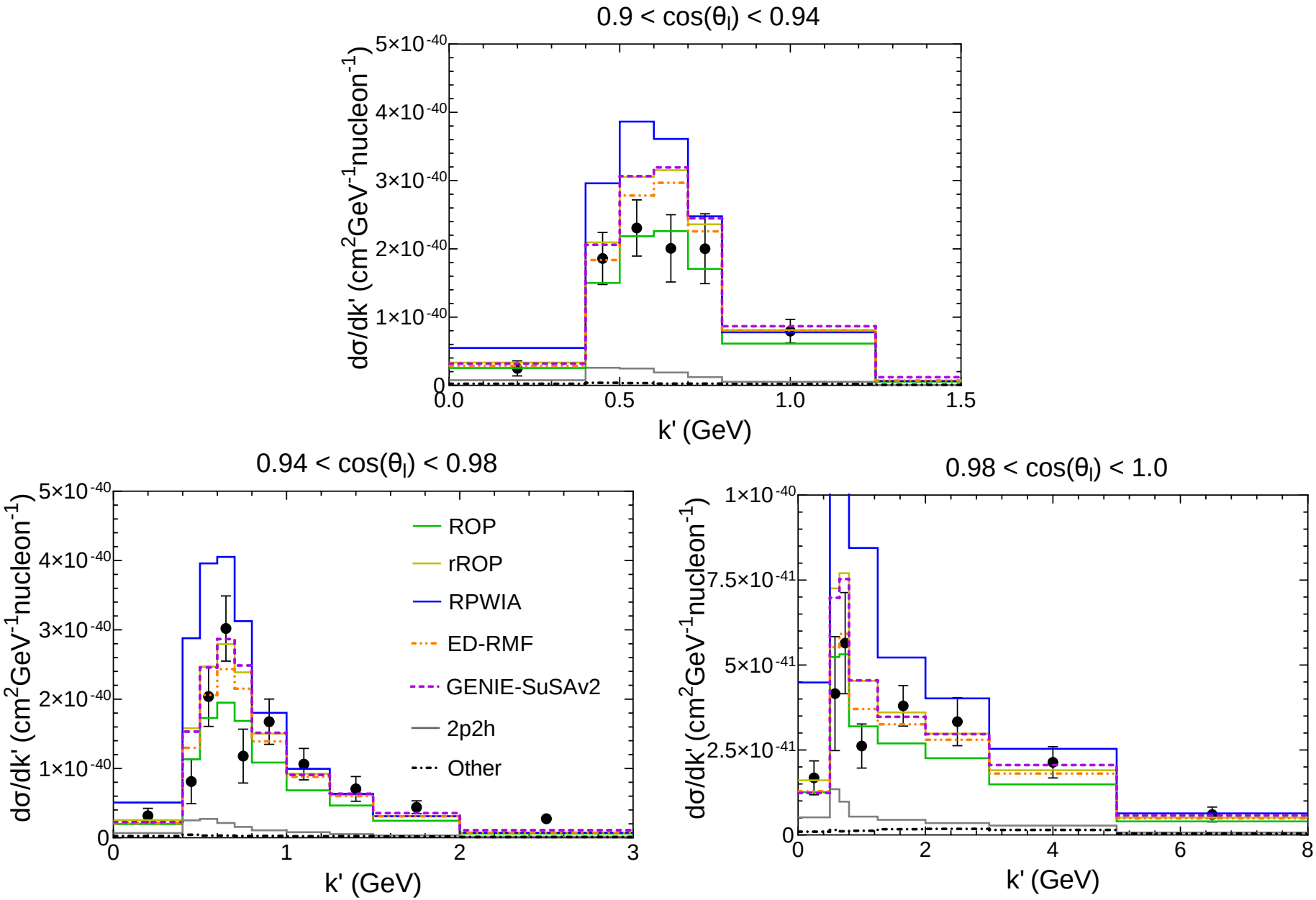

T2K semi-inclusive cross sections: $p_N > 0.5$ GeV

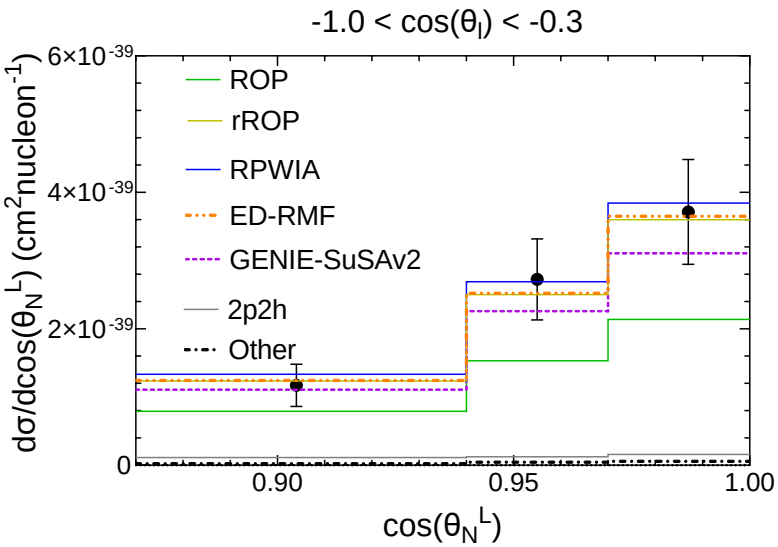

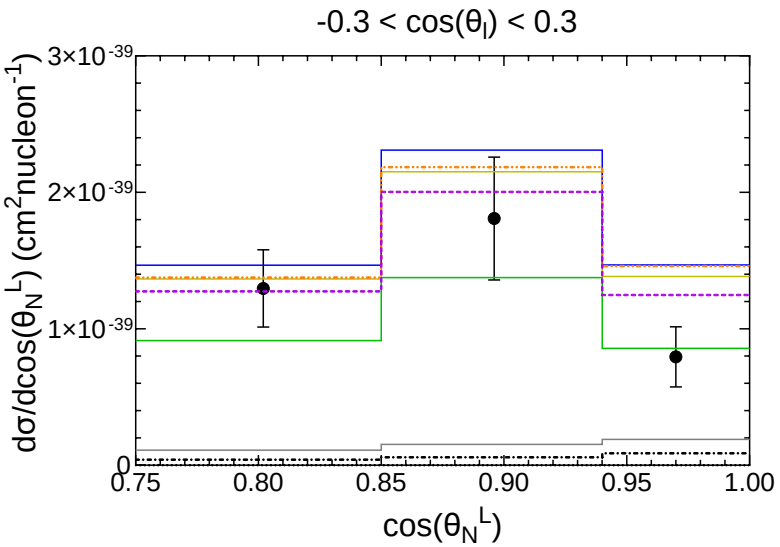

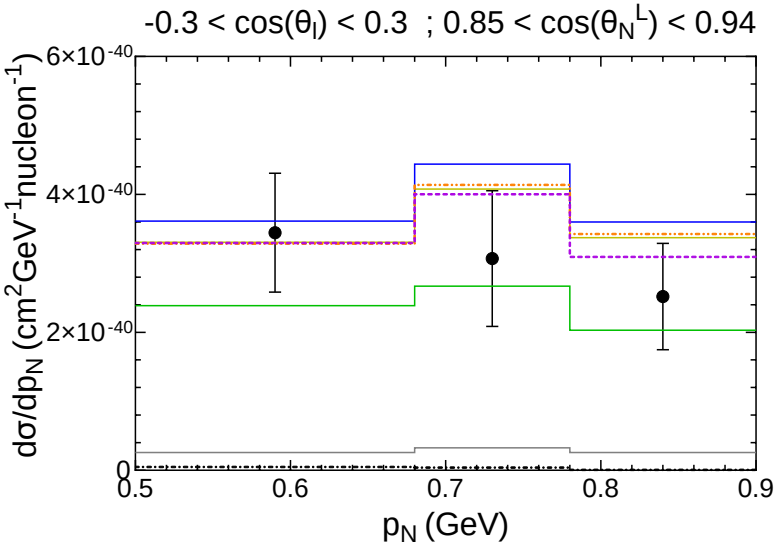

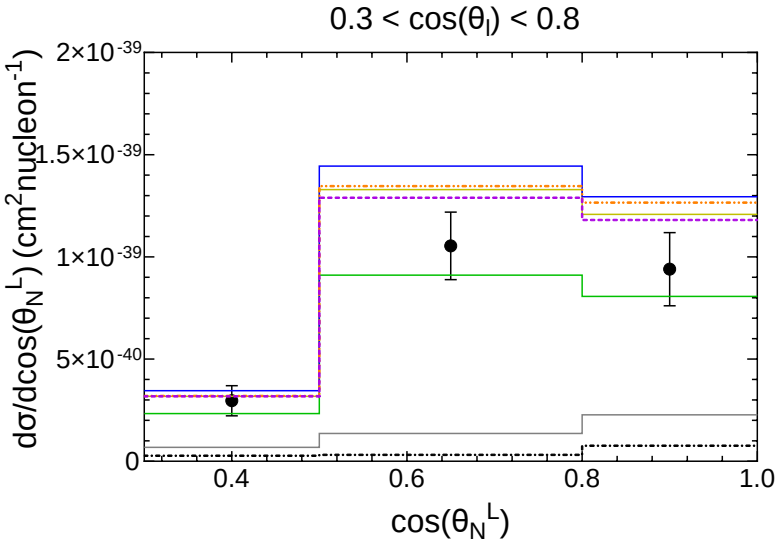

T2K semi-inclusive cross sections: $p_N > 0.5$ GeV

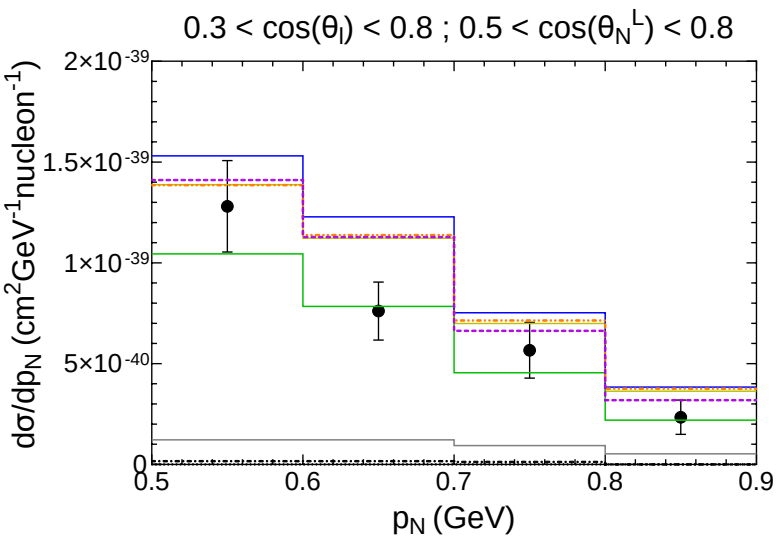

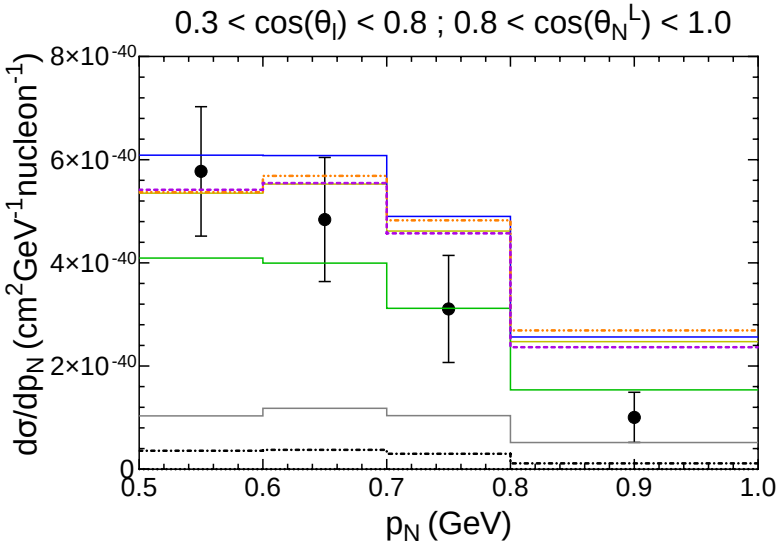

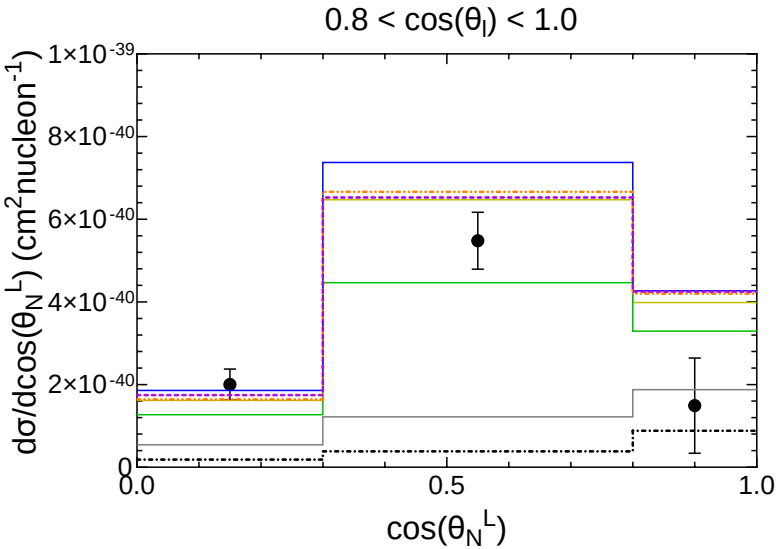

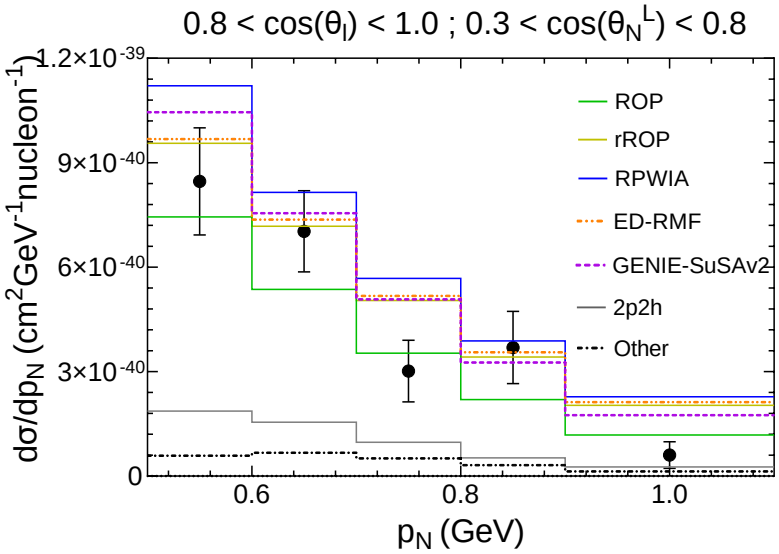

T2K semi-inclusive cross sections: $p_N > 0.5$ GeV

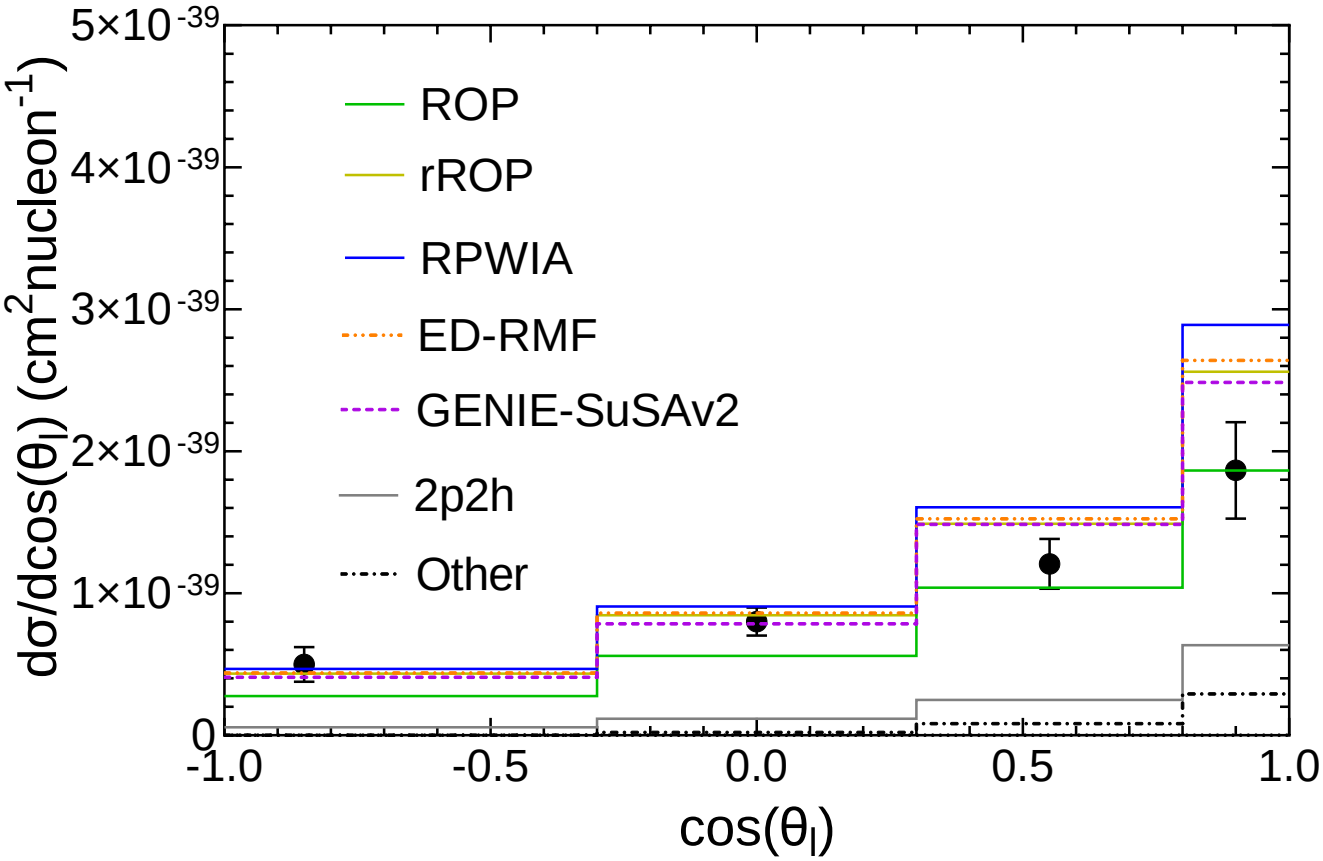

T2K semi-inclusive cross sections: Δp

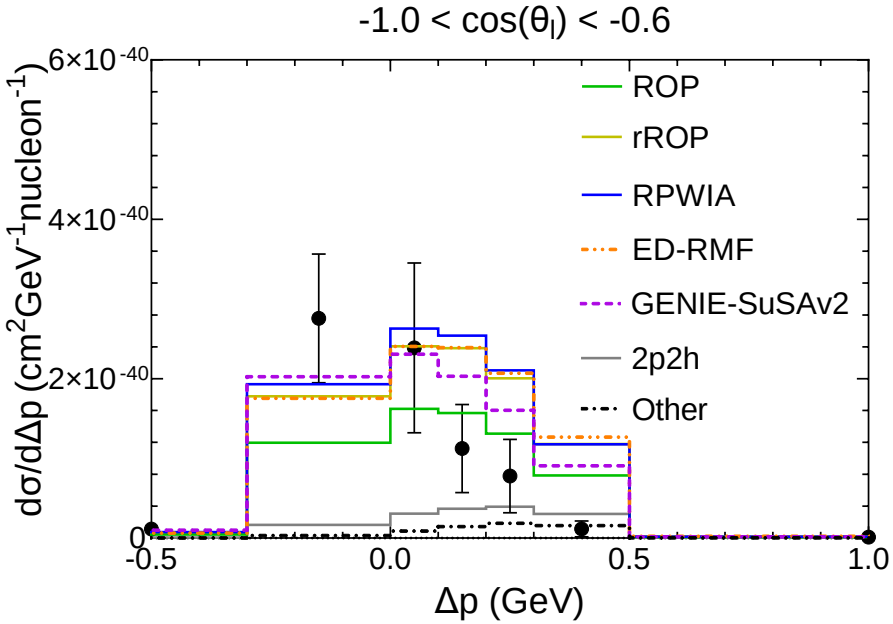

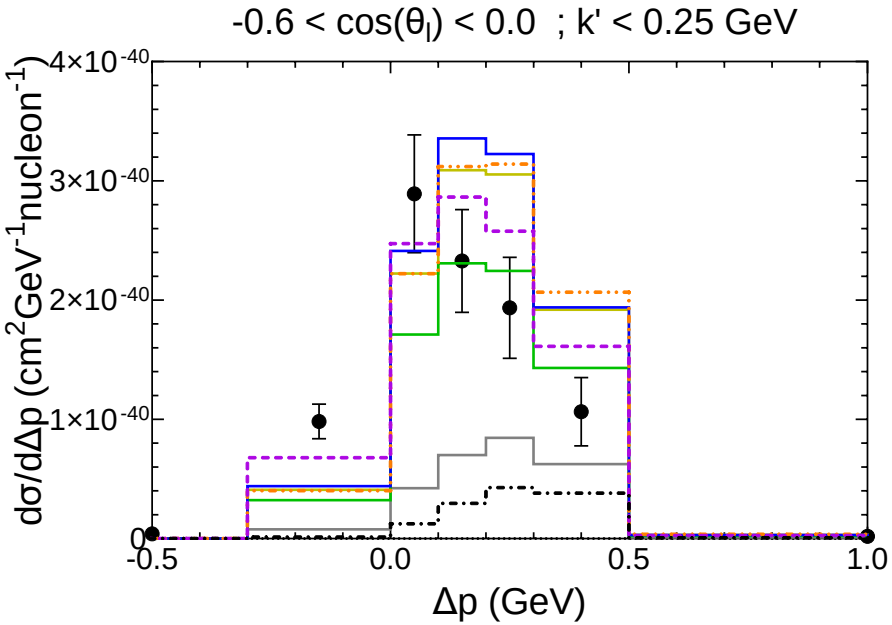

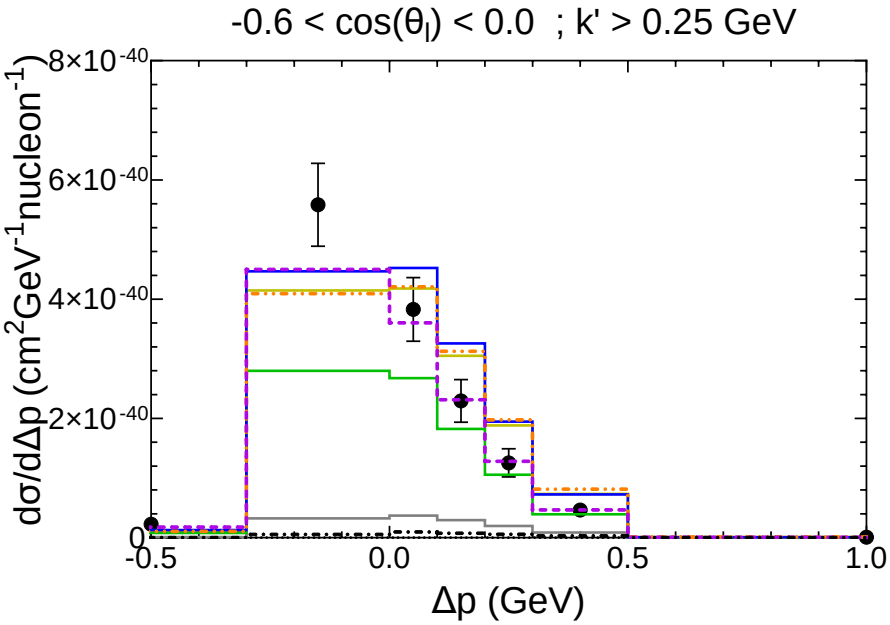

T2K semi-inclusive cross sections: Δp

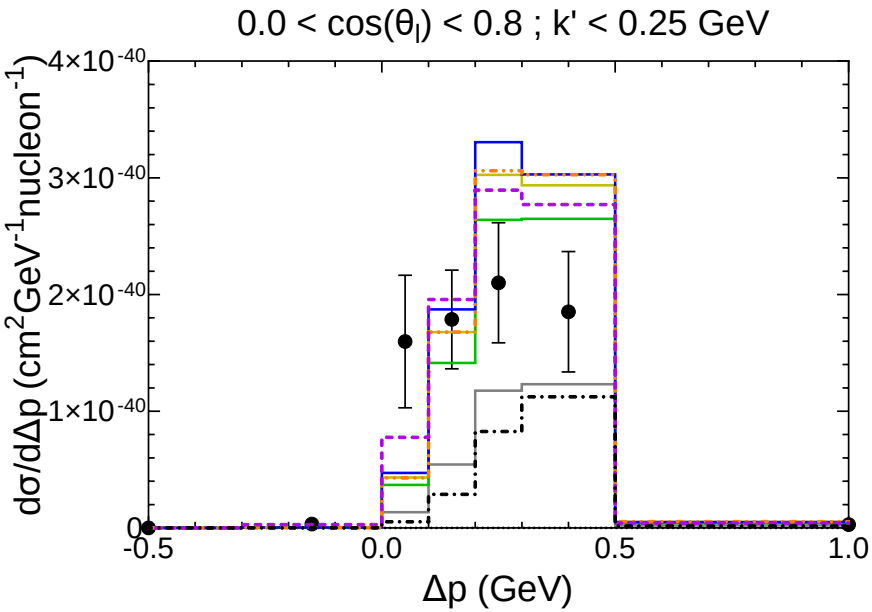

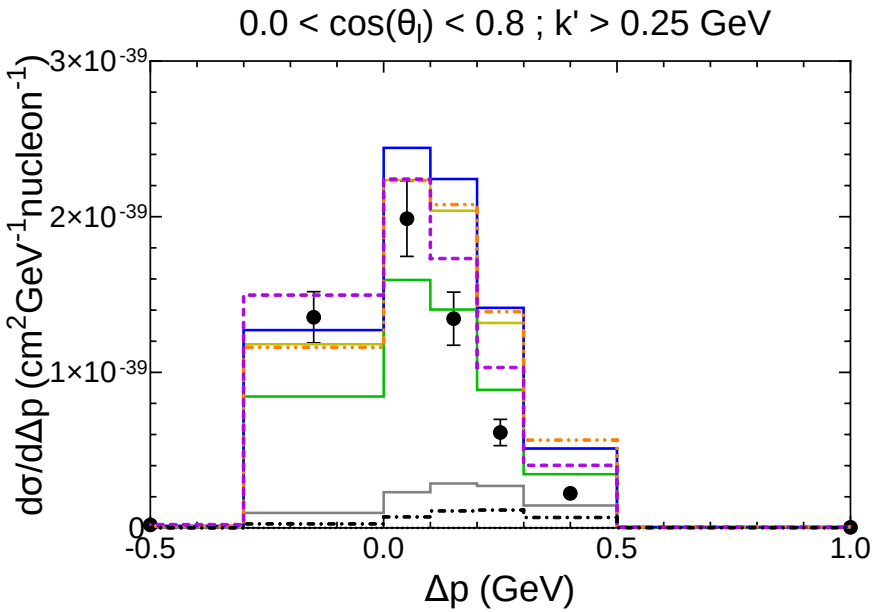

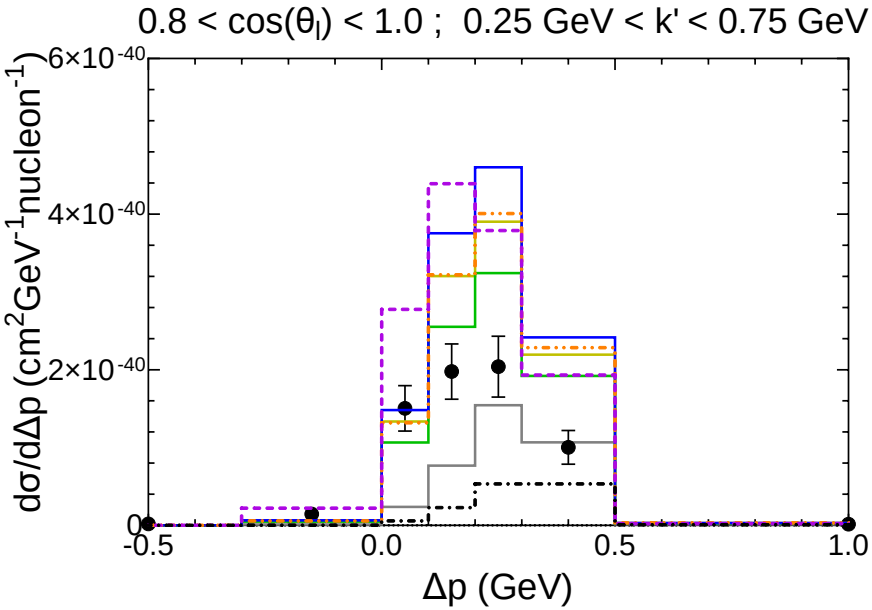

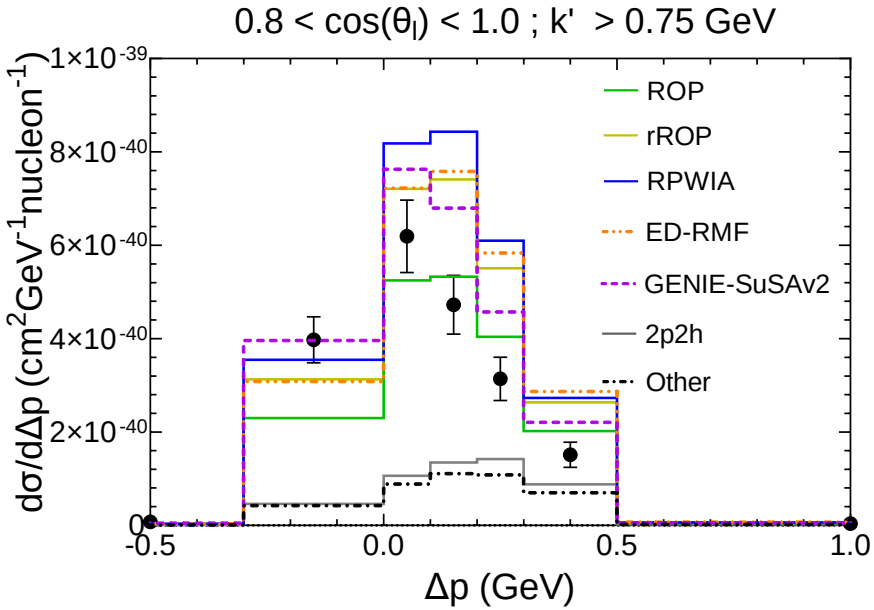

T2K semi-inclusive cross sections: $\Delta\theta$

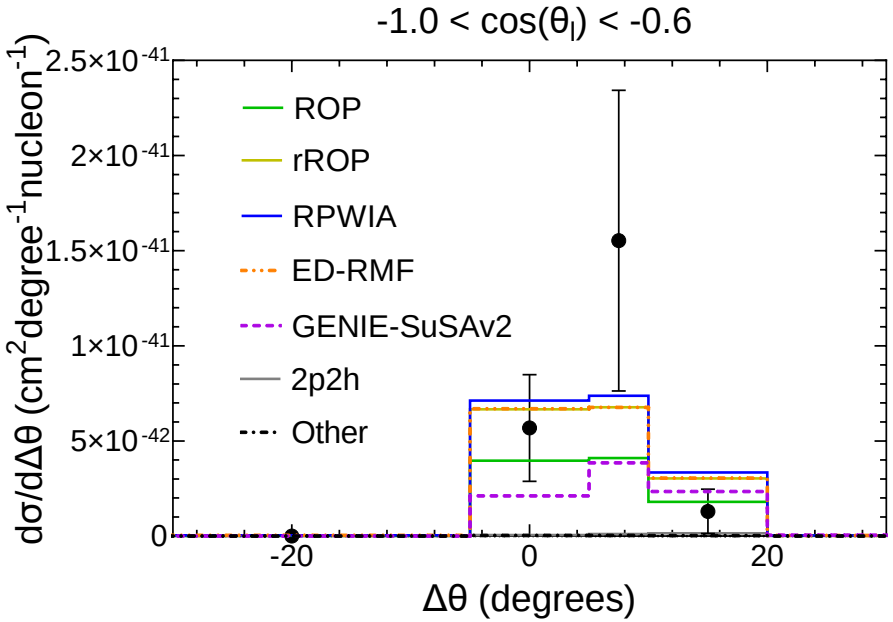

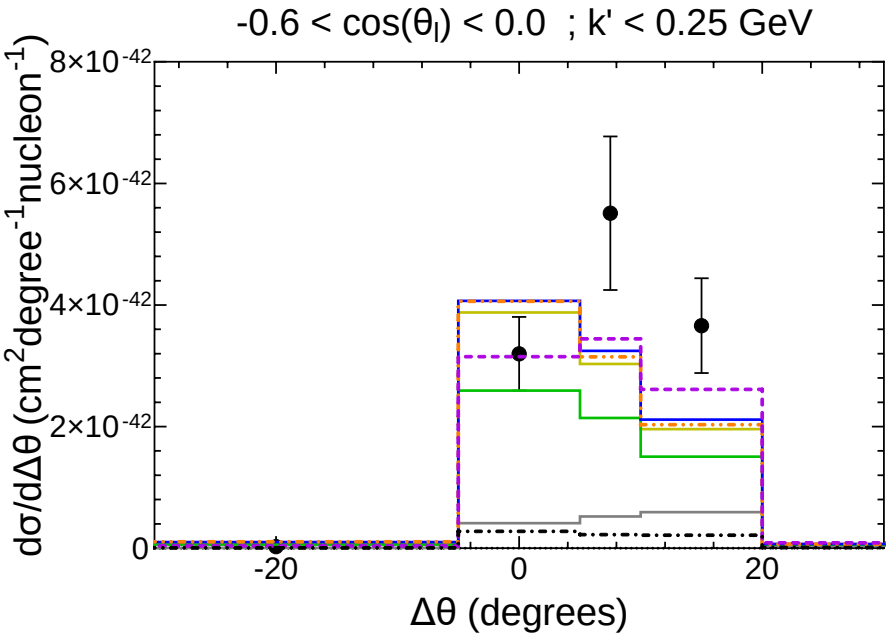

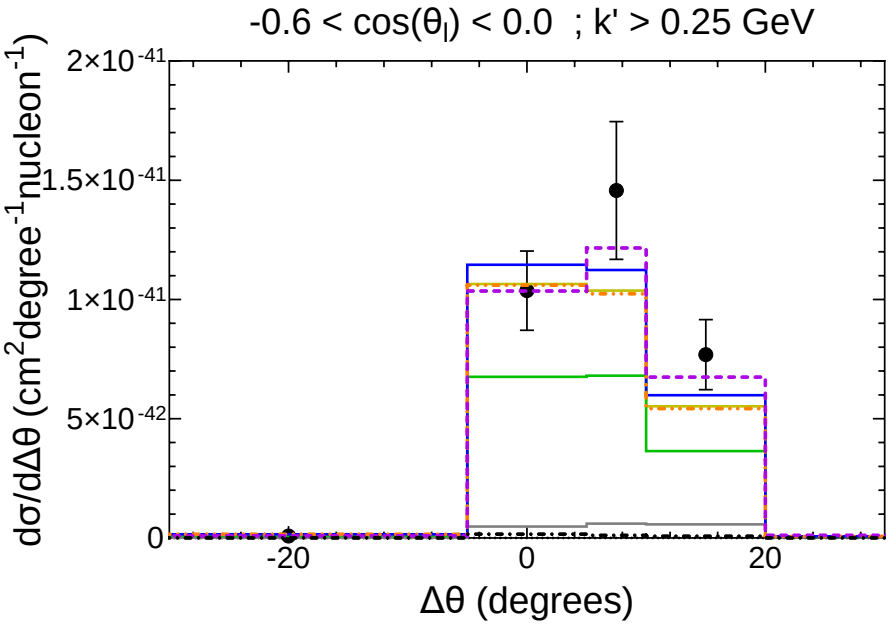

T2K semi-inclusive cross sections: $\Delta\theta$

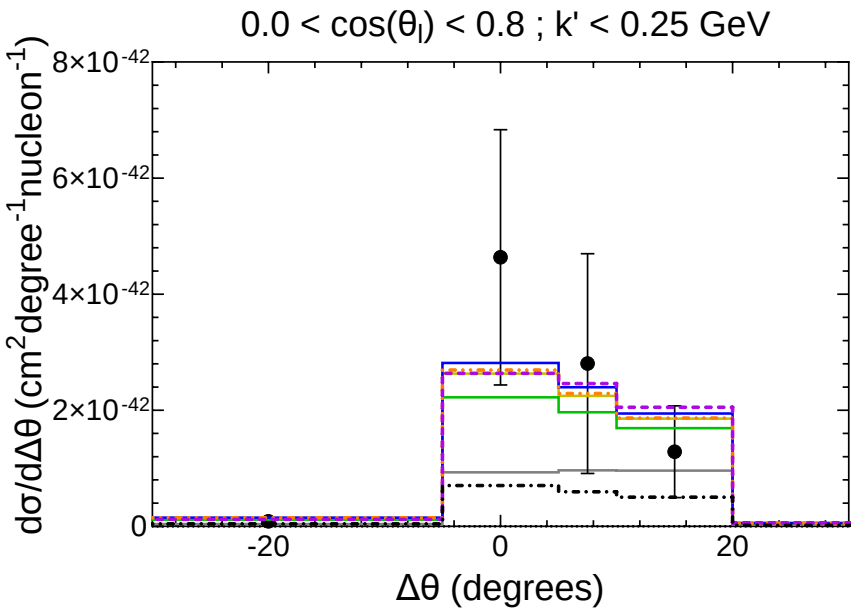

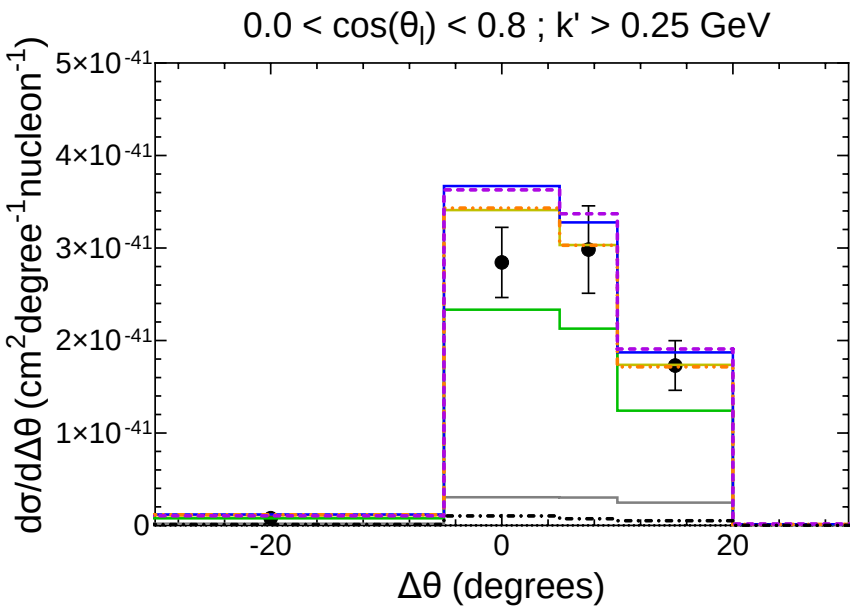

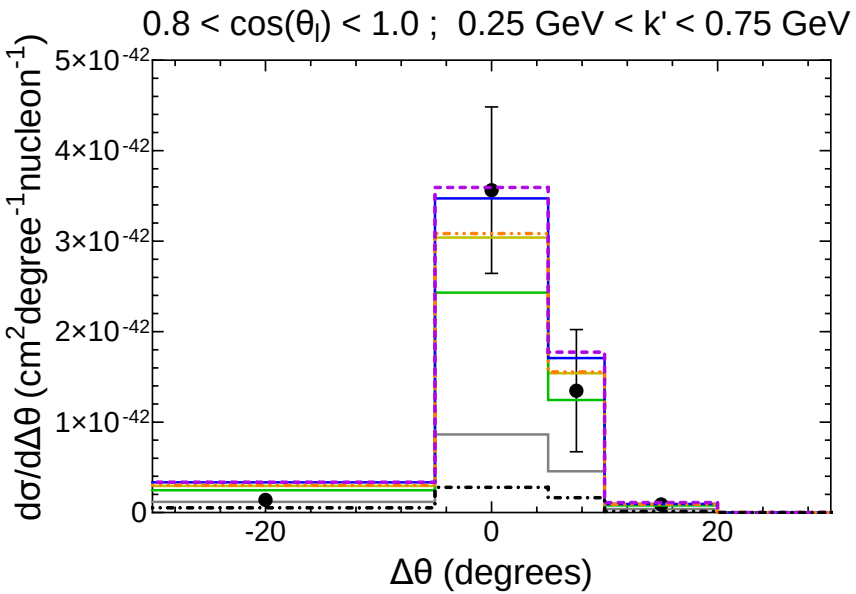

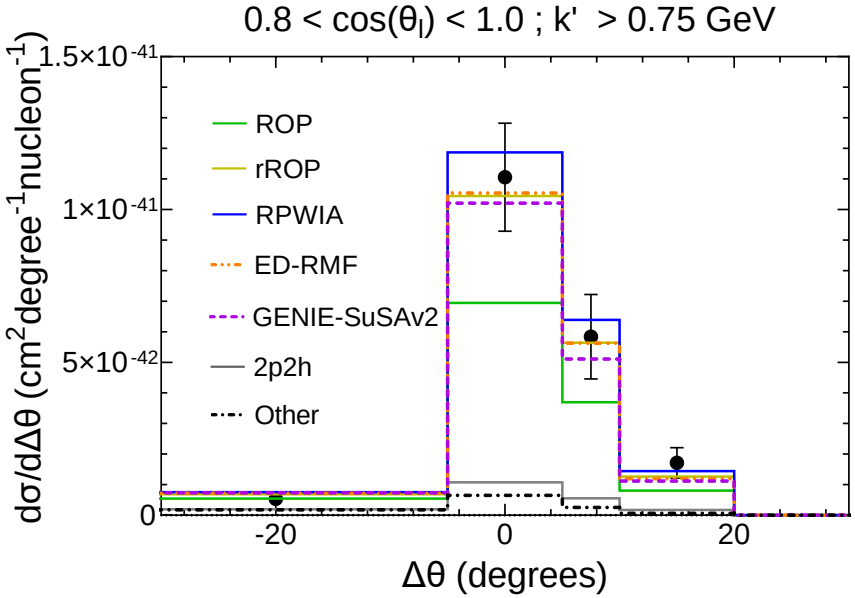

T2K semi-inclusive cross sections: $|\Delta \mathbf{p}|$

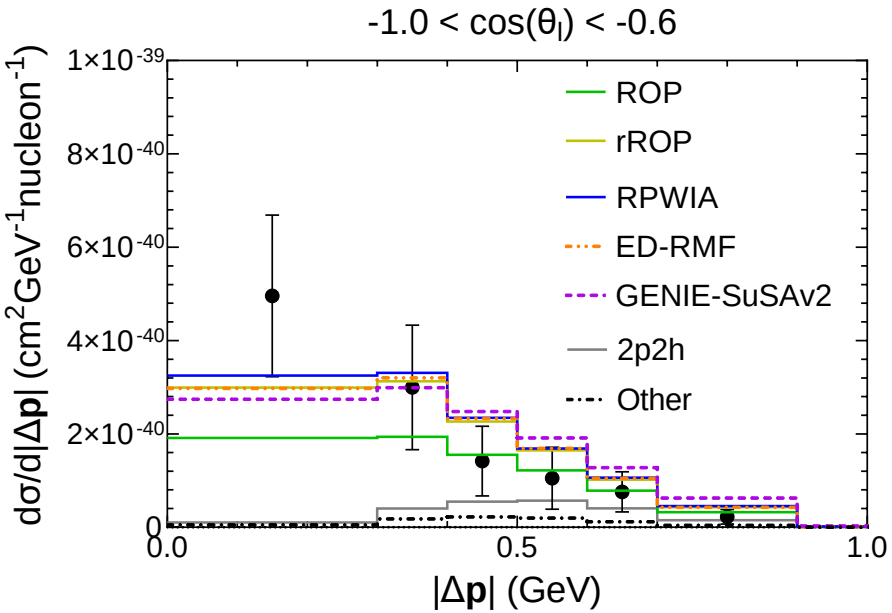

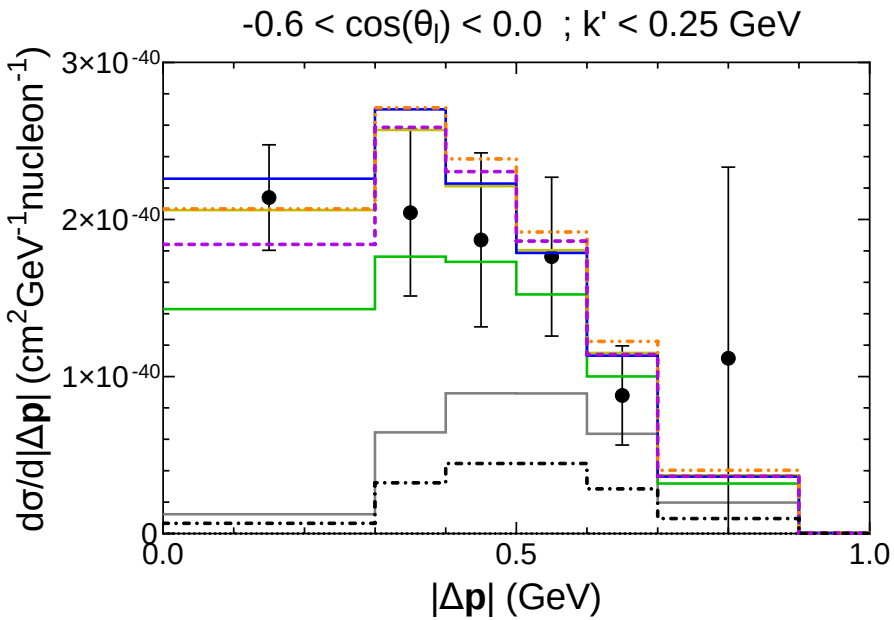

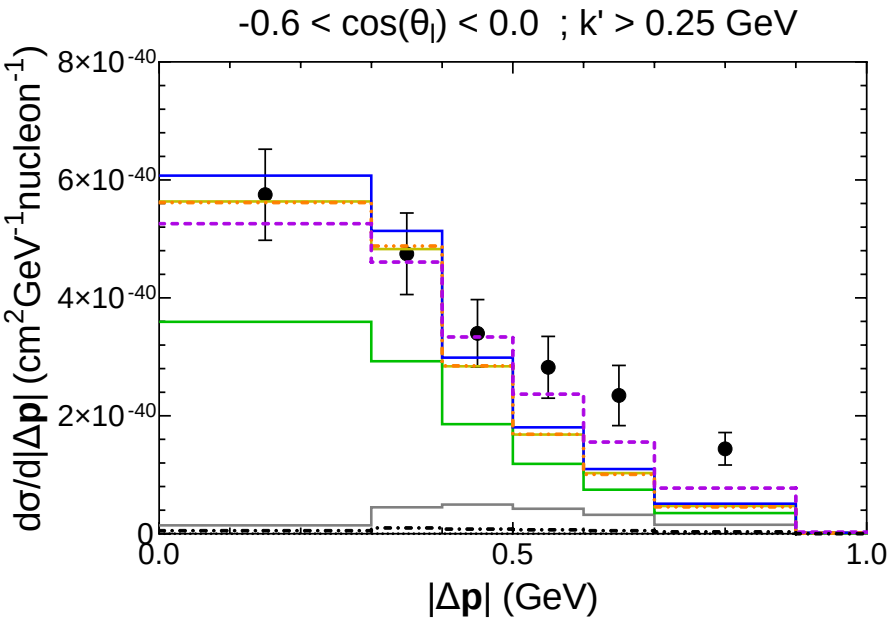

T2K semi-inclusive cross sections: $|\Delta \mathbf{p}|$

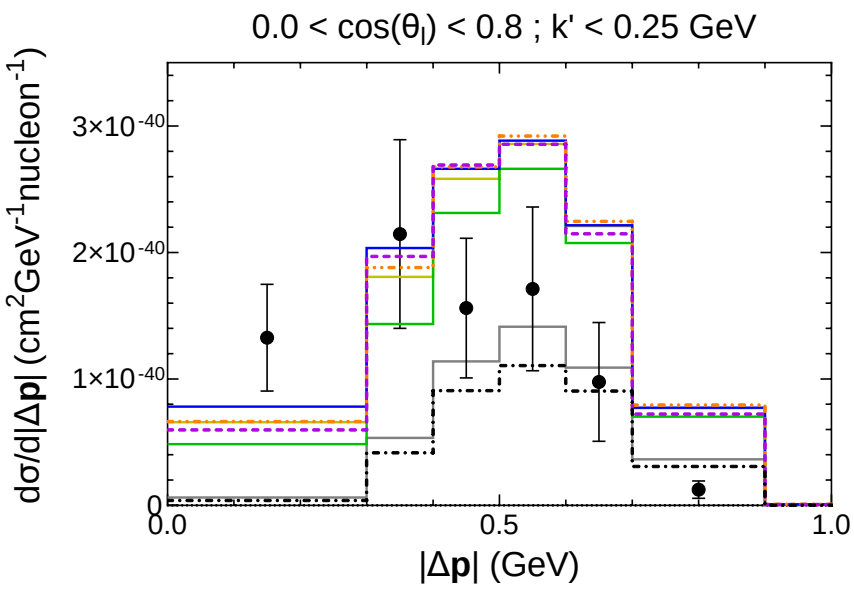

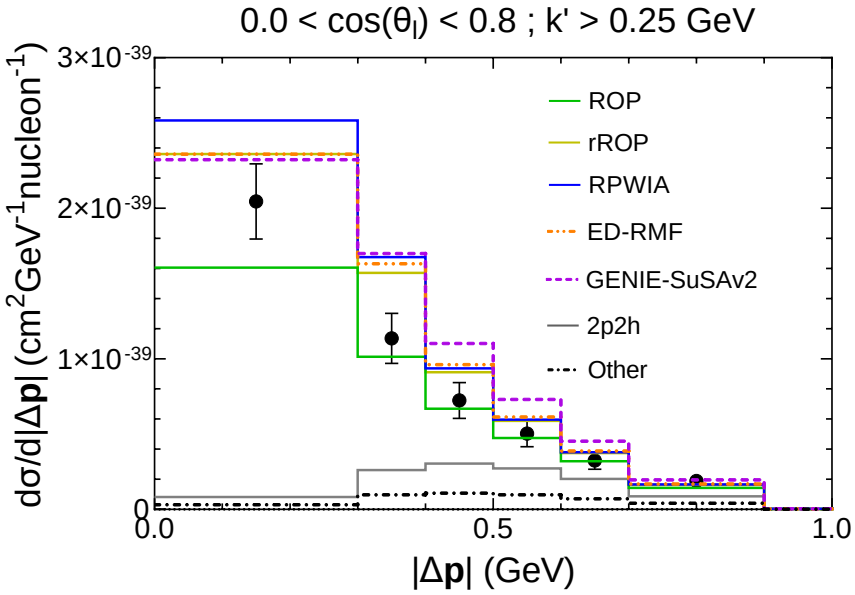

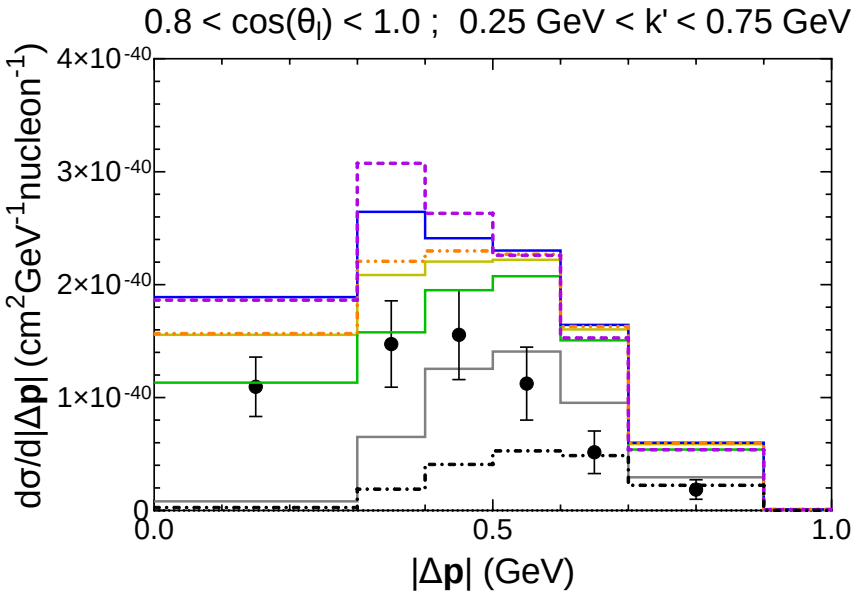

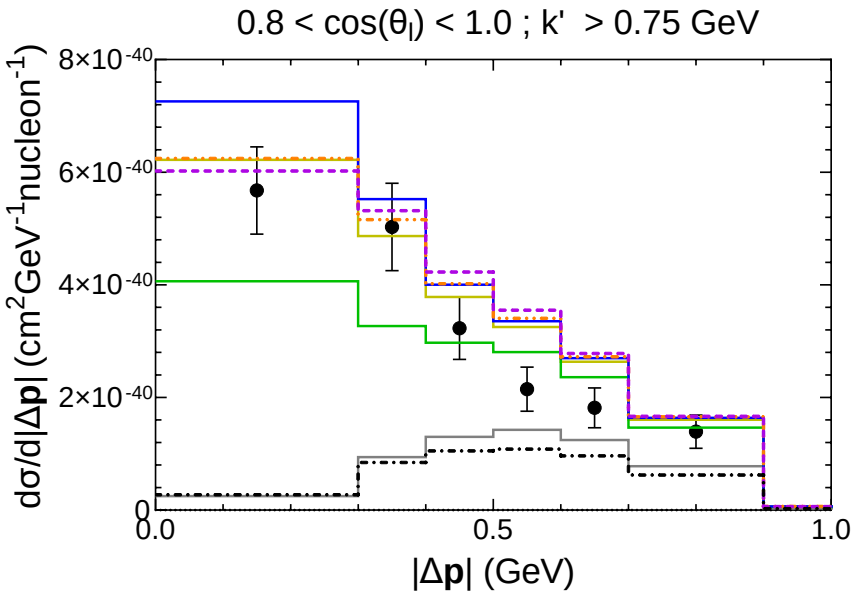

MINERνA semi-inclusive cross sections: muon and proton kinematics

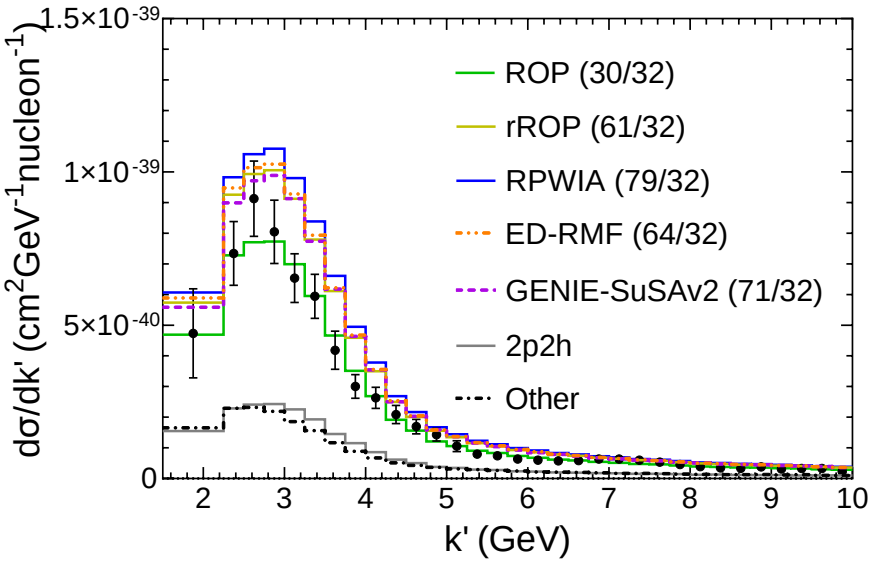

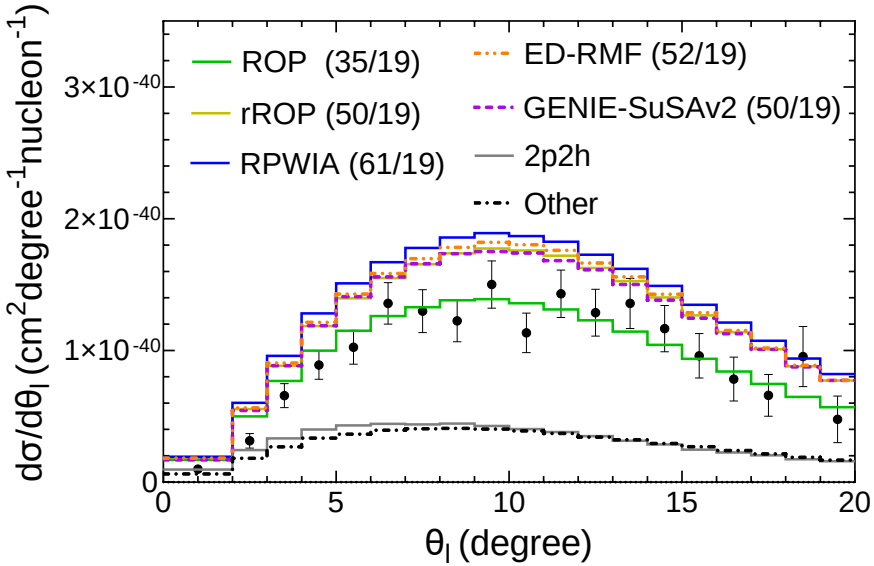

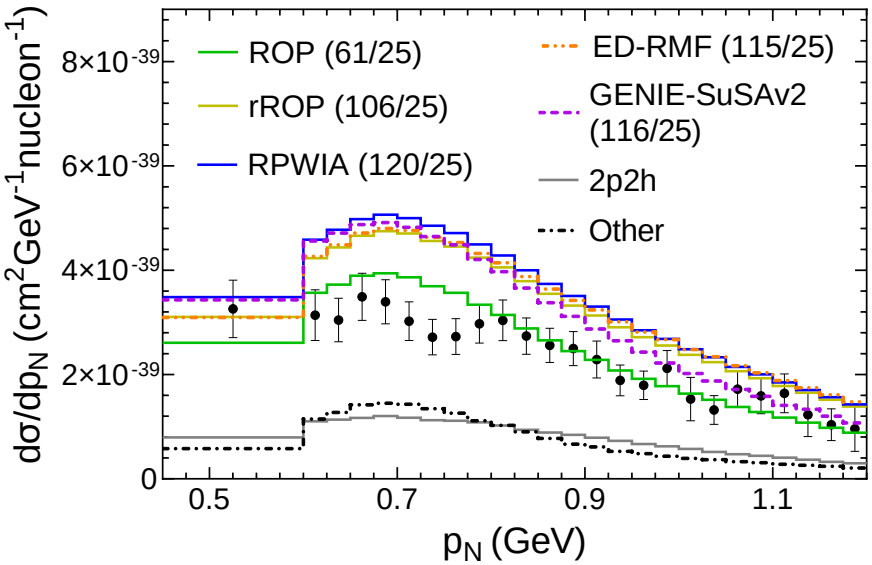

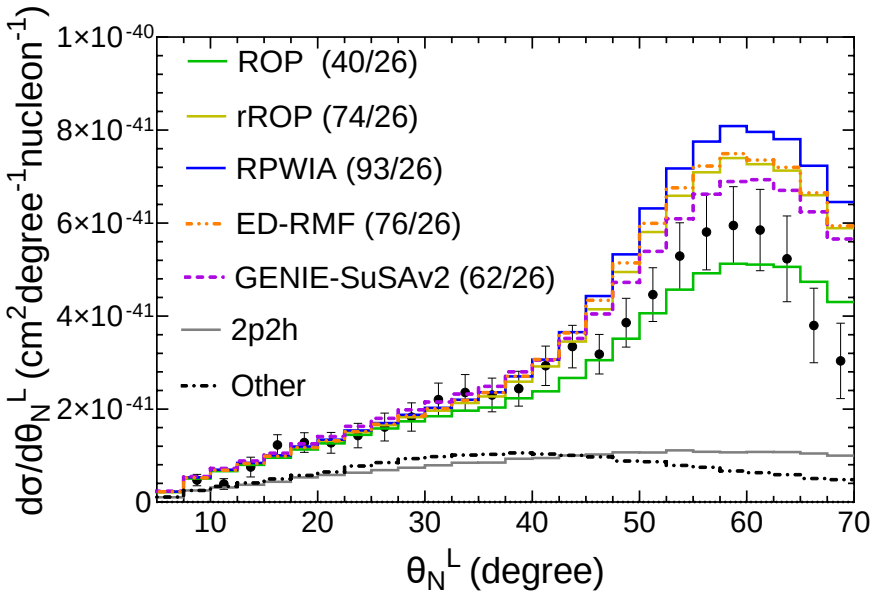

MicroBooNE kinematic cuts

1μCC0πNp	k' (GeV)	$\cos\theta_l$	p_N (GeV)	$\cos\theta_N^L$	ϕ_N^L (°)	$\theta_{\mu p}$ (°)	δp_T (GeV)
	> 0.1	-	0.3-1.2	-	-	-	-
1eCC0πNp							
	> 0.0305	-	> 0.3105	-	-	-	-
1μCC0π1p							
	0.1-1.5	-0.65-0.95	0.3-1.0	> 0.15	145-215	35-145	< 0.35

MicroBooNE semi-inclusive cross sections: $1\mu CC0\pi Np$

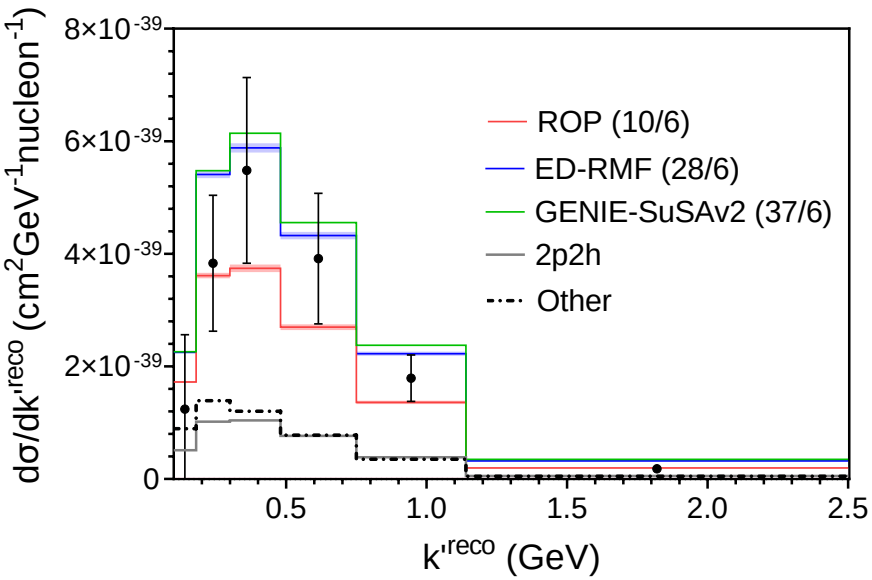

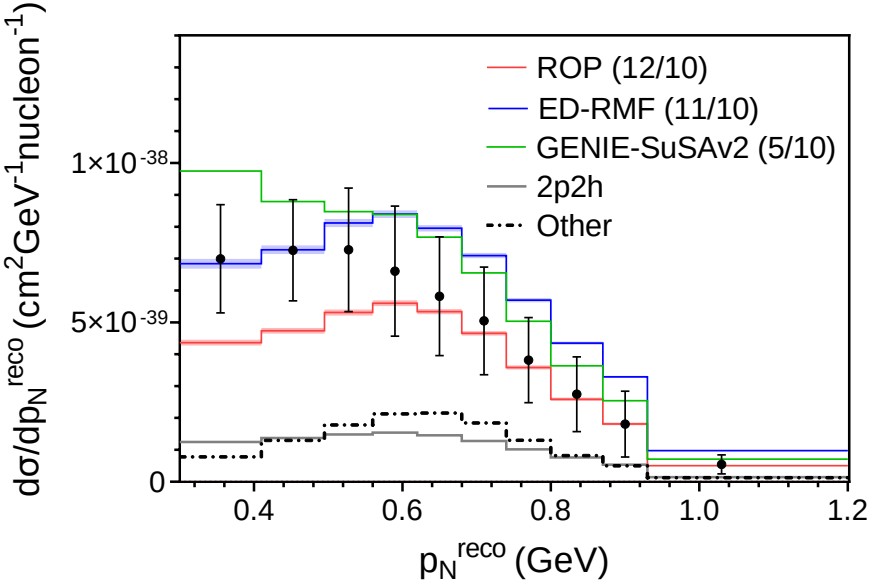

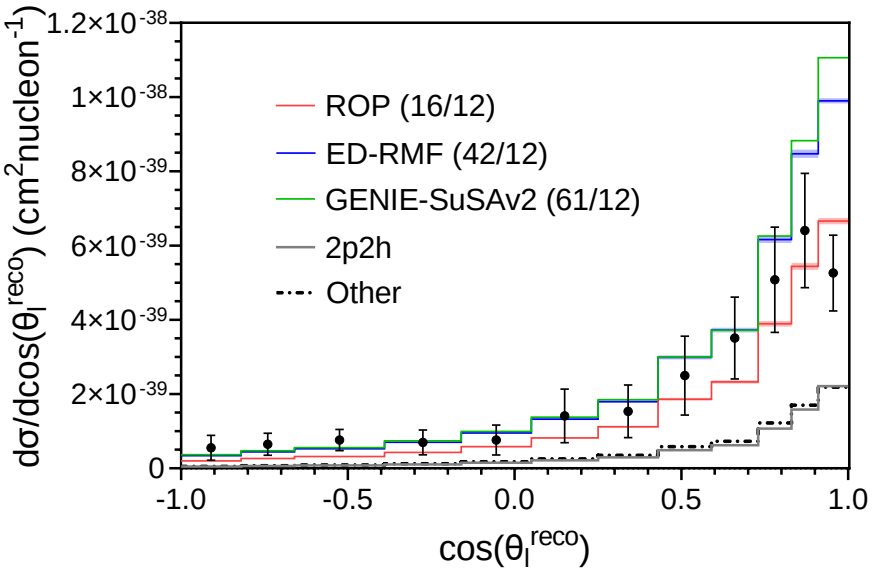

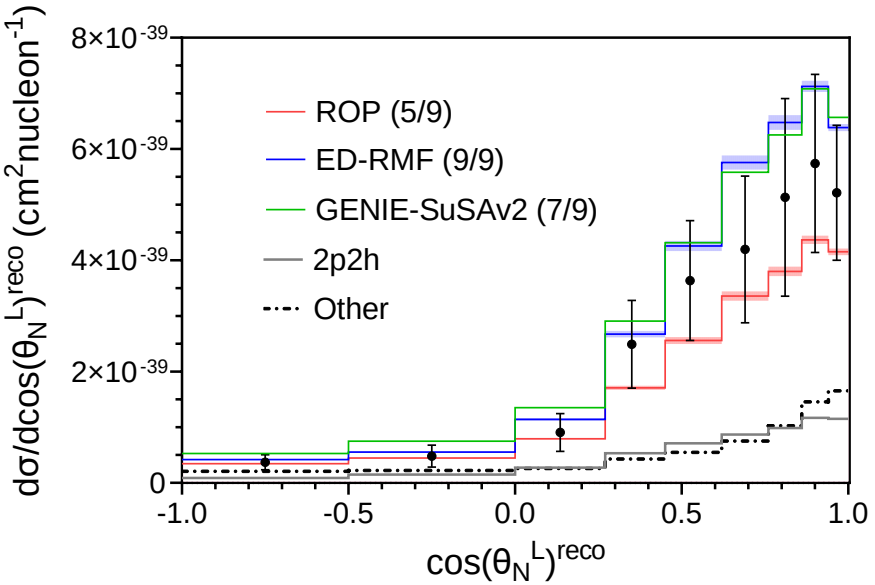

MicroBooNE semi-inclusive cross sections: $1\mu CC0\pi Np$

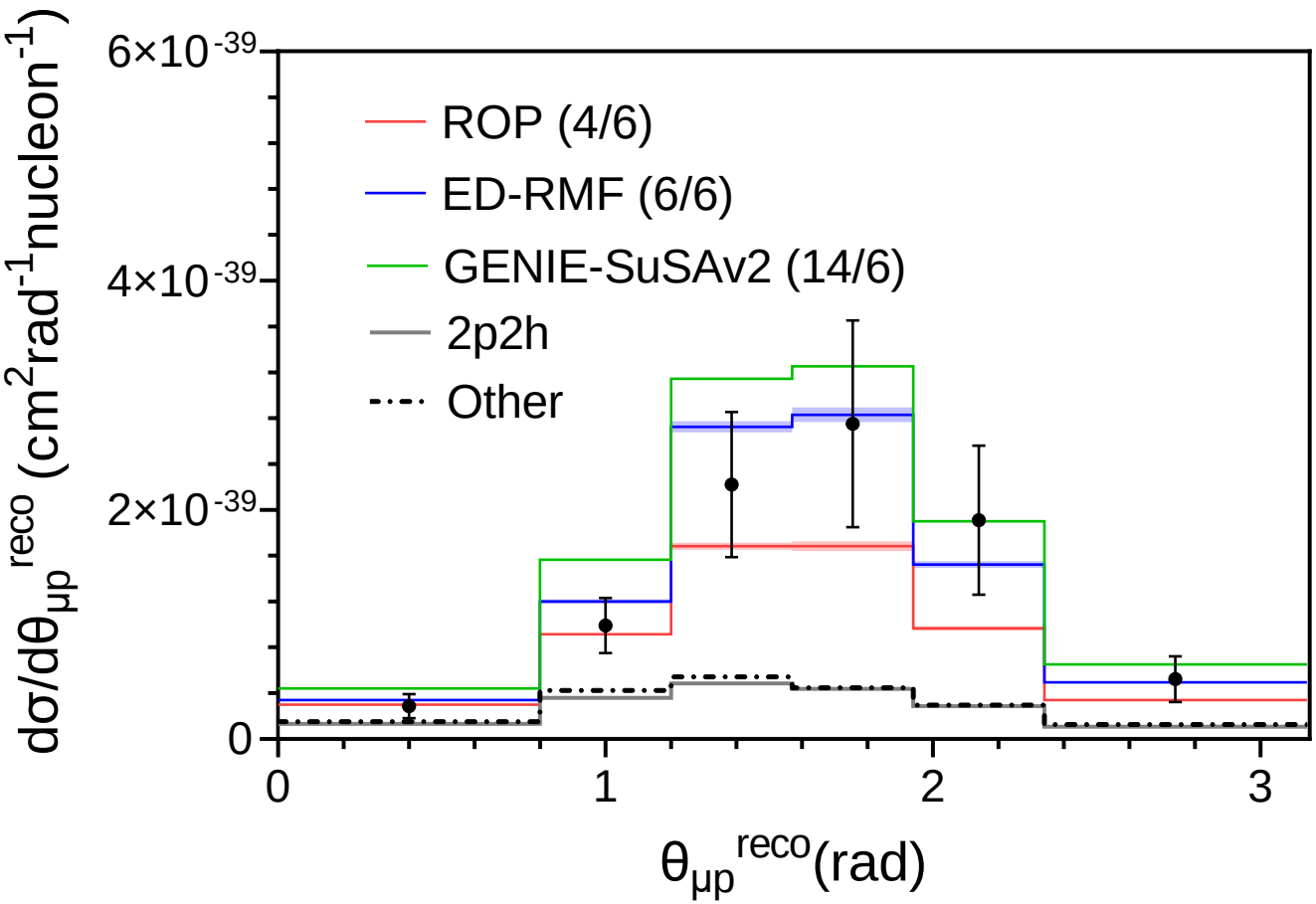

MicroBooNE semi-inclusive cross sections: $1eCC0\pi Np$

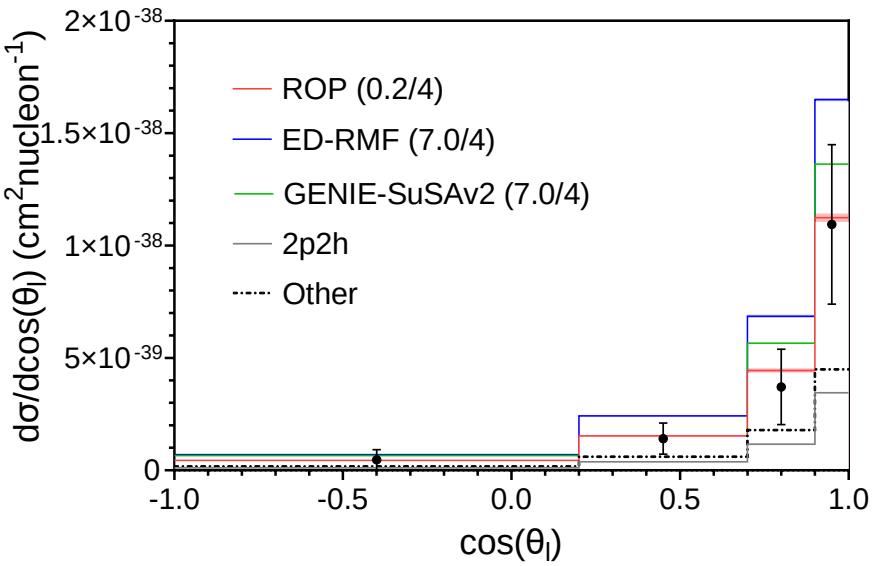

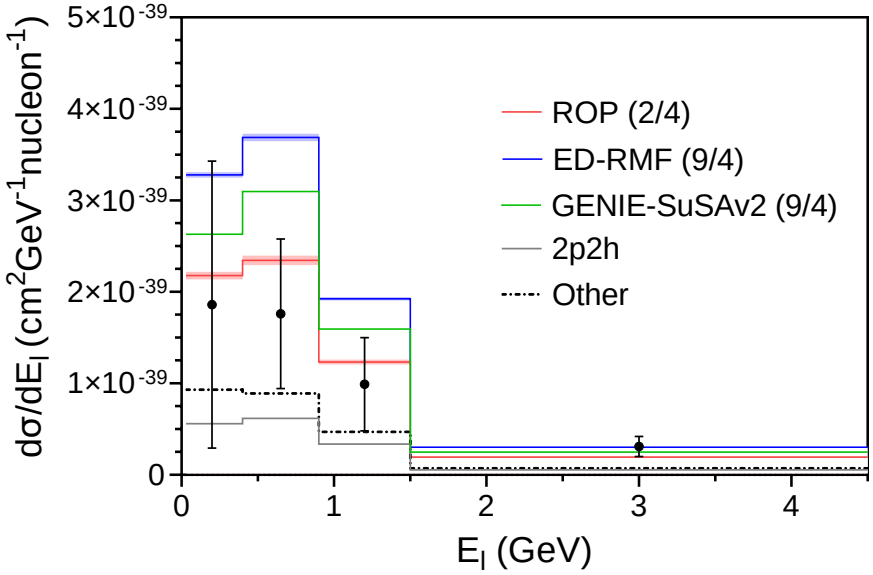

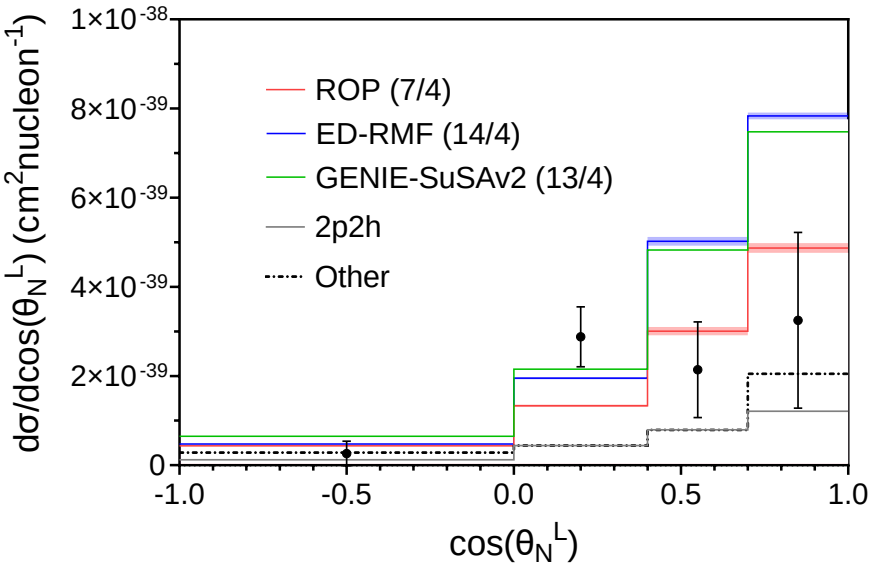

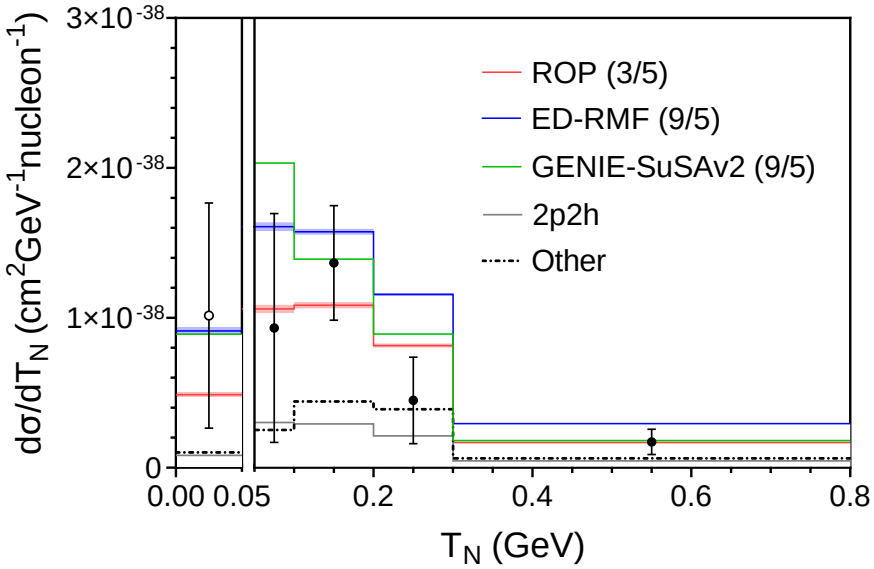

MicroBooNE semi-inclusive cross sections: $1\mu CC0\pi 1p$

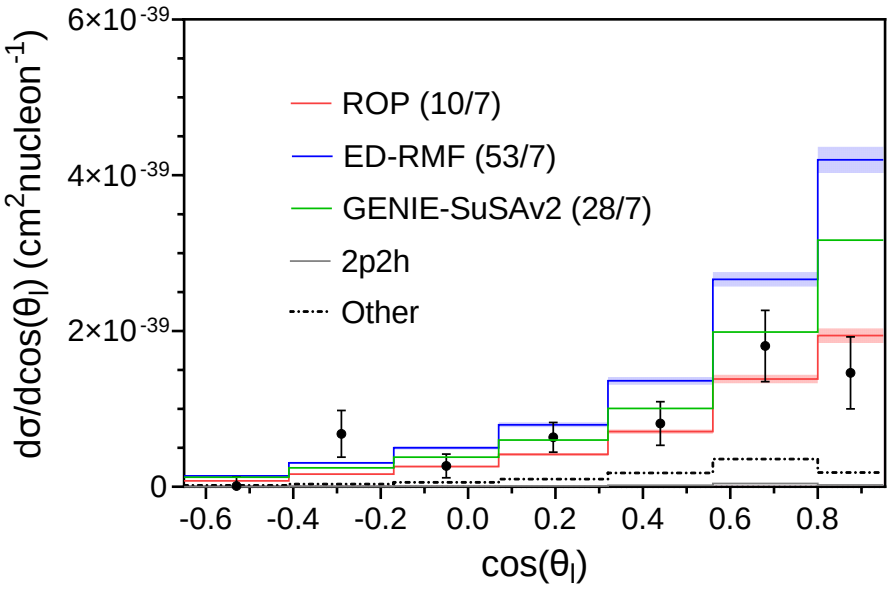

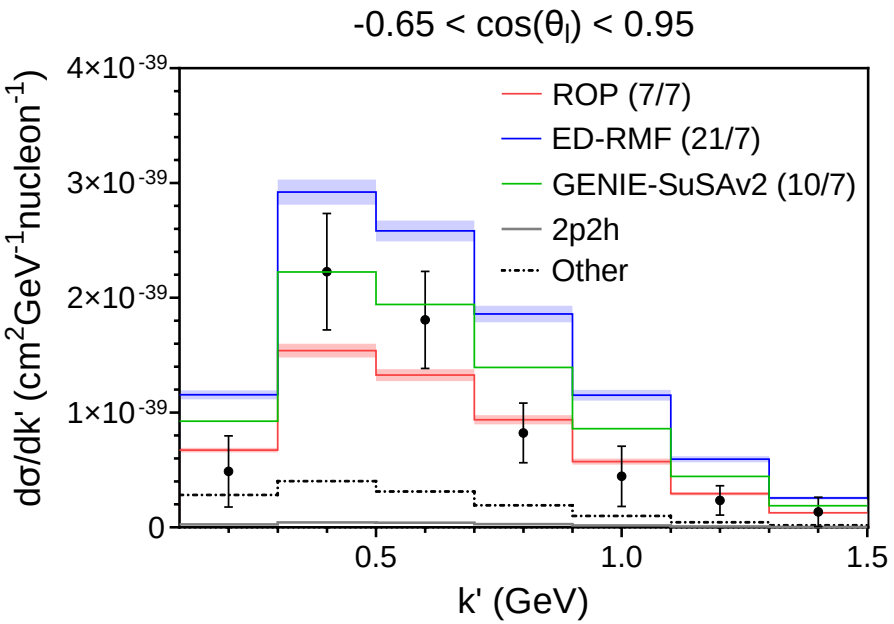

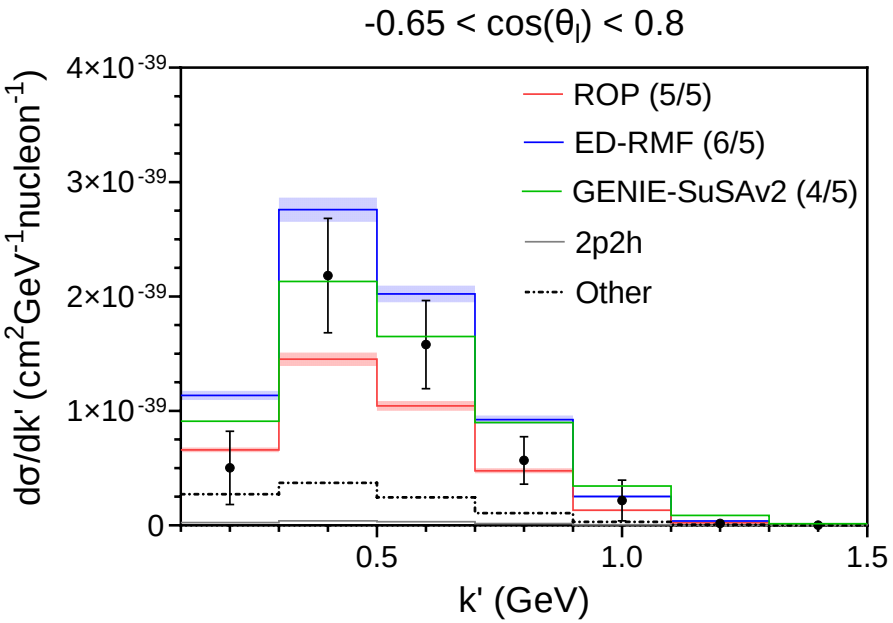

MicroBooNE semi-inclusive cross sections: $1\mu CC0\pi 1p$

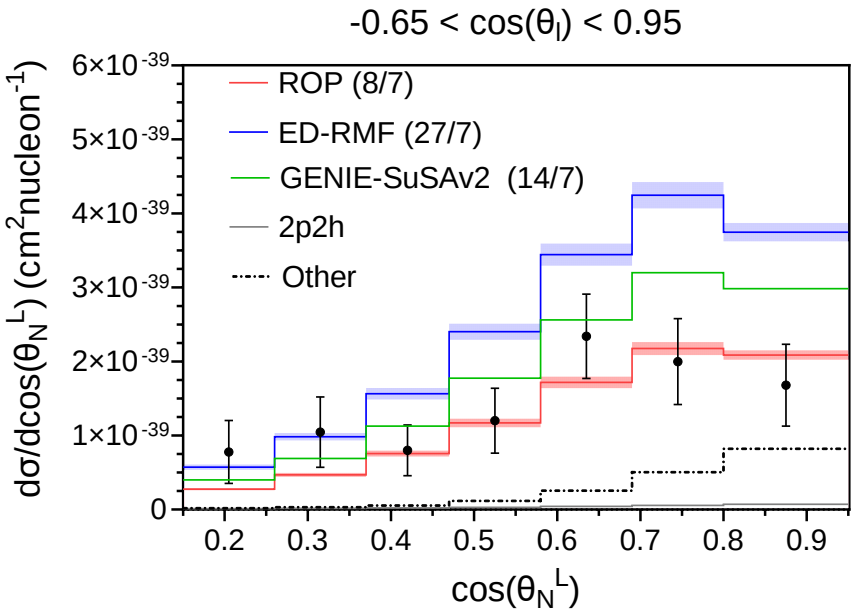

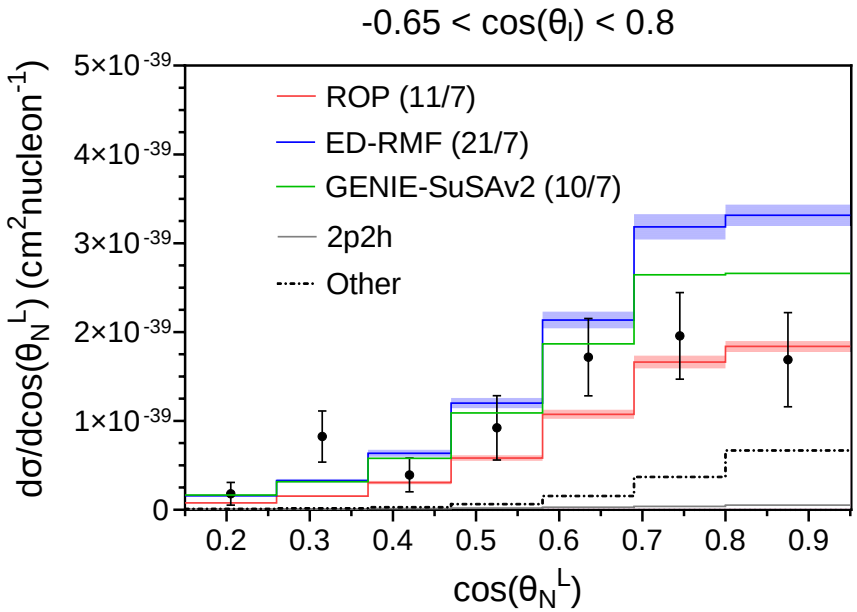

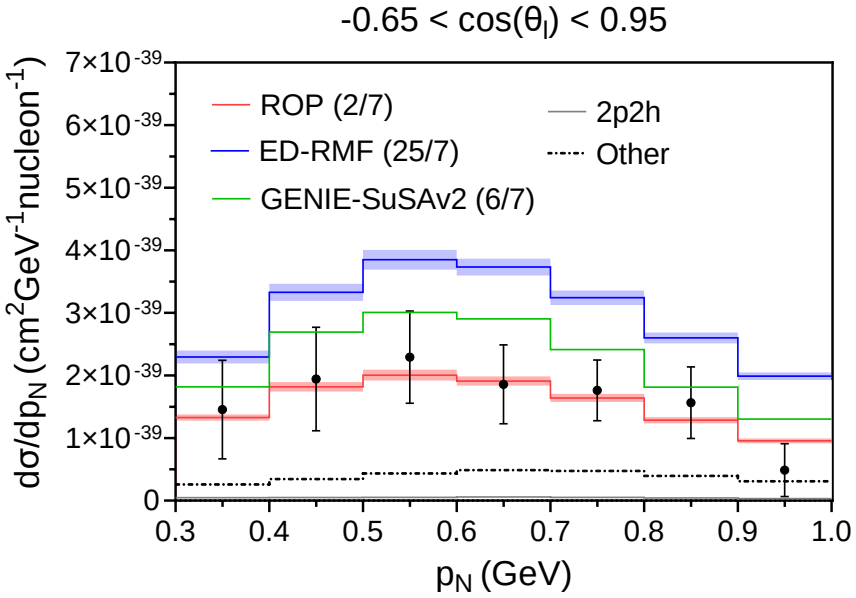

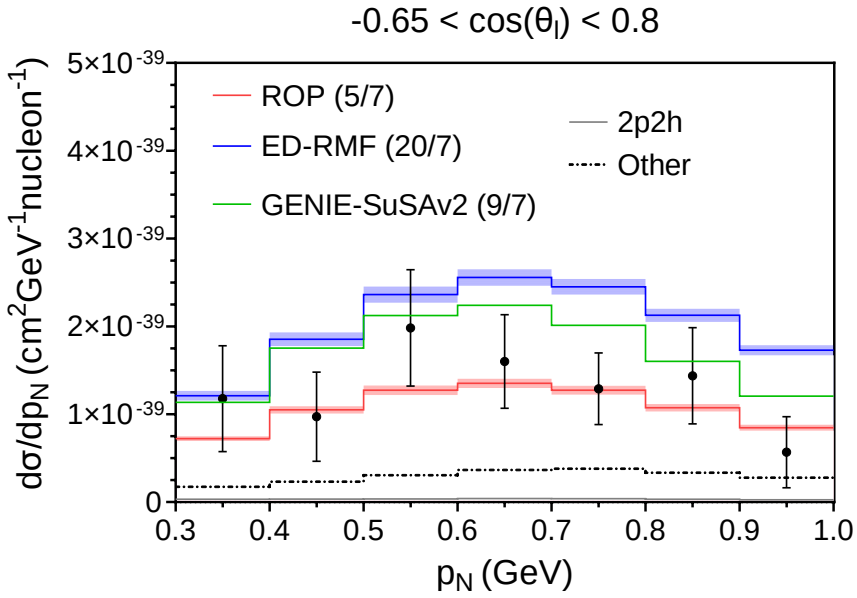

MicroBooNE semi-inclusive cross sections: $1\mu CC0\pi 1p$

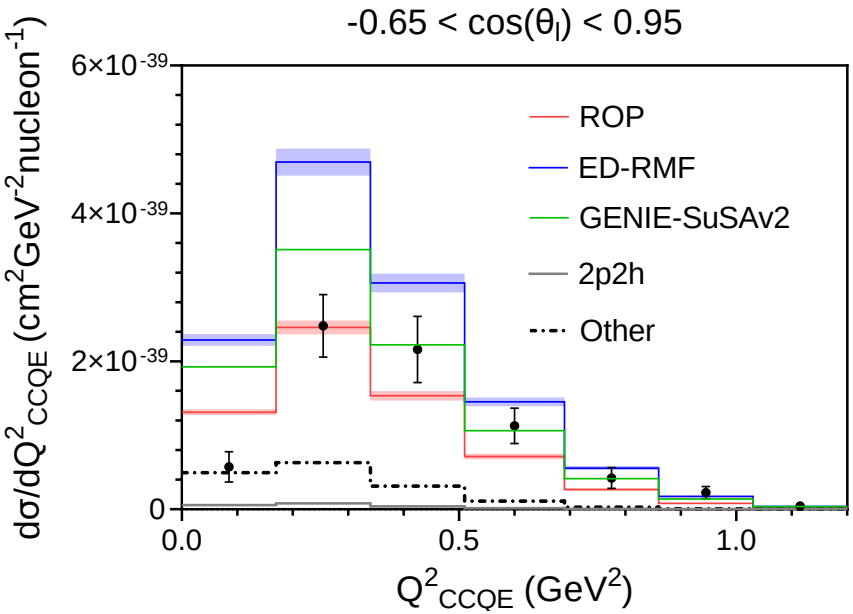

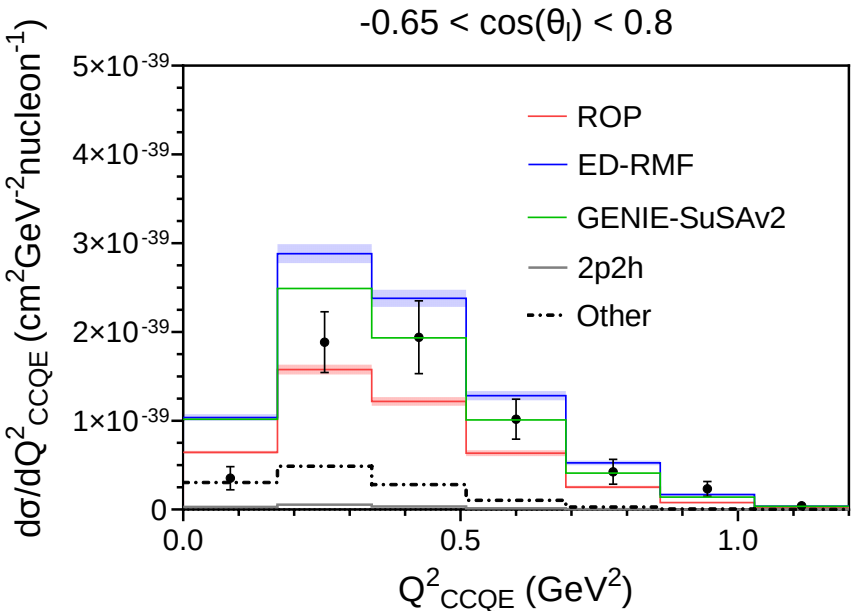

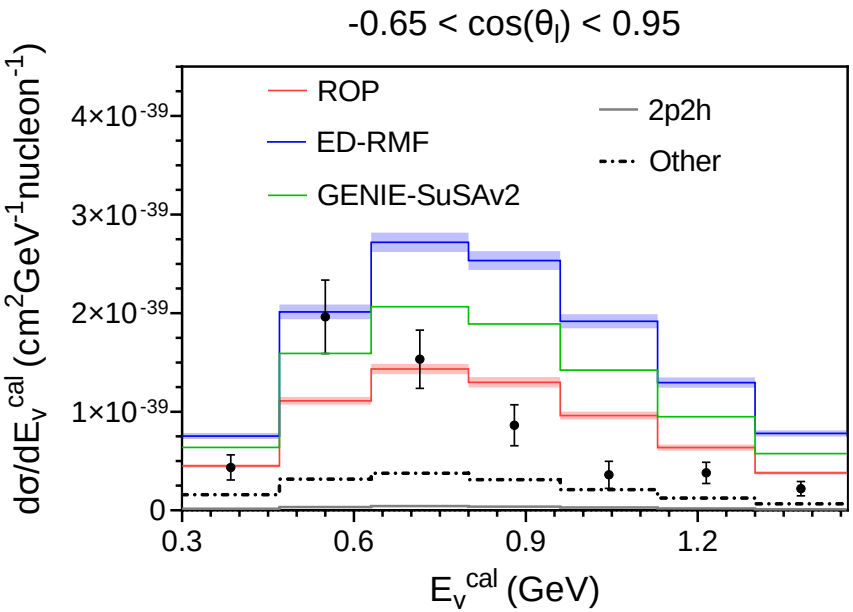

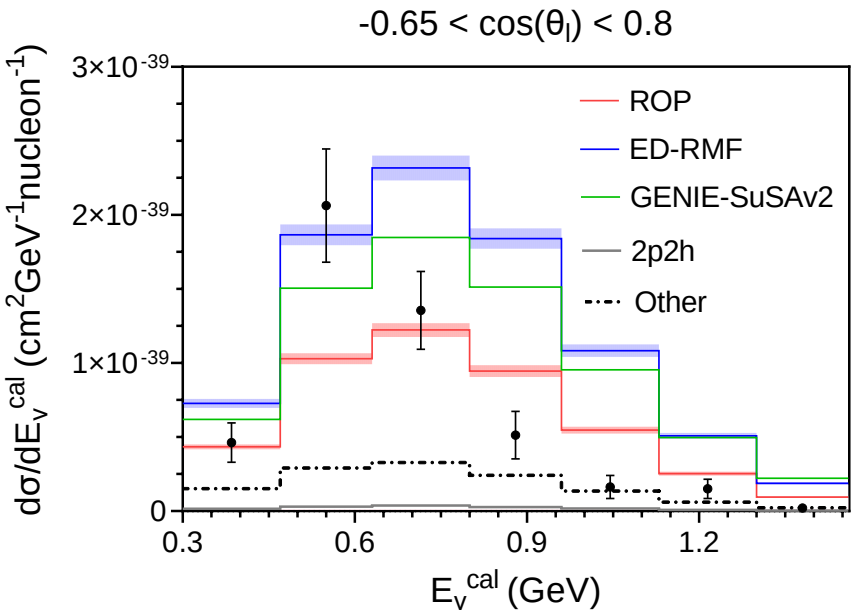

Reference systems

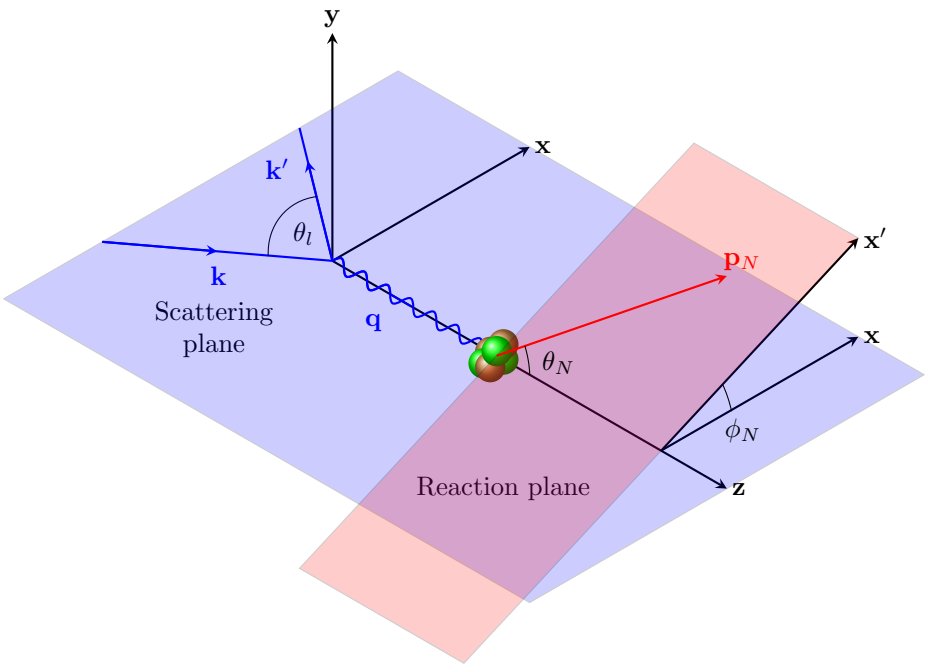

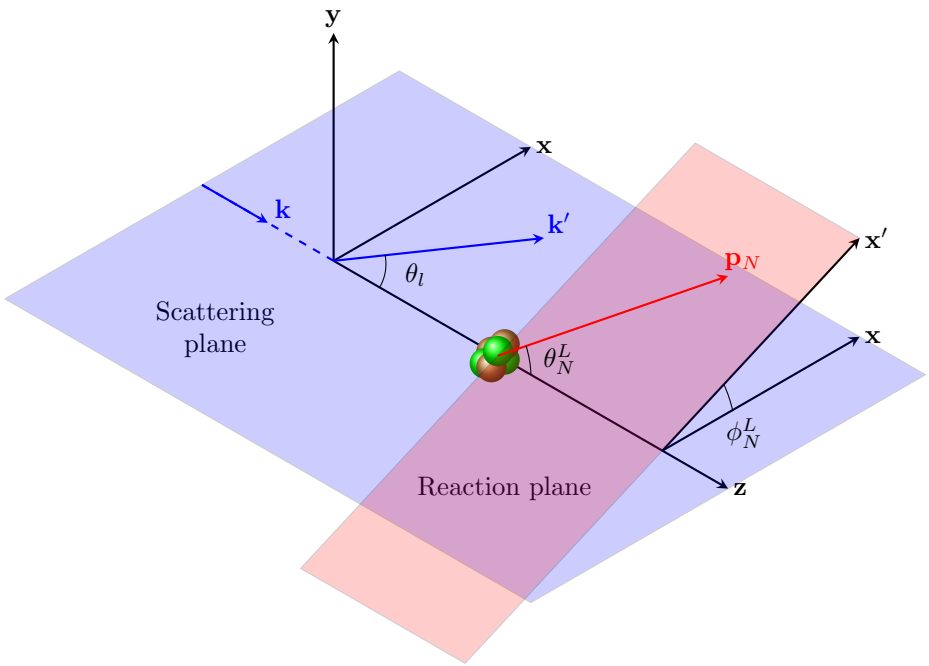

T2K χ^2 table

	rROP	ROP	RPWIA	ED-RMF	GENIE-SuSAv2
1μCC0π0p (59)	232	127	1172	180	209
1μCC0πNp (24)	64	28	82	76	69
Δp (49)	666	373	756	773	366
$\Delta\theta$ (35)	1170	466	1285	1379	159
$\Delta\theta^*$ (33)	129	92	152	146	123
$\lvert\Delta\mathbf{p}\rvert$ (49)	348	290	357	376	336
δp_T (8)	38	16	60	41	36
$\delta\alpha_T$ (8)	29	13	41	33	49
$\delta\phi_T$ (8)	23	20	38	24	40

RMF parameters

Parameter	HS	NL1	NL2	NLSH
m (MeV)	939	938	938	939
m_σ (MeV)	520	492.25	504.89	526.059
m_ω (MeV)	783	795.359	780	783
m_ρ (MeV)	770	763	763	763
g_σ	10.47	10.138	9.111	10.444
g_ω	13.8	13.285	11.493	12.945
g_ρ	4.035	4.976	5.507	4.383
g_2 (fm^{-1})	0	-12.172	-2.304	-6.9099
g_3	0	-36.265	13.783	-15.8337
ρ_0 (fm^{-3})	0.148	0.151	0.146	0.146
E/A (MeV)	-15.731	-16.426	-17.018	-16.346
K (MeV)	546.3	211.11	399.2	355.4
m^*/m	0.541	0.573	0.670	0.597
J (MeV)	34.9	43.5	45.1	36.1